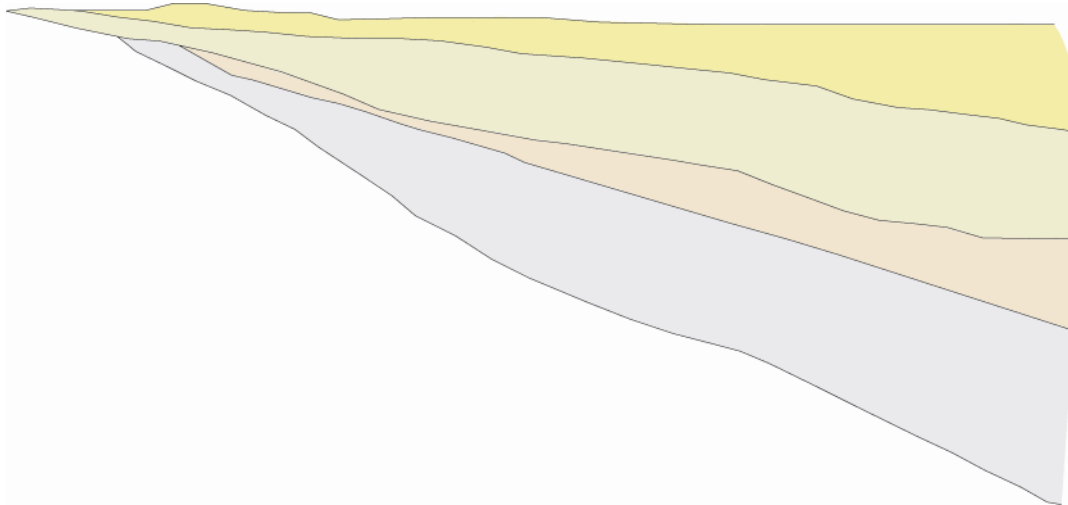


Groundwater Resource Evaluation and Availability Model of the Gulf Coast Aquifer in the Lower Rio Grande Valley of Texas



Report 368

By
Ali Chowdhury, Ph.D, P.G.
Robert E. Mace, Ph.D, P.G.

Texas Water Development Board

P.O. Box 13231, Capitol Station
Austin, Texas 78711-3231

June 2007





Texas Water Development Board

Report 368

Groundwater Resource Evaluation and Availability Model of the Gulf Coast Aquifer in the Lower Rio Grande Valley of Texas

by
Ali H. Chowdhury, Ph.D., P.G.
Robert E. Mace, Ph.D., P.G.

June 2007

This page is intentionally blank.

Texas Water Development Board

E.G. Rod Pittman, Chairman, Lufkin

James E. Herring, Member, Amarillo

Jack Hunt, Vice Chairman, Houston

Thomas Weir Labatt III, Member, San Antonio

Dario Vidal Guerra Jr., Member, Edinburg

William W. Meadows, Member, Fort Worth

J. Kevin Ward, Executive Administrator

Authorization for use or reproduction of any original material contained in this publication, i.e., not obtained from other sources, is freely granted. The Board would appreciate acknowledgment. The use of brand names in this publication does not indicate an endorsement by the Texas Water Development Board or the State of Texas.

Published and distributed
by the
Texas Water Development Board
P.O. Box 13231, Capitol Station
Austin, Texas 78711-3231

June 2007
Report 368
(Printed on recycled paper)

This page is intentionally blank.

Table of Contents

1.0	Executive summary.....	1
2.0	Introduction.....	2
3.0	Study area.....	3
	3.1 Physiography, climate, and vegetation.....	3
	3.2 Geology	10
4.0	Previous work	14
5.0	Hydrogeologic setting.....	16
	5.1 Hydrostratigraphy.....	16
	5.2 Structure	18
	5.3 Water levels and regional groundwater flow	28
	5.4 Rivers, streams, lakes, and canals	33
	5.5 Recharge.....	39
	5.6 Hydraulic properties	43
	5.7 Discharge.....	48
6.0	Groundwater quality	61
7.0	Conceptual model of groundwater flow in the aquifer	66
8.0	Model design.....	68
	8.1 Code and processor	68
	8.2 Layers and grid.....	68
	8.3 Model parameters	74
9.0	Model boundaries.....	76
10.0	Modeling approach	76
11.0	Steady-state model	77
	11.1 Calibration.....	78
	11.2 Water budget	85
12.0	Sensitivity analysis.....	88
13.0	Transient model	90
	13.1 Calibration	91
14.0	Predictions.....	98
	14.1 Drought of record	98
	14.2 Predictive runs	99
15.0	Limitations of the model.....	107
	15.1 Input data.....	107
	15.2 Assumptions	109
	15.3 Applicability.....	109
16.0	Future improvements	110
17.0	Conclusions.....	110
18.0	Acknowledgments.....	111
19.0	References.....	112

List of Figures

3-1	Location of the study area	4
3-2	Locations of regional water planning areas and groundwater conservation districts in model area.....	5
3-3	Location of the major aquifers and model boundaries.....	6
3-4	Land-surface elevation.....	6
3-5	Major physiographic features in the study area	7
3-6	Historical annual precipitation	8
3-7	Net lake evaporation	9
3-8	Stratigraphic and hydrostratigraphic section	12
5-1	General structural setting	19
5-2	Elevation of the base of the Chicot Aquifer.....	21
5-3	Elevation of the base of the Evangeline Aquifer	21
5-4	Elevation of the base of the Burkeville Confining System.....	22
5-5	Elevation of the base of the Jasper Aquifer	22
5-6	Location of control points to define structural bases	23
5-7	Typical well log used to delineate formation contacts.....	24
5-8	Thickness of the Chicot Aquifer	26
5-9	Thickness of the Evangeline Aquifer.....	26
5-10	Thickness of the Burkeville Confining System	27
5-11	Thickness of the Jasper Aquifer.....	27
5-12	An east-west cross section in the study area.....	28
5-13	Water level elevation comparisons for different time periods.....	29
5-14	Water level elevations in the Chicot Aquifer.....	30
5-15	Water level elevations in the Evangeline Aquifer	30
5-16	Hydrographs for wells in the Chicot and Evangeline aquifers	31
5-17	Hydrographs for wells in the Chicot and Evangeline aquifers	32
5-18	River basins.....	33
5-19	Streamflow data from the Rio Grande	35
5-20	Streamflow data from Arroyo Colorado	36
5-21	Lakes in the study area.....	37
5-22	Precipitation distribution for 1930–1980	41
5-23	Location of rain gages.....	42
5-24	Location of pumping and specific-capacity tests.....	47
5-25	Histograms of measured hydraulic conductivity	48
5-26	Variogram analyses of hydraulic conductivity	49
5-27	Kriged distribution of hydraulic conductivity in the Chicot Aquifer	50
5-28	Kriged distribution of hydraulic conductivity in the Evangeline Aquifer	50
5-29	Vegetation map of the study area.....	52
5-30	Total groundwater withdrawal in the study area.....	54
5-31	Population density distribution for 1990.....	59
5-32	Population density distribution for 2000.....	59
5-33	Total groundwater withdrawal from each county	60
6-1	Total dissolved solids distribution versus depth	64
6-2	Spatial distributions of total dissolved solids	65

7-1	Conceptual model of groundwater flow	67
8-1	Active cells and boundary assignments in Layer 1 (Chicot Aquifer)	69
8-2	Active cells and boundary assignments in Layer 2 (Evangeline Aquifer)	70
8-3	Active cells and boundary assignments in Layer 3 (Burkeville Confining System).....	71
8-4	Active cells and boundary assignments in Layer 4 (Jasper Aquifer)	72
8-5	Surface geology in the study area.....	73
11-1	Calibrated hydraulic conductivity zones in the Chicot Aquifer	79
11-2	Calibrated hydraulic conductivity zones in the Evangeline Aquifer.....	79
11-3	Calibrated recharge for 1980	80
11-4	Calibrated evapotranspiration for 1980.....	81
11-5	Cross-plot of simulated and measured water levels for 1980	82
11-6	Simulated water level elevations for the Chicot Aquifer	82
11-7	Simulated water level elevations for the Evangeline Aquifer	83
11-8	Simulated water level elevations for the Burkeville Confining System	83
11-9	Simulated water level elevations for the Jasper Aquifer.....	84
11-10	Spatial distribution of water level residuals in the Chicot Aquifer for 1980	84
11-11	Spatial distribution of water level residuals in the Evangeline Aquifer for 1980	85
12-1	Sensitivity of simulated water levels for the steady-state model	89
13-1	Cross plot of simulated and measured water levels for 1990 and 2000	92
13-2	Comparison of simulated to measured water levels from 1980 to 2000	93
13-3	Sensitivity of model to specific yield	96
13-4	Sensitivity of model to specific storage	97
14-1	Historical precipitation and Palmer Drought Severity Indices.....	99
14-2	Simulated water level declines in 2010.....	101
14-3	Simulated water level declines in 2020.....	102
14-4	Simulated water level declines in 2030.....	103
14-5	Simulated water level declines in 2040.....	104
14-6	Simulated water level declines in 2050.....	105
14-7	Predictive pumping extrapolated using historical groundwater pumping.....	106

List of Tables

5-1	Recharge estimates for the Gulf Coast Aquifer.....	40
5-2	Hydraulic properties of the Gulf Coast Aquifer in the Lower Rio Grande Valley	46
5-3	Rate of groundwater withdrawal in the Chicot Aquifer	55
5-4	Rate of groundwater withdrawal in the Evangeline Aquifer.....	57
5-5	Estimates of predictive groundwater withdrawal through 2050	61
11-1	Water budget from the steady-state, transient, and predictive models.....	86
12-1	Sensitivity of the Rio Grande stage in the steady-state model calibration.....	90

This page is intentionally blank.

1.0 Executive summary

The Gulf Coast Aquifer in the Lower Rio Grande Valley of South Texas is composed of the Jasper, Evangeline, and Chicot aquifers and is an important groundwater resource to agricultural, municipal, and domestic users. In the Lower Rio Grande Valley, groundwater in many areas often does not meet drinking water or irrigation water quality standards. Most of the groundwater in the valley is slightly saline (1,000 to 3,000 milligrams per liter of total dissolved solids) with local occurrences of high nitrate, sodium, chloride, and boron. Because of advances in desalination technology, this region has a renewed interest in identifying, developing, and treating its groundwater resources to supplement its limited water supply.

The Texas Water Development Board (TWDB) developed a three-dimensional, numerical groundwater flow model of the Gulf Coast Aquifer in the Lower Rio Grande Valley to help estimate groundwater availability and water level responses due to future drought and projected amounts of pumping. The model includes historical information on water levels, structure, hydraulic properties, and recharge rates. We calibrated a steady-state model to mean annual water levels from 1930 through 1980 when there were no significant changes in water levels across the study area. We also calibrated a transient model to reproduce seasonal fluctuations in water levels by incorporating recharge, storage coefficients, and pumpage information from 1980 through 2000. When we made predictive runs from 2000 through 2050, we used water demand numbers for drought conditions from the 2001 regional water plans and included drought-of-record recharge conditions. The 2007 State Water Plan was released after completion of this study. Therefore, we were unable to use drought-of-record demand numbers from the 2006 regional water plans. We will publish predictive runs from 2010 to 2060 using the 2006 regional water plans at a later date.

The model generally replicates the spatial distribution of water levels and reproduces groundwater flow to the Gulf of Mexico and to and from the Rio Grande. The root mean squared error of the calibrated steady-state model is 23 feet, which is about 4.4 percent of the hydraulic head drop across the study area. The recharge rate is about 0.52 percent of the average annual rainfall for 1930 to 1980 (0.08 to 0.14 inches per year). Modeling results indicate that about 88,000 acre-feet of groundwater annually flows through the aquifer in the study area. Of the total annual flow through the aquifer, 47 percent of the recharge comes from rainfall, and 53 percent seeps in from the Rio Grande. Cross-formational flow is a significant component of the total flow for each aquifer, with deeper groundwater from the Evangeline Aquifer flowing upward near the coast and resulting in greater salinity in the overlying Chicot Aquifer.

The model suggests that water levels may fall by about 14 feet in the Chicot Aquifer and about 34 feet in the Evangeline Aquifer by 2010 based on projected pumping and drought-of-record recharge. By 2050, water levels may decline by as much as 22 feet in the Chicot Aquifer and as much as 52 feet in the Evangeline Aquifer. However, when we used average recharge through 2050, predicted water levels and aquifer storage remain at about the same level as in 1990.

2.0 Introduction

The Gulf Coast Aquifer in the Lower Rio Grande Valley of South Texas is an important groundwater resource to agricultural, municipal, and domestic users. The Lower Rio Grande Valley is often exposed to severe droughts and has very limited water resources, depending primarily on the Rio Grande for most of its water needs. With recent droughts, a limited source of water from the Rio Grande, and a projected doubling of the population over the next 50 years, there is considerable interest in better using the groundwater resources of the area. Drought and decreased river flow for nearly a decade have recently caused the Rio Grande to stop flowing into the Gulf of Mexico for the first time in recorded history. Water supplies may diminish even more as a result of pumping the shallow aquifer along both sides of the Rio Grande. Water levels have declined in the past near major pumping centers in Hidalgo and Brooks counties.

Although the Gulf Coast Aquifer has been extensively studied, most of these investigations have focused on the Houston area where water levels have declined by as much as 250 feet, resulting in land subsidence (Kasmarek and Strom, 2002). In the Lower Rio Grande Valley, groundwater quality in many areas does not meet drinking water or irrigation water quality standards. Most of the groundwater in the valley is slightly saline (1,000 to 3,000 milligrams per liter of total dissolved solids), with local occurrences of high nitrate, sodium, chloride, and boron concentrations. However, the continued scarcity of water in the region and the greater availability and affordability of desalination technology have renewed interest in identifying, developing, and treating groundwater resources in the area (HDR, 2000).

A numerical groundwater flow model can help provide information on the quantity of water available in an aquifer and how water levels might respond to increased pumping or reduced recharge under drought conditions. In addition, a groundwater flow model can be used as a tool to quantitatively compare and contrast the effects of regional water resource management decisions. A groundwater flow model is also useful to groundwater conservation districts, regional water planning groups, or anyone else interested in evaluating the groundwater resources in the Lower Rio Grande Valley.

In this study, TWDB developed a three-dimensional, finite-difference groundwater flow model for the Gulf Coast Aquifer in the Lower Rio Grande Valley of Texas to

- (1) better understand and characterize groundwater flow in the region,
- (2) develop a management tool to support water planning efforts of groundwater conservation districts and regional water planning groups in the area,
- (3) help determine fresh to moderately saline groundwater availability,
- (4) assess brackish water availability for desalination, and
- (5) evaluate potential water level declines due to pumping increases and future droughts.

In this report, we describe the construction and calibration of the numerical groundwater availability model for the Gulf Coast Aquifer in the Lower Rio Grande Valley. We also present predictive groundwater results through 2050, using pumping projections provided by the regional water planning groups for the 2002 State Water Plan.

In addition, this report contains detailed analyses of the (1) study area, previous investigations, hydrostratigraphic framework of the Gulf Coast Aquifer, and conceptualization of the flow system; (2) code, grid, and parameters used in model construction and calibration; (3) results of the steady-state and transient model simulation; (4) predictive water level changes over the next 50 years; and (5) limitations and potential future improvements of the model. We also present an estimate on the amount of brackish water present in the Chicot and Evangeline aquifers, using aquifer thickness, porosity, and the distribution of total dissolved solids in the groundwater.

3.0 Study area

The study area is located in the Lower Rio Grande Valley of South Texas and includes all or parts of Jim Hogg, Brooks, Kenedy, Starr, Hidalgo, Cameron, and Willacy counties (Figure 3-1). The study area includes two regional water planning areas: (1) the Rio Grande Region (Region M) and (2) the Coastal Bend Region (Region N). There are three groundwater conservation districts located within the study area (Kenedy County Groundwater Conservation District, Starr County Groundwater Conservation District (not yet confirmed at time of publication), and Red Sands Groundwater Conservation District) (Figure 3-2). The study area covers the southern part of groundwater management area 16. We defined the limits of the study area according to the hydrologic boundaries and lateral extent of the aquifer. These boundaries include (1) the outcrop limit of the aquifer to the west; (2) the Rio Grande to the south; (3) a groundwater flow line through Jim Hogg, Brooks, and Kenedy counties to the north; and (4) the Gulf of Mexico to the east (Figure 3-3). We chose the position of the northern groundwater flow line to avoid major pumping centers. We placed the eastern boundary 10 miles offshore from the coastline to include the flow of groundwater through the aquifer and into the Gulf of Mexico. Including this offshore area into the model is consistent with suggestions that the freshwater part of the Chicot and Evangeline aquifers extends at least 5 to 10 miles beneath the Gulf of Mexico (Groschen, 1985; Kasmarek and Strom, 2002).

3.1 Physiography, climate, and vegetation

The Lower Rio Grande Valley is a flat plain extending from the Gulf of Mexico in the east to the Bordas Escarpment in the west where surface elevation rises to more than 500 feet in Starr and Jim Hogg counties (Figure 3-4). Near the southern edge of the escarpment, the plain gently slopes southeastward. Low clay ridges and mounds formed by wind deposition give the appearance of a “blowout and dune” topography that rises to an elevation of 25 feet in the eastern plain (Baker and Dale, 1961).

The central and western part of the plain has broad, shallow depressions. In southeastern Hidalgo County, a ridge known as Mission Ridge arises near Mission and extends westward

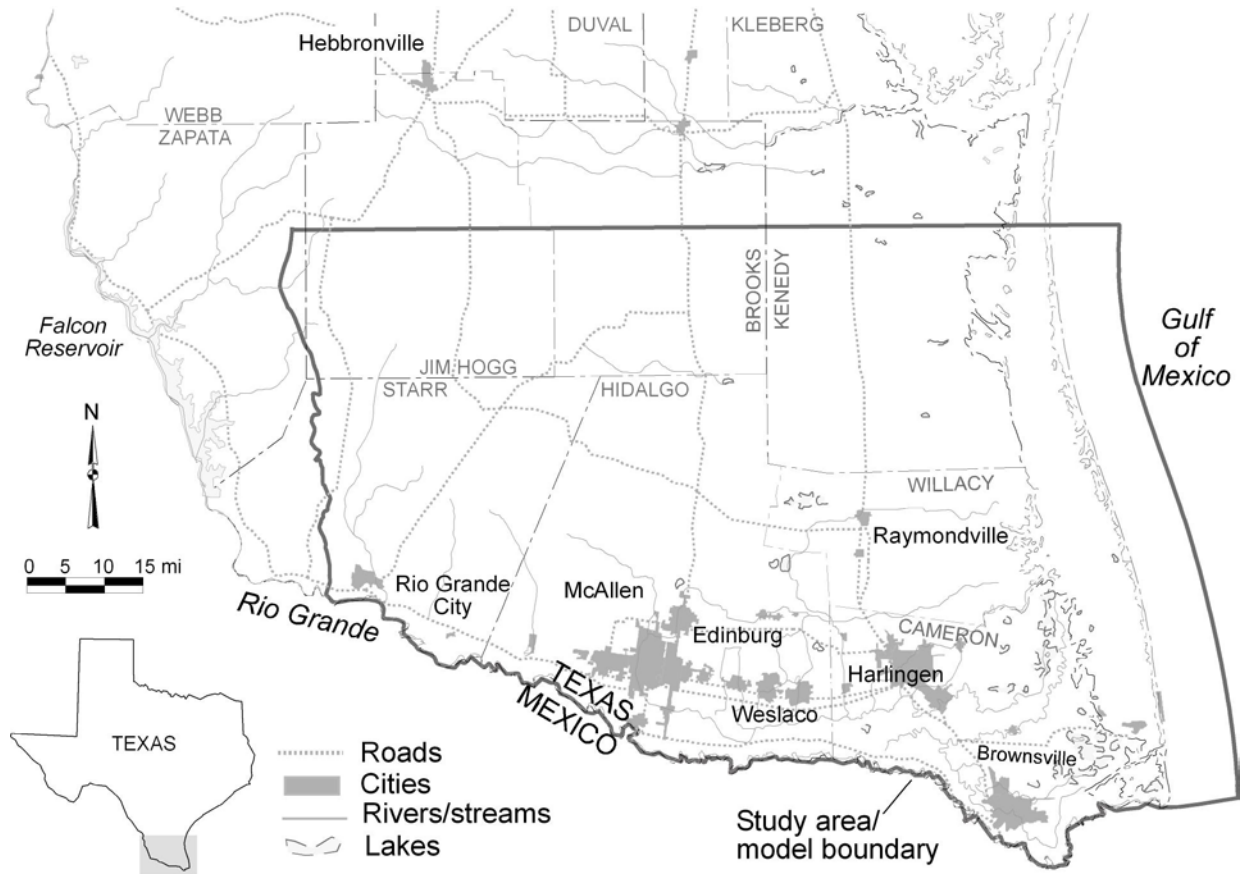


Figure 3-1. Location map of the study area showing model boundaries, major cities, rivers, and lakes. Note that the eastern boundary extends 10 miles offshore into the Gulf of Mexico (mi = miles).

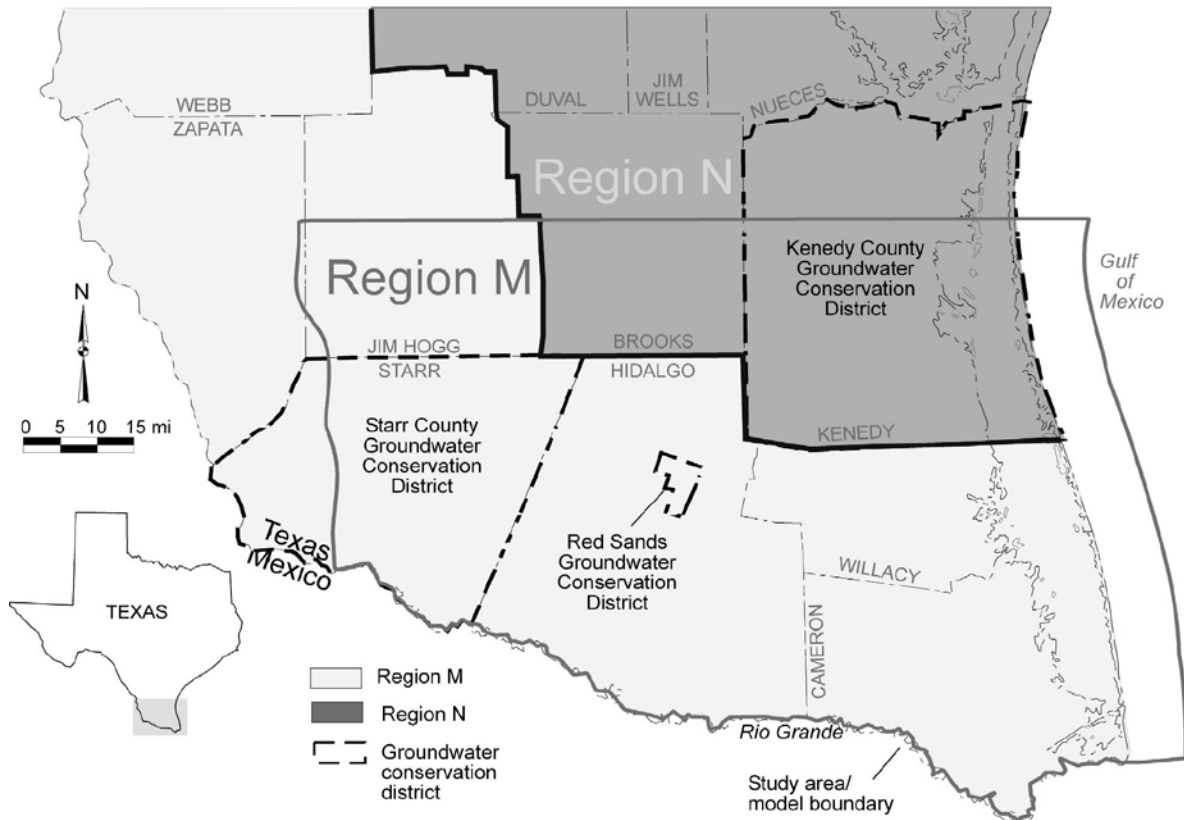


Figure 3-2. Locations of the regional water planning areas, the Red Sands Groundwater Conservation District, the Kenedy County Groundwater Conservation District (boundary approximate), and the Starr County Groundwater Conservation District (unconfirmed at present time). Regions N and M extend outside the area shown (mi = miles).

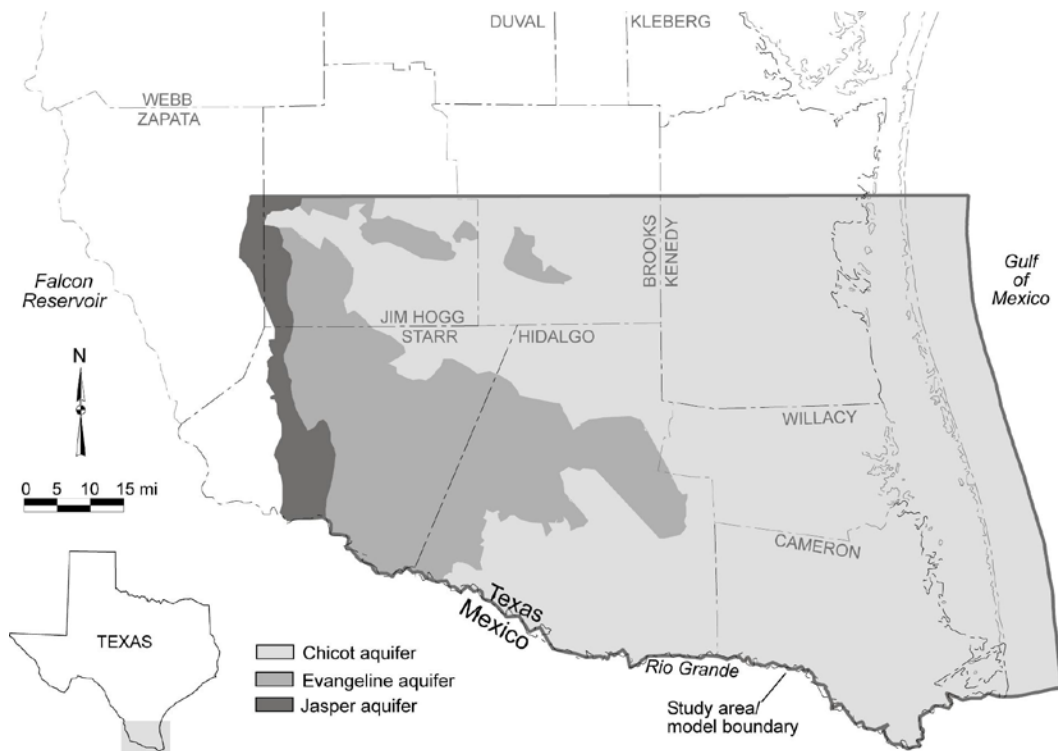


Figure 3-3. Outcrop areas of the Chicot, Evangeline, and Jasper aquifers in the study area. These aquifers together make up the Gulf Coast Aquifer (mi = miles).

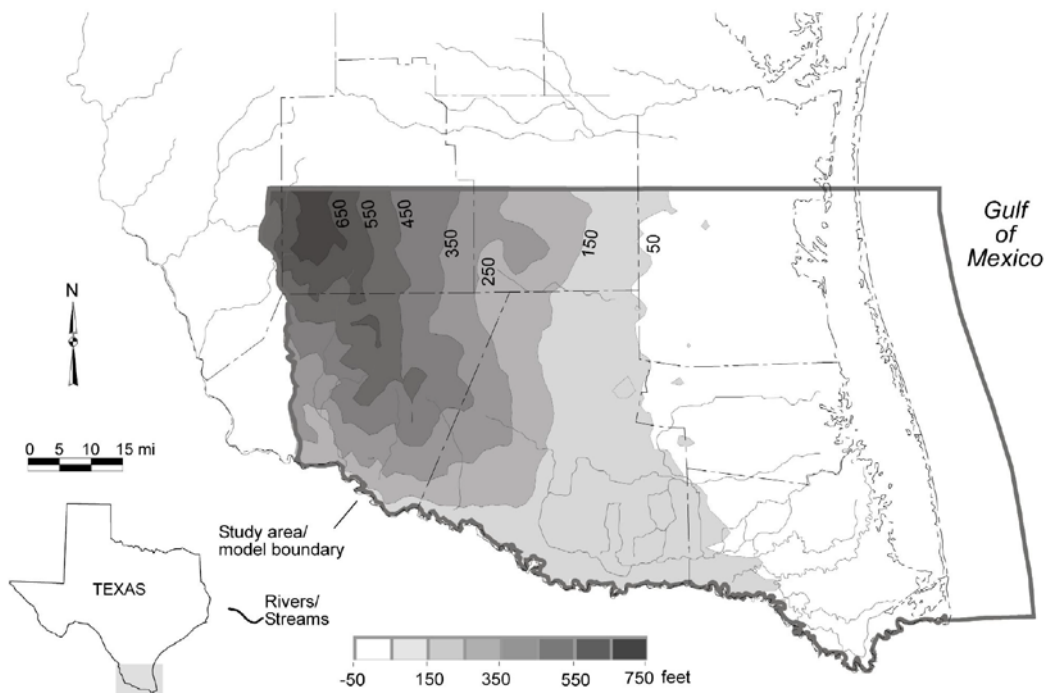


Figure 3-4. Land surface elevation in the study area (data from USGS, 1990; mi = miles).

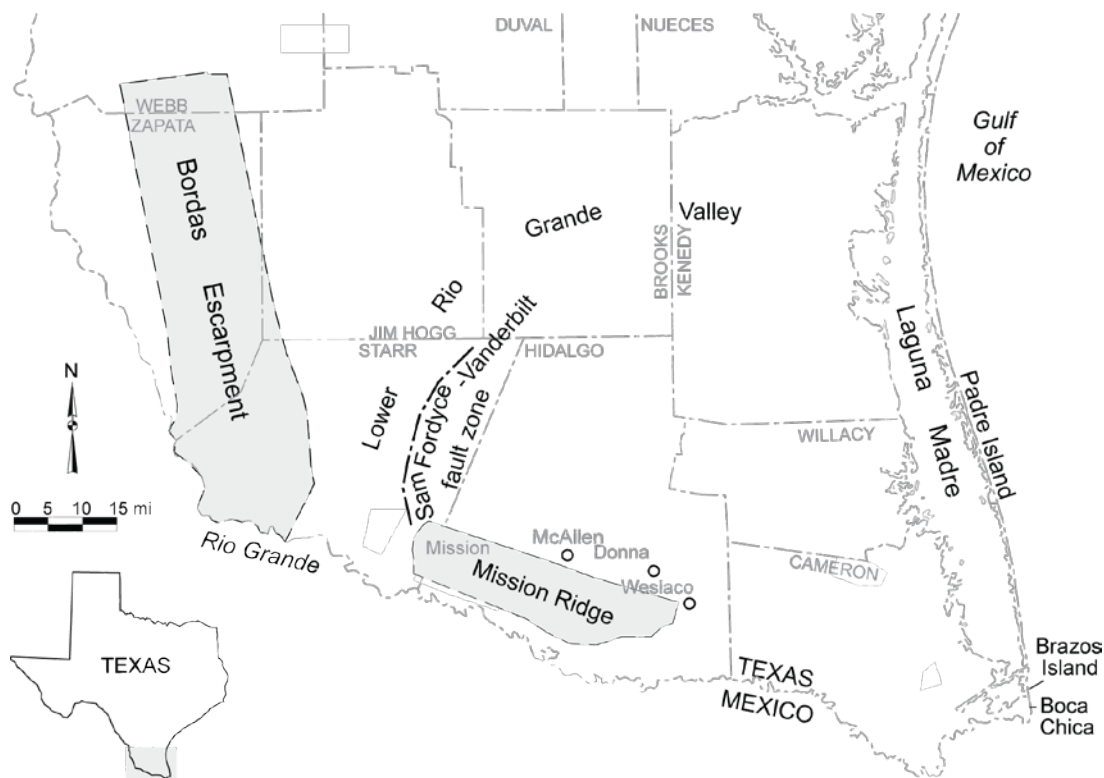


Figure 3-5. Major physiographic features in the study area (modified after Baker and Dale, 1961, and McCoy, 1990; mi = miles).

to the upland plain. To the east near Donna, the Mission Ridge becomes imperceptible. Rounded hills and broad valleys occur west of the Bordas Escarpment (Figure 3-5). The valleys contain intermittent streams that form tributaries to the Rio Grande.

The Rio Grande Valley has a maximum width of about 9 miles near Weslaco and contains one or more terraces. Both the width of the valley and the number of terraces vary locally. The Rio Grande empties into the Gulf of Mexico in the southeastern corner of the valley. The river has a slope lower than the plain to the north. To the east, the river lowland and the plain merge into the delta of the Rio Grande (Baker and Dale, 1961).

Padre Island, located 8 miles east of the mainland, forms a barrier between the Gulf of Mexico and the mainland. The island is less than a mile wide and is covered with sand dunes. Boca Chica and Brazos Island are a continuation of the barrier south of Padre Island and are connected with the mainland near the mouth of the Rio Grande. Laguna Madre lies between the mainland and these offshore barrier islands (Baker and Dale, 1961).

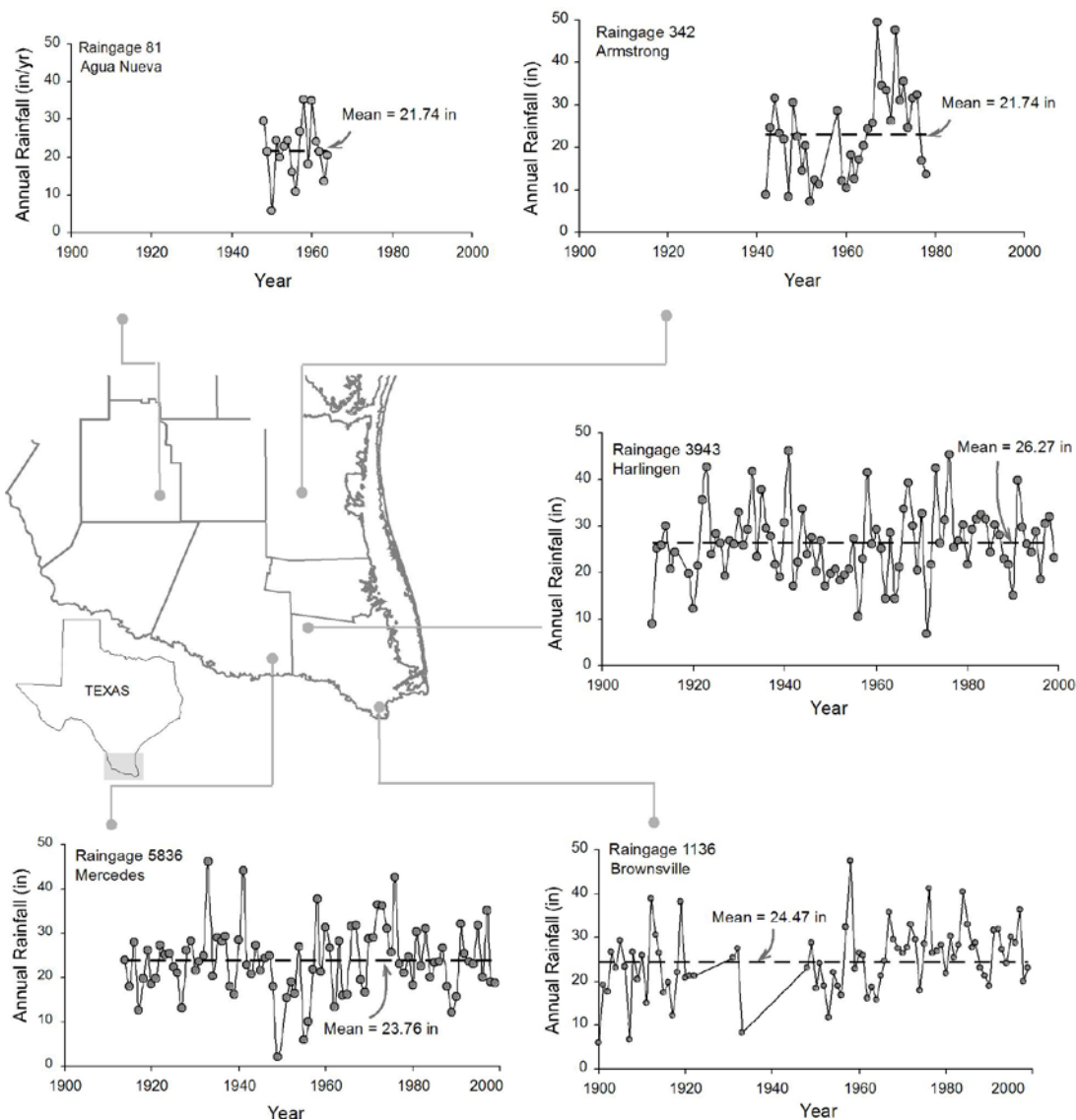


Figure 3-6. Annual rainfall in the study area. Dashed line indicates mean annual rainfall for each rain gage (data from NCDC, 2002; in = inches).

The Rio Grande and several streams flow through the lower Rio Grande Valley and empty into Laguna Madre. Numerous, extremely sinuous channels—locally known as resacas—cross the plain near the coast. Meander scars of the ancestral Rio Grande, resacas and occupy low lying areas often exposed to frequent flooding (Preston, 1983). The streams in most of the study area rarely flow continuously during normal climatic conditions. Therefore, runoff collects in shallow depressions where it subsequently evaporates into the atmosphere or seeps into the ground.

The climate in the valley fluctuates from semitropical to semiarid with annual average precipitation decreasing from 28 inches in the east to 18 inches in the west (Baker and Dale, 1961; Figure 3-6). Prevailing winds are southeasterly with hot, humid air from the

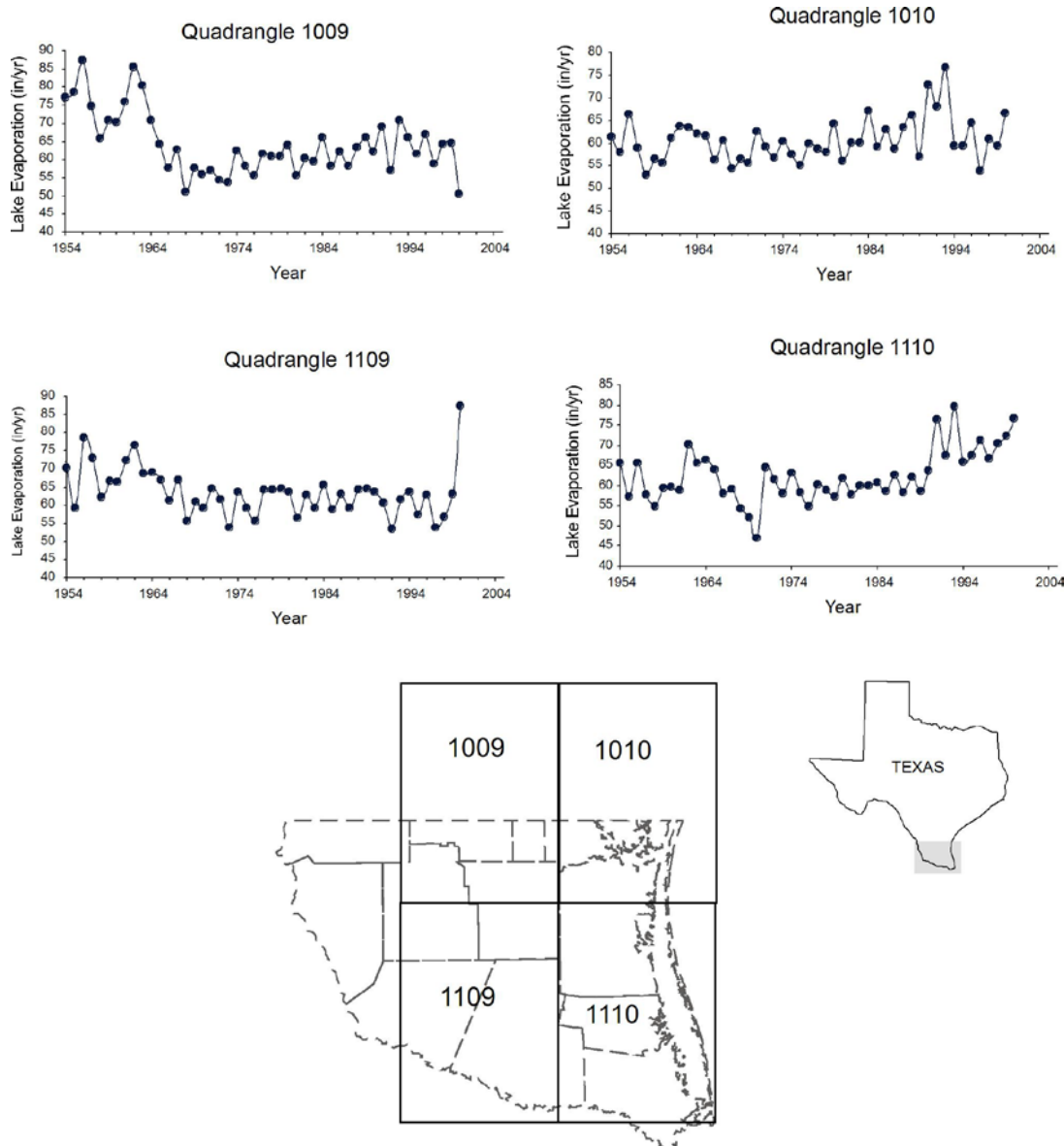


Figure 3-7. Average annual net lake evaporation rates in the study area (in/yr = inches per year).

Gulf of Mexico producing humid summers and relatively mild and dry winters. Most precipitation falls from April through June and from August through October. Hurricanes moving from the Gulf of Mexico in the summer and the early fall also frequently bring heavy rains that occasionally cause flooding of the valley (TCB, 2000). Average annual temperature is about 63°F, and the average annual daily high temperature is 84°F (McCoy, 1990). Average annual net lake evaporation ranges from 60.62 to 62.35 inches near the coast (quadrangles 1010 and 1110) and from 63.52 to 64.19 inches in the upland areas (quadrangles 1009 and 1109; Figure 3-7).

Savannas—areas dominated by drought-tolerant, mostly small-leaved, and often thorn-laden small trees and shrubs—are common in the Lower Rio Grande Valley (Weakly and others, 2000). The most dominant species is mesquite, which occurs as scattered individuals or as a canopy species overtopping a dense undergrowth of shrub savannas. Barbed-wire cactus is dominant on the clay soils of the Beaumont Formation in Cameron and Willacy counties (Ideker, 1991). On the sandy plains of the Goliad Formation in Hidalgo and Starr counties, the dominant vegetation is a canopy of mesquite, Texas paloverde, and Texas ebony overtopping brush species including blackbrush, granjeno, and Mission fiddlewood (Weakly and others, 2000).

Extensive grasslands persist in the coastal sands of Brooks, Kenedy, Jim Hogg, Hidalgo, and Willacy counties. Seacoast bluestem and live oak occur on coastal sand ridges and barrier islands. Floodplain terraces support riparian forests containing sugarberry, cedar elm, and ash. Diverse brush communities called Iomas thrive on better-drained, clay hills composed of sediments transported by winds from coastal bays or inland salt lakes (Weakly and others, 2000). In Cameron and Willacy counties, these Iomas are surrounded by coastal wetlands, grasslands, or periodically inundated wind-tidal flats and dunes (Carr, 2000).

3.2 Geology

The Lower Rio Grande Valley is underlain by sand, silt, and clay of nonmarine to marine origin deposited during Tertiary period to the present (65 million years ago to present). Periodic fluctuation in sea levels and changes in the sediment source areas gave rise to a heterogeneous assemblage of river, windblown, and lake sediments onto a delta (Galloway, 1977). Coarser fluvial and deltaic sand, silt, and clay predominate in inland areas near sediment source areas and grade into finer brackish and marine sediments in offshore areas.

Isostatic adjustment that caused subsidence of the basin and a simultaneous rise of the land surface resulted in a progressive thickening of the stratigraphic units toward the Gulf. Faults that remained active during sedimentation (growth faults) contributed to additional sediment thickness over short, lateral distances. Occurrences of numerous paleo-caliche horizons (calcium carbonate that occurs between interstitial pores from near-surface evaporation of groundwater) in the Gulf Coast indicate that a steady and dry climate existed when the sediments were deposited during the Miocene (from 23 million to 5 million years ago) and the Pleistocene (from 1.8 million years to 11,000 years ago) periods (Galloway, 1977).

Older Eocene- to Miocene-aged sediments in the western portion of the study area are composed of thickly bedded fluvial sands. Progressively younger sediments outcrop toward the coast. The sands are occasionally interbedded with tuffaceous ash that was probably derived from source areas in the Davis Mountains and other volcanic centers in Trans-Pecos Texas (Sellards and others, 1932).

Stratigraphic framework of the Gulf Coast Aquifer is complex and controversial, with disagreement on which units in the surface or subsurface are equivalent in age and what their relationships are (Baker, 1979). Considerable heterogeneity of the sediments and a general

absence of index fossils and diagnostic electric log signatures in the subsurface often make correlating the units difficult.

Baker (1979) grouped the various stratigraphic units in the Gulf Coast using well logs and faunal occurrences from the Sabine River in the northeast to the Rio Grande in the south (Figure 3-8). From oldest to youngest, he classified the Tertiary rocks into the Frio Formation, the Anahuac Formation, and the Catahoula Tuff or Sandstone (Early Miocene); the Oakville Sandstone and the Fleming Formation (Mid- to Late-Miocene); the Goliad Sand (Pliocene); and the Willis Sand, Bentley Formation, Montgomery Formation, Beaumont Clay (Pleistocene), and Alluvium (Holocene) (Baker, 1979). The Catahoula Tuff or Sandstone, Goliad Sand, Willis Sand and Beaumont Clay are often interchangeably referred to in the literature as formations (Sellards and others, 1932; Baker, 1979). We follow this convention in this report because these sediments are mappable over considerably large geographic areas.

Given the complexity of identifying the base of the Pleistocene from electric logs, several nomenclatures have been used to characterize these sediments. For example, Solis (1981) defined the base of the Pleistocene to be the Lissie Formation. The undifferentiated Lissie Formation has also been considered equivalent in age to the Montgomery and the Bentley formations with the bottom of the latter being considered the base of the Pleistocene (Dutton and Richter, 1990). The Montgomery Formation is also occasionally included within the Beaumont Clay (Baker and Dale, 1961). In place of the Montgomery and the Bentley formations, the undifferentiated Lissie Formation of equivalent age occurs in the Lower Rio Grande Valley (Baker and Dale, 1961; Bureau of Economic Geology, 1976).

The Frio Formation has been mapped from Live Oak County to the Rio Grande. In Live Oak County, the Frio Formation outcrop is about a mile wide, and its thickness is about 100 feet. Stratigraphic placement of the Frio Formation remains controversial. The Frio Formation at the surface (mainly clay) has been identified as the nonmarine time equivalent of the Vicksburg Group of Oligocene age, but it may be equivalent to the Catahoula Tuff or Sandstone down dip (Baker, 1979).

The width of the outcrops of the Catahoula Tuff or Sandstone in East Texas ranges from 4 to 6 miles and narrows to 1 mile in Central Texas. The basal contact of the Catahoula Tuff or Sandstone is marked by coarse-grained sand and conglomerate cemented by tuffaceous and siliceous clays. The Catahoula Tuff or Sandstone is distinguished from other formations by the preponderance of volcanic tuffs, opaline cement, glass, irregular bedding, polished sand grains, absence of carbonate cements, and absence of fossils (Sellards and others, 1932).

Both the Frio Formation and the Catahoula Tuff or Sandstone crop out in the western portion of Starr and Jim Hogg counties in a north-south trending band. Outcrops of the Frio and the Catahoula formations widen to about 8 to 10 miles and the thickness increases to about 800 to 1,000 feet in South Texas. The Frio Formation contains characteristic greenish-gray, massive clay. In South Texas, tuff beds of the Catahoula Tuff or Sandstone rest unconformably upon the greenish-gray, nontuffaceous clays of the Frio Formation (Sellards and others, 1932).

System	Series	Stratigraphic Units		Groundwater Sources	Hydrostratigraphy
				Baker and Dale (1961)	Baker (1979)
Quaternary	Holocene	Alluvium		Lower Rio Grande Groundwater Reservoir	Chicot Aquifer
	Pleistocene	Beaumont Clay		*Mercedes-Sebastian Groundwater Reservoir	
		Lissie Formation	Montgomery Formation	*Linn-Faysville Groundwater Reservoir	
			Bentley Formation		
Willis Sand					
Tertiary	Pliocene	Goliad Sand		*Linn-Faysville Groundwater Reservoir	Evangeline Aquifer
	Miocene	Fleming Formation/ Lagarto Clay			Burkeville Confining System
		Oakville Sandstone		Oakville Sandstone	
		Oligocene	1 Catahoula tuff or sandstone		2 Upper part of Catahoula tuff
			2 Anahuac Formation		
			2 Frio Formation		
1 Frio Clay	2 Vicksburg Group equivalent				

Gulf Coast Aquifer

1 = outcrop
2 = subsurface
* includes the Lower Rio Grande Groundwater Reservoir

Figure 3-8. Stratigraphic and hydrostratigraphic classification of the Gulf Coast Aquifer in South Texas (after Baker and Dale, 1961, and Baker, 1979).

The Anahuac Formation is one of the most discernible formations in the subsurface because it contains a rich assemblage of marine microfauna. The updip limit of the marine facies of the Anahuac Formation ranges from about 2,500 feet below land surface in East Texas to about 4,000 feet in South Texas (Baker, 1979). The Anahuac Formation is shaley from San Patricio County to the Sabine River in contrast to its sandy nature in South Texas (Baker, 1979).

The Oakville Sandstone crops out in a belt 8 miles wide from Grimes County to the southwest part of Lavaca County. The Oakville Sandstone is overlain by the Fleming Formation (Lagarto Clay and Fleming Formation are equivalent designations with the former nomenclature being abandoned [Solis, 1981]) and is underlain by the Catahoula Tuff or Sandstone. The basal portion of the Oakville Sandstone hosts a conglomerate bed containing Cretaceous fossils and pebbles (Sellards and others, 1932). The Oakville Sandstone is composed of thick sand sheets characterized by lenticular cross-bedded sand beds, shells, and bone-bearing clay beds (Sellards and others, 1932). To the south in the Lower Rio Grande Valley, the Oakville Sandstone pinches out in the subsurface in western Starr and Jim Hogg counties (Baker, 1979).

The Fleming Formation overlies the Oakville Sandstone and is in turn overlain by the Goliad and the Willis sands (Solis, 1981). The Fleming Formation is separated from the underlying Oakville Sandstone by higher clay content and thinner, less massive sand beds (Baker and Dale, 1961). The strata of the Fleming Formation often contain yellow and green clays, chalky limestone, and ferruginous nodules (Sellards and others, 1932). In parts of South Texas, the Fleming Formation is covered by caliche crusts at or near the ground surface (Solis, 1981).

The Goliad Sand crops out in a northeast-southwest band from Lavaca County to as far south as Starr and Hidalgo counties. The Goliad Sand, which covers a belt about 15 miles wide in the north, is a coarse fluvial deposit consisting of multilateral lenticular sand bodies (McCoy, 1990). The basal strata are coarse-grained with cobbles and gravel and have the irregular bedding of river-bottom deposits. These strata show a fining-upward sequence indicating sediment accumulation on flood plains (Sellards and others, 1932).

In Starr and Hidalgo counties to the south, the Goliad Sand extends over 60 miles. In many outcrops—particularly south of McAllen and in Reynosa, Mexico—sand and gravel within the Goliad Sand are cemented by caliche. Some areas contain more than 30 percent calcium carbonate, giving the caliche a whitish or pinkish-gray color. In places, the Goliad Sand has so many chert grains that it takes on a salt-and-pepper appearance (Sellards and others, 1932). The Goliad Sand has been eroded into ridges, valleys, and cuestas and is indurated enough in some places to be used as building stones (Sellards and others, 1932).

The Willis Sand was used to describe a sequence of unfossiliferous and gravelly sands overlying the Fleming sediments in southeast Texas (Doering, 1935; Solis, 1981). Plummer (1933) described these sediments as reddish, coarse, and gravelly sands and subordinate clays that grade into the Goliad Formation in the southwest of the Gulf Coast (Doering, 1935). In the Rio Grande region, the Willis Sand has not been identified (Weeks, 1937).

The Lissie Formation is unconformably contained between the Goliad Sand and the overlying Beaumont Clay. The Lissie Formation crops out in a belt about 30 miles wide from the Sabine

River to the Rio Grande. The sediments of the Lissie Formation in the outcrop are partly continental deposits deposited on flood plains and partly delta sands, silts, and muds deposited at river mouths (Sellards and others, 1932). The Lissie Formation hosts flatter, gently undulating topography and has much lower-dipping beds than the Goliad Sand. Lissie sediments consist of reddish, orange, and gray fine- to coarse-grained, cross-bedded sands.

Over most of Brooks and Hidalgo counties to the south, the Lissie Formation is either eroded or covered by sand dunes. Thin slivers of the Lissie Formation crop out over a small area in southern Hidalgo and northern Willacy counties. The sands in the Lissie Formation are fine textured and contain relatively less conglomerates than the underlying Goliad Sand. Caliche beds often mark the base of the Lissie Formation (Price, 1934).

The Beaumont Clay is contained between the underlying Lissie Formation and overlying stream deposits and wind blown sands. It crops out from the Sabine River in the east to Kleberg County to the south. The Beaumont Clay is made up of poorly bedded clay and marl interbedded with lenses of sand in the north (Sellards and others, 1932). In the Lower Rio Grande Valley, the Beaumont Clay forms a thin mantle that extends from Rio Grande City in Starr County eastward into Hidalgo County (Weeks, 1937). In Starr and western Hidalgo counties, the Beaumont Clay is sandy but is composed of reddish-brown clay and some sand beds farther east (Weeks, 1937).

The Quaternary Alluvium consists of gravel, sand, silt, and clay and underlies most of the Rio Grande delta, with the thickest sections occurring adjacent to the present course of the Rio Grande (Rose, 1954). Wind blown sand dunes and sand sheets composed of clay, sand, and silt with dense live oak mottes (small stands of trees) and scrubs occur in most of the northern and western part of the study area.

4.0 Previous work

Several state and federal agencies have conducted studies on the geology and hydrogeology of the Gulf Coast Aquifer (for example, Wood and Gabrysch, 1965; Jorgensen, 1975; Baker and Wall, 1976; Baker, 1979; Meyer and Carr, 1979; Carr and others, 1985; Groschen, 1985; Baker, 1986; Ryder, 1988; Dutton and Richter, 1990; McCoy, 1990; Hay, 1999; Harden and Associates, 2002). Most of these studies involved characterizing the hydrogeology of the aquifers in support of groundwater model development with emphasis on major pumping centers in the Houston area. Other researchers have presented information on groundwater resources, stratigraphy, and water quality (for example, Rose, 1954; Preston, 1983; Baker, 1986; McCoy, 1990).

Modeling efforts in the Gulf Coast Aquifer of Texas have evolved from the construction of a very simplistic electric-analog model covering a small area to more complex numerical models covering large areas and multiple aquifers (for example, Wood and Gabrysch, 1965; Jorgensen, 1975; Meyer and Carr, 1979). Five groundwater flow models have been constructed for the Gulf Coast Aquifer that also include parts of the Lower Rio Grande Valley (Carr and others, 1985; Groschen, 1985; Ryder, 1988; Hay, 1999; Harden and Associates, 2002).

Carr and others (1985) constructed and calibrated a numerical groundwater flow model of the Chicot and Evangeline aquifers extending from the Texas-Louisiana border to the northern half

of Jim Hogg, Brooks, and Kenedy counties. This model had four layers that incorporated hydraulic properties of distinct horizons of clay and sand beds of the Chicot and the Evangeline aquifers. Carr and others (1985) found that vertical leakage through clays into the Chicot Aquifer was significant in the Upper Gulf Coast Aquifer but decreased considerably in the southern portions of the Lower Rio Grande Valley. Transmissivity and unconfined storage were most sensitive to model calibration.

Groschen (1985) constructed a groundwater flow and solute transport model to assess saline water movement in the Evangeline Aquifer using projected pumping through 2020. The model covered an area of 4,680 square miles from San Patricio County in the north to the northern parts of Jim Hogg, Brooks, and Kenedy counties in the south. The model included the Chicot, Evangeline, and Jasper aquifers and the Burkeville Confining System; had 38 square grids with each cell 2 miles long; and used constant heads in the outcrop to simulate recharge. The model suggested that the saline water/fresh water interface would not be affected by increased pumping and that most of the salinity in the Evangeline Aquifer was due to leakage from the overlying Chicot Aquifer.

Ryder (1988) developed a three-dimensional, variable-density model covering the entire Texas Gulf Coast and parts of Louisiana and Mexico. He included all 14 geologic units contained within the Gulf Coast and Carrizo-Wilcox aquifers above the geo-pressured zone in the model to simulate flow under predevelopment conditions. Recharge was simulated using constant heads at the outcrop representing water levels in the top 100 feet of the aquifer. The model did a better job of matching the water levels in the outcrop than in the deeper parts of the aquifers. Ryder (1988) indicated that evapotranspiration by phreatophytes was the main mechanism of groundwater discharge in the Gulf Coast.

Hay (1999) developed a three-dimensional, steady-state model for Region N as part of regional water planning in Texas. This model included the Chicot, Evangeline, and Jasper aquifers and the Burkeville Confining System. Constant heads were assigned in the outcrop to simulate recharge into the aquifers.

Harden and Associates (2002) developed a model covering an area of about 90 miles by 60 miles to evaluate water availability and drawdown in the Rio Grande alluvium near Brownsville. Rather than using actual structure surfaces for the model layers, the model used average thickness of the Rio Grande alluvium and included four layers based on levels of groundwater production (surface zone, primary zone, separation zone, and secondary zone).

The five models mentioned above are not ideal for regional water planning in the Lower Rio Grande Valley. The Carr and others (1985) model extends only to the northern part of the Lower Rio Grande Valley. The Groschen (1985) model is a cross-sectional representation of the flow system that does not properly simulate the three-dimensional effect of pumping. This model also covers only small areas in the northern parts of the Lower Rio Grande Valley. Although the Ryder (1988) model covers the entire Lower Rio Grande Valley, it is a super-regional model with a large grid size (5 miles by 5 miles) and simulates groundwater flow only for predevelopment conditions. The Hay (1999) model does not include large areas of Hidalgo and Starr counties and excludes all of Cameron and Willacy counties. The Harden and Associates

(2002) model only covers a small area near Brownsville and includes only the alluvium of the Chicot Aquifer.

5.0 Hydrogeologic setting

The hydrogeologic setting describes the aquifer geometry, hydrologic boundaries, and the hydraulic and storage properties that determine groundwater flow and fluxes in the aquifer. We based the hydrogeologic setting for the aquifers on previous investigations (Baker, 1979; Meyer and Carr, 1979; Carr and others, 1985; Ryder, 1988) and additional information that we collected in support of the modeling effort. The additional information included (1) examining geophysical logs to identify formation contacts in areas where information was unavailable, (2) using geology to develop a structure map, (3) developing water level maps for each aquifer and hydrographs for selected wells, (4) estimating recharge rates, (5) estimating evapotranspiration, (6) compiling hydraulic conductivity and storage parameters from pumping and specific-capacity tests, and (7) assembling pumping information.

5.1 Hydrostratigraphy

There are several different interpretations of the hydrostratigraphy of the Gulf Coast Aquifer. Baker and Dale (1961) divided major sources of groundwater in the Lower Rio Grande Valley into four types based on stratigraphic position, geographic location, lateral continuity, well yield, and water quality: (1) the Oakville Sandstone in northeast Starr and northwest Hidalgo counties, (2) the Linn-Faysville Groundwater Reservoir in central Hidalgo County, (3) the Lower Rio Grande Groundwater Reservoir along the Rio Grande in southern Hidalgo and parts of southern Cameron counties, and (4) the Mercedes-Sebastian Groundwater Reservoir in western Cameron County. Although this classification scheme is locally useful, it is not widely applicable because (1) it has a limited areal extent; (2) parts of the different formations were grouped together, and the entire formation was not considered; (3) identical groundwater reservoirs occur at different stratigraphic positions; and (4) overlaps occur between water quality and source areas.

Baker (1979) divided the Gulf Coast Aquifer in South Texas into five hydrostratigraphic units: (1) the Catahoula Confining System, (2) the Jasper Aquifer, (3) the Burkeville Confining System, (4) the Evangeline Aquifer, and (5) the Chicot Aquifer. This hydrostratigraphic classification scheme roughly coincides with Ryder's (1988) five permeable zones borrowed from type sections in Louisiana that, from oldest to youngest, include (1) the Middle-Miocene permeable zone, (2) the Middle-Miocene confining unit, (3) the Lower Pliocene-upper Miocene permeable zone, (4) the Lower Pleistocene-upper Pliocene permeable zone, and (5) the Holocene-upper Pleistocene permeable zone. The permeable zones were designated based on the volumes of water that could be produced from each and the differences in the distribution of vertical hydraulic heads between these zones (Weiss and Williamson, 1985).

There are considerable differences in the stratigraphic placement of the Catahoula Confining System and the Jasper Aquifer in the literature. For example, Baker (1979) includes the Frio Formation, Anahuac Formation, and the upper part of the Catahoula Tuff as part of the Catahoula Confining System. He placed the Oakville Sandstone and the lower part of the

Fleming Formation in the Jasper Aquifer. In contrast, Ryder (1988) considered the Oakville Sandstone and the Fleming Formation parts of the Burkeville Confining System. He also considered the Middle-Miocene permeable zone and the Anahuac and Frio formations in the downdip areas of the basin as parts of the Jasper Aquifer.

For this study, we adopted Baker's (1979) hydrostratigraphy because it included (1) detailed faunal occurrences, lithology, and electric log signatures along with several cross sections across the study area; (2) hydraulic characteristics of the sediments; and (3) covered the entire southern Gulf Coast area (Figure 3-8).

The configuration of the Jasper Aquifer in the subsurface is geometrically irregular as the delineation was based on the aquifer being treated as a rock stratigraphic unit (Baker, 1979). The lower boundary of the aquifer coincides with the stratigraphic lower boundary of the Oakville or the Fleming formations, or it may be contained within or coincide with the base of the Catahoula Formation. The top of the aquifer lies locally within the Fleming Formation or coincides with the top of the Oakville Formation.

The Burkeville Confining System separates the Jasper and Evangeline aquifers. It is predominantly composed of silt and clay but may occasionally contain isolated sand lenses locally containing fresh water. It occurs as clayey sediments in the upper part of the Oakville Sandstone and the middle part of the Fleming Formation. Given the predominance of silt and clay in the Burkeville Confining System, it primarily acts as a confining unit (Ryder, 1988). The Burkeville Confining System pinches out in the subsurface in western Starr, Jim Hogg, and part of Duval counties.

The Evangeline Aquifer consists of the Goliad Sand and may include sections of sand and clay of the Fleming Formation. The aquifer is wedge shaped and contains mostly sand with individual sand beds that are tens of feet thick. The Evangeline Aquifer is underlain by the Burkeville Confining System downdip but directly overlies the Jasper Aquifer updip where the Burkeville Confining System has pinched out.

The Chicot Aquifer includes the Montgomery Formation, Lissie Formation, Beaumont Formation, and the overlying alluvial/sand plain deposits, including the Rio Grande Alluvium. The Pleistocene/Upper Pliocene forms the base of the Chicot Aquifer. The Chicot Aquifer consists of discontinuous sand and clay beds of nearly equal thickness for most of the coastal areas. Carr and others (1985) subdivided the Chicot Aquifer into lower and upper units in the Houston area based on differences in water levels. In Galveston and southeast Harris counties, the basal part of the Chicot Aquifer holds a massive sandstone (Alta Loma Sands) with high permeability (Carr and others, 1985). We could not identify this basal unit in any of the electric logs we examined in the Lower Rio Grande Valley. Although the Chicot Aquifer generally has a higher sand-clay ratio than the underlying Evangeline Aquifer (McCoy, 1990), the two aquifers are difficult to distinguish from each other using geophysical logs.

In central Hidalgo County, the upper part of the Goliad Sand and the lower part of the Lissie Formation consist of interbedded layers of sand and clay with some caliche and form an important source of groundwater for irrigation (Baker and Dale, 1961). Farther south near the

Rio Grande, in southeastern Starr, southern Hidalgo, and western Cameron counties, the water-bearing sediments of the Goliad Sand, Lissie Formation, Beaumont Formation, and the alluvium, though locally separated by clay layers, are hydraulically connected and acts as a hydraulic unit (Baker and Dale, 1961).

The Beaumont Formation also hosts considerable groundwater in central Hidalgo, Willacy, and northern Cameron counties (Baker and Dale, 1961). These permeable deposits probably represent a relict channel of the former course of the Rio Grande.

The Rio Grande Alluvium consists of gravel, sand, silt, and clay that underlie most of the Rio Grande delta (Rose, 1954). Thickness of the deposit ranges from 50 to 300 feet with the thickest sections occurring adjacent to the present course of the Rio Grande. In the lower part of the alluvium, a zone of water-bearing material extends from the vicinity of Rio Grande City to Brownsville. The extent of the aquifer can also be defined by a string of irrigation wells that were installed around the fringes of the aquifer. The permeable zones in the alluvium are in hydraulic connection with the adjacent and underlying beds of the Goliad Sand, Lissie Formation, and Beaumont Formation (Baker and Dale, 1961).

5.2 Structure

The major structural elements in the area include the Rio Grande and Houston embayments that act as sediment sources for the Gulf Coast (Figure 5-1). The Balcones Fault Zone and the Pearsall-Luling-Mexia fault zones rim the basin in the west and the north and form a divide between Upper Cretaceous and Eocene strata (McCoy, 1990). Most of the regional structures, embayments, arches, and flexures were created from a combination of differential subsidence of the basement floor and thick sediment piles flowing as viscous fluids on sloping surfaces (Bornhauser, 1958). Others suggest that deep-seated vertical intrusions of salt in the form of narrow ridges pushed up the gulfward dipping beds to form deep-seated anticlines (Quarles, 1952; Cloos, 1962). Growth faults that are common in the Tertiary strata of the Gulf Coast consist of deformed zones a few feet to tens of feet thick containing sheared sediments (Berg, 1995). The sheared fault zones can act as a seal or conduit to fluid flow, thereby reducing the drainage areas into smaller hydraulic compartments (Berg, 1986). All regional and local structures in the Texas Gulf Coast were developed by shallow tectonics in rapidly subsiding basins that led to sediment burial to considerable depths (Bornhauser, 1958) while still preserving most of the initial porosity. If the sediments were affected by deeper tectonic events, a higher temperature associated with metamorphic processes would have destroyed most of the transmissive capacities of the sandstone.

The post-Eocene Texas Gulf Coastal Plain forms a relatively flat surface that dips gradually toward the gulf. The older formations dip more steeply than the younger units. Locally, the occurrence of salt domes, faults, and folds may cause reversals of regional dip and thickening or thinning of the formations (Carr and others, 1985). However, the salt domes only locally pierce the Chicot or Evangeline aquifers in the northern part of the Gulf Coast (Carr and others, 1985). In addition to the regional dip and thickening of the units toward the east, a major fault (Sam Fordyce-Vanderbilt) and an associated anticlinal fold occur in eastern Starr County. However, this fault does not impede groundwater flow in the area (Baker and Dale, 1961).

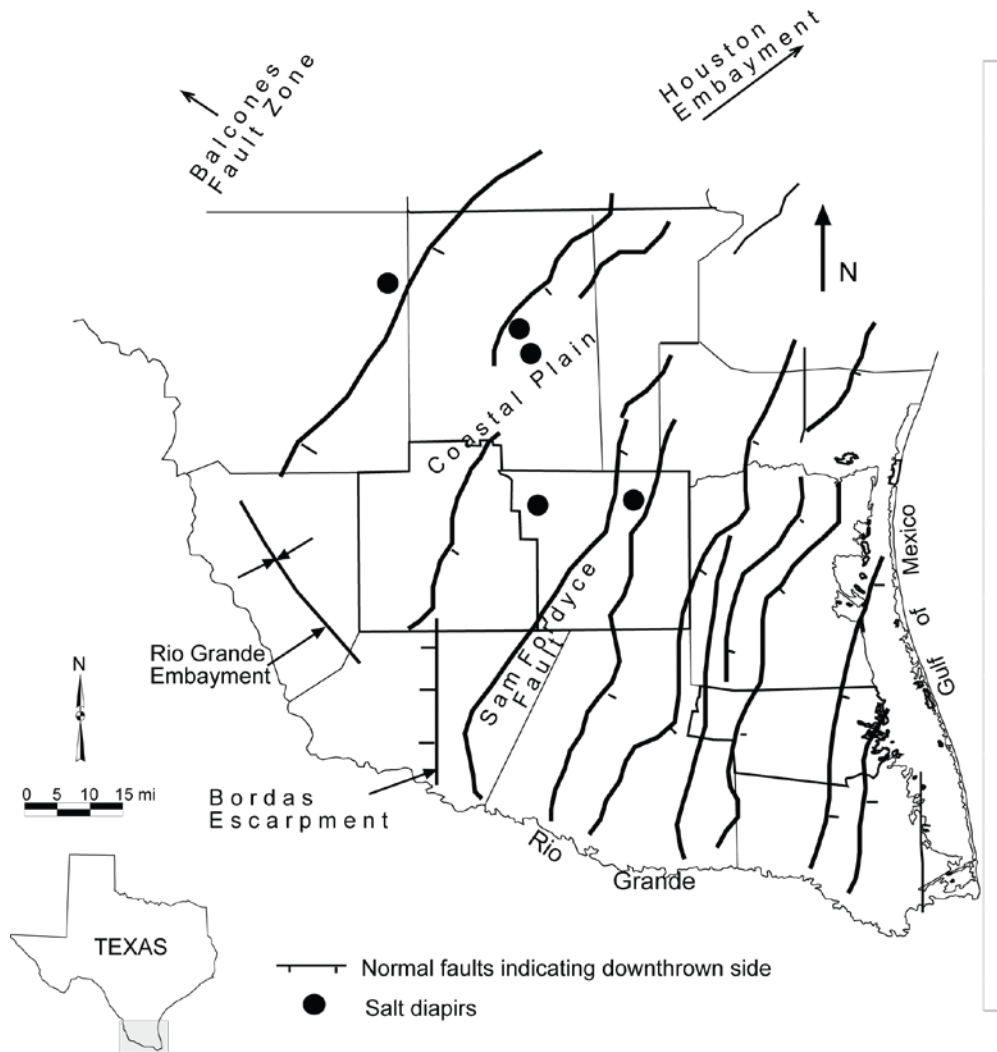


Figure 5-1. General structural setting of the study area. (Normal faults after Bureau of Economic Geology, 1997; Bordas Escarpment and the Rio Grande Embayment after McCoy, 1990; and San Fordyce fault after Baker and Dale, 1961; mi = miles).

TWDB used structural information from the U.S. Geological Survey (Strom and others, 2003) to develop the structural elevation maps for the base of the Chicot and Evangeline aquifers (Figures 5-2 and 5-3). We used additional resistivity and spontaneous potential logs to determine formation contacts for the Burkeville Confining System and the Jasper Aquifer where U.S. Geological Survey data were unavailable. We then developed a structure grid by combining these two data sets with outcrop data (Figures 5-4 and 5-5). Control points used in developing structural surfaces include both outcrop points and well information (Figure 5-6). We collected all well logs from the Surface Casing Unit of the Texas Commission on Environmental Quality (Figure 5-7).

Geophysical logs are essential in delineating formation contacts for sediments deposited in a deltaic setting characterized by cyclic sedimentation (Selley, 1970). These logs are useful in correlating lithologic units from one well to another and in interpreting grain size profiles, permeability, and quality of water in water-bearing units (Baker and Dale, 1961). Spontaneous potential logs detect the differences in electrical potential between the formation water and the drilling mud. Deflection of a spontaneous potential log to the left (lower potential) indicates presence of sandy layers (sand line) and to the right (higher potential) clay layers (shale line). Deflection amplitude is small when the differences between the drilling mud and the formation water are small. The larger the deflection is toward the left, the more likely that there are more dissolved solids in the formation water.

Resistivity logs measure salinity and continuity of the formation waters. Resistivity is lowest in such units as clean sandstone and vuggy dolomite and highest in impermeable rocks such as clays and tight carbonates. The short normal curve reflects the resistivity of the drilling fluid and aquifer materials at short distances from the borehole wall. The long normal curve indicates apparent resistivity at a greater distance from the borehole wall. In sand zones, if the long normal curve is lower than the short normal curve, then highly saline water is suspected. Fresh water is inferred if the reverse succession is detected (Baker and Dale, 1961).

We closely matched the geophysical logs with the type logs (Baker, 1979) for locating the aquifer contacts. All contacts were determined based on the spontaneous potential, resistivity, and conductivity curves where available. The key information initially established for each log was the borehole location in latitude and longitude, elevation of the ground surface, drill floor elevation, and kelly bushing elevation where all down-hole measurements originate. Maximum kelly bushing elevation is about 25 feet above the ground surface in South Texas and about 40 to 50 feet above the ground surface in Laguna Madre near the coastline.

We included all units above the top of the Goliad Sand in the Chicot Aquifer. We also included the units containing the Goliad Sand and the sandy sections of the Fleming Formation overlying the Burkeville Confining System in the Evangeline Aquifer (Baker, 1979). The contact between the Chicot and Evangeline aquifers in the outcrop generally lies at the base of the primary clay. In the thicker downdip sections, a more prolific sand-clay section underlying a mostly clay section was used as the marker between the Chicot and Evangeline aquifers. Stratigraphically, this contact represents the boundary between the base of the Pleistocene and the top of the Pliocene.

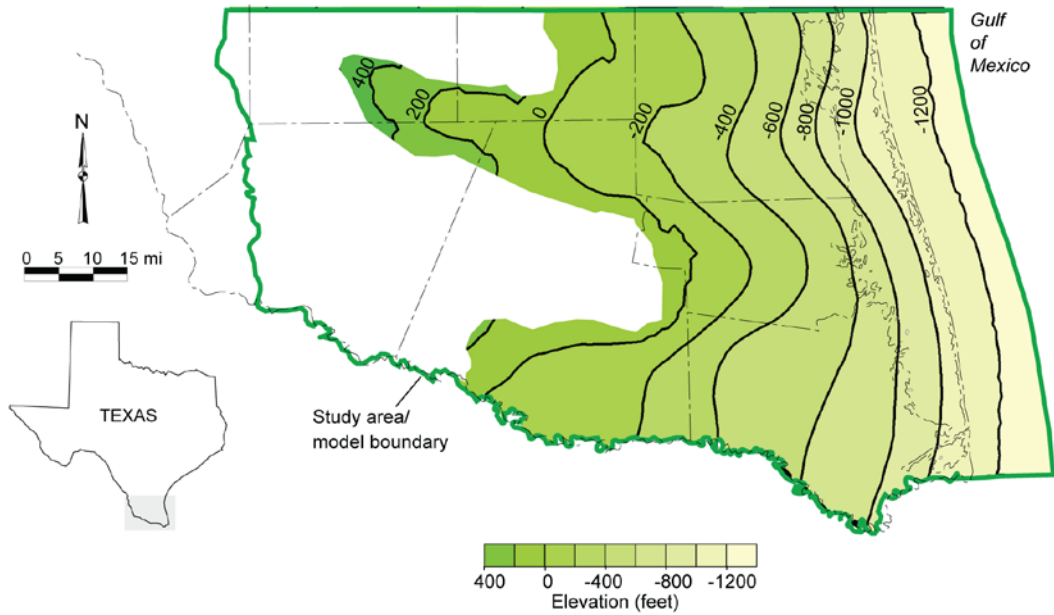


Figure 5-2. Elevation of the base of the Chicot Aquifer (data from Strom and others, 2003; mi = miles)

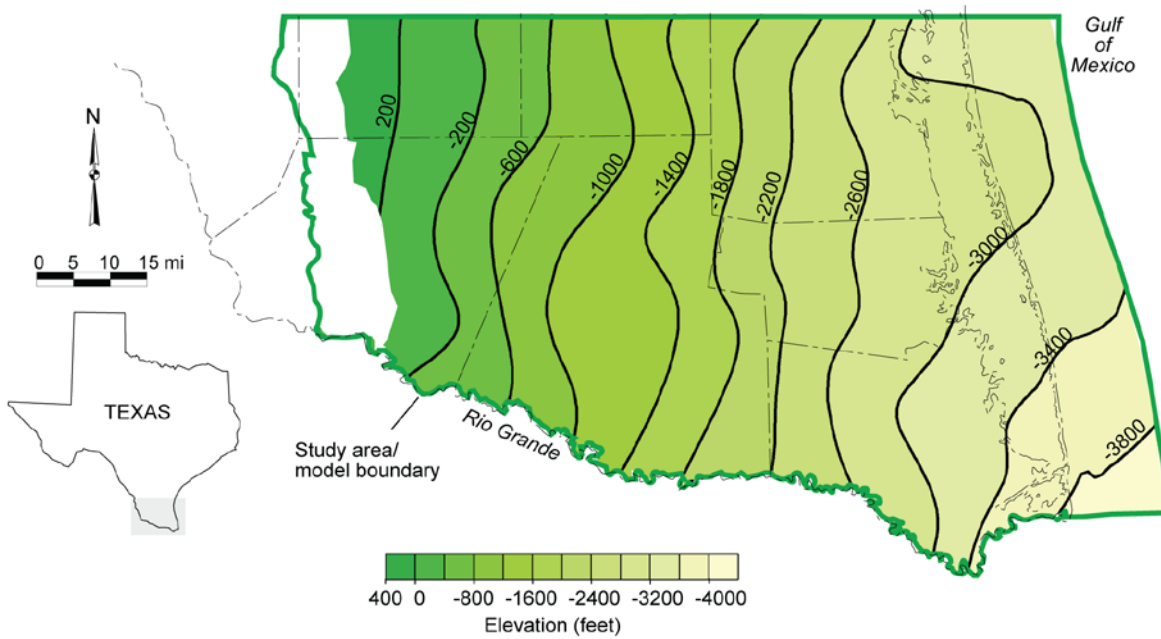


Figure 5-3. Elevation of the base of the Evangeline Aquifer (data from Strom and others, 2003; mi = miles).

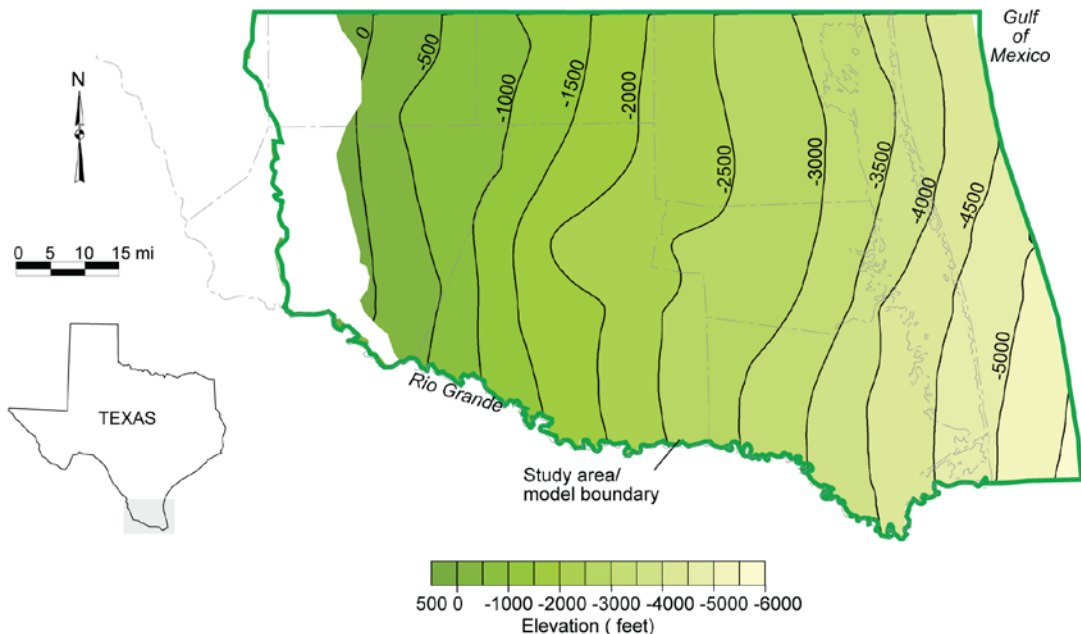


Figure 5-4. Elevation of the Burkeville Confining System (data from Strom and others, 2003; mi = miles).

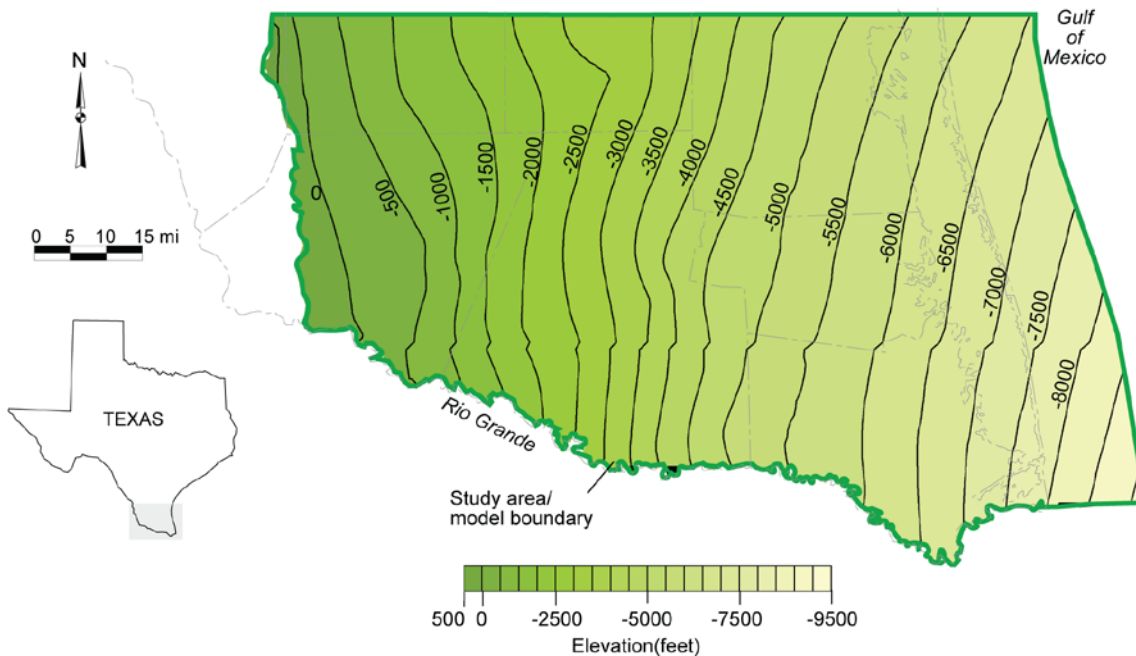


Figure 5-5. Elevation of the base of the Jasper Aquifer. Note that the sands in the outcrop sections of the Catahoula Formation have been included in the Jasper Aquifer (data from Strom and others, 2003; mi = miles).

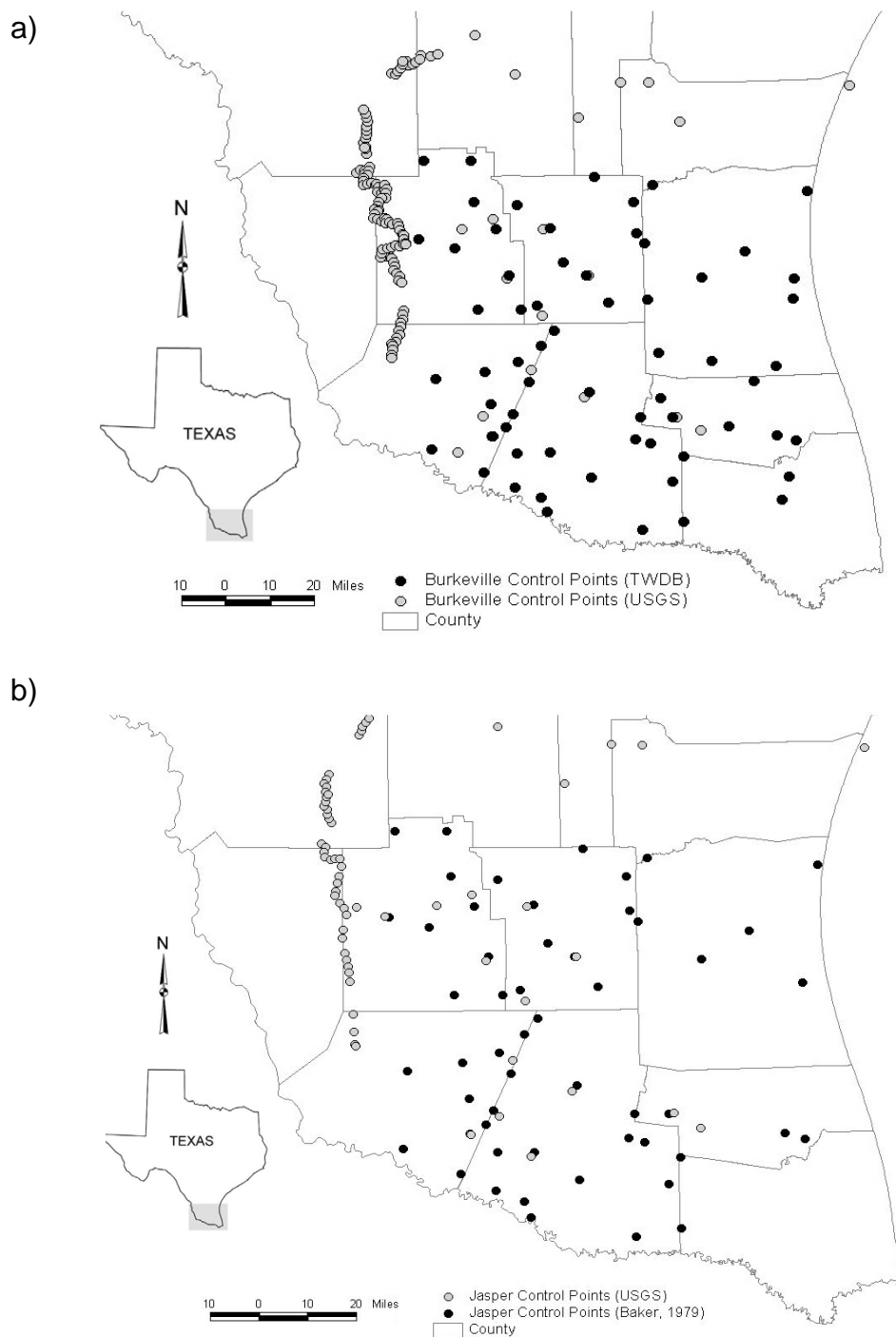


Figure 5-6. Locations of control points in the (a) Burkeville Confining System and (b) the Jasper Aquifer. Structure bases for the Chicot and the Evangeline aquifers were drawn from the U.S. Geological Survey structure compiled for the entire Gulf Coast Aquifer (data from Strom and others, 2003).

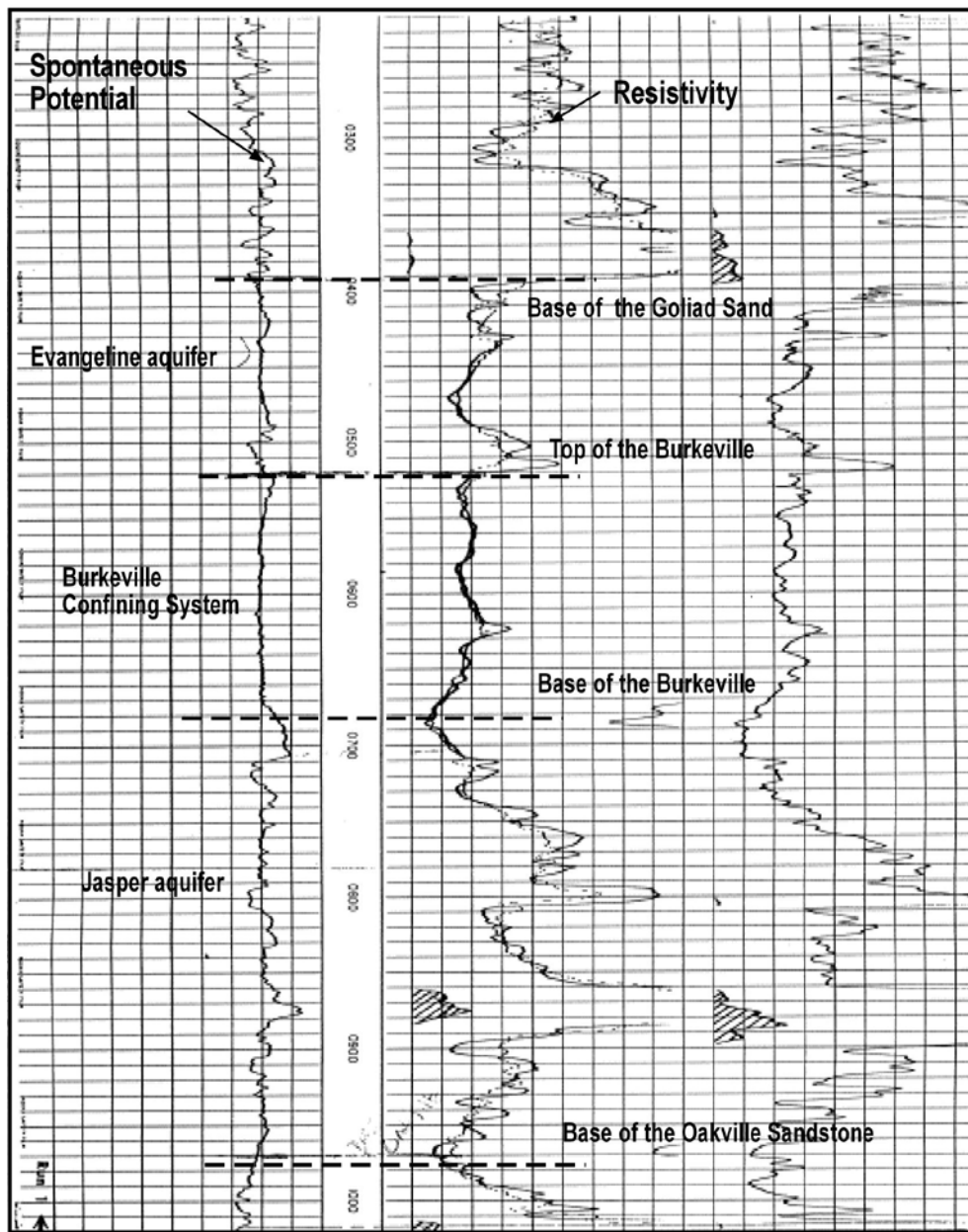


Figure 5-7. A typical geophysical log used to identify and delineate contacts between the different geological formations.

There was rarely any difference in electric log signatures between the Upper Fleming Formation and the basal Goliad Sand except for a slight increase in the sand/shale ratio. The base of the Evangeline Aquifer is the top of the Burkeville Confining System. This interface is the top of the Miocene, although the Burkeville Confining System is actually shown within the Fleming Formation (Baker, 1979).

The Burkeville Confining System is a relatively continuous stratigraphic unit. The top of the Burkeville Confining System is generally seen as the beginning of a highly clayey section, which is in sharp contrast to the overlying sandy-clay section of the Fleming and Goliad formations. Likewise, the base of the Burkeville Confining System is characterized by the reappearance of a sandy-clay section that marks the top of the Jasper Aquifer.

We defined the bottom of the Jasper Aquifer at the base of the Oakville Sandstone, where a significant decrease in the sand content and a prominent increase in the shale content were observed. The underlying Catahoula Tuff or Sandstone has a log signature dominated by a strong shale line and low resistivity, making it easy to identify. Baker (1979) included the sands in the outcrop areas of the Catahoula Tuff or Sandstone with the Jasper Aquifer and drew the bottom of the Jasper Aquifer at the base of the Oakville Sandstone in the downdip areas. We followed the same approach as Baker (1979) and included the Catahoula Tuff or Sandstone in the outcrop within the Jasper Aquifer.

We supplemented the formation picks obtained from well logs with land-surface elevations where each of the formations was extrapolated to meet the outcrop points. We adapted the locations of the formation contacts from the Geologic Atlas of Texas plates as digitized by Texas A&M University, Corpus Christi. We then intersected the locations with the U.S. Geological Survey digital elevation model to generate outcrop points in ArcView. These outcrop points were added to the structural elevations for the Jasper, Evangeline, and Chicot aquifers and the Burkeville Confining System to produce final structural surfaces for the model layers.

All basal surfaces of the Chicot, Evangeline, and Jasper aquifers and the Burkeville Confining System show sediment deposition on slopes steeply dipping toward the Gulf. Dip of the beds is nearly perpendicular to the coastline. Slopes of the aquifer bases are highly variable, with abrupt changes observed between nearby wells. The deeper aquifers generally have a base with higher slopes than the shallower aquifers. Given the structural history of the Gulf Coast, we presume that the steep slopes of the aquifers were probably caused by a combination of growth faulting and deep-seated movements of salt domes. The Burkeville Confining System and the Jasper Aquifer host irregular bottoms that locally thicken to develop sediment wedges. Near the coastline, the bottom of the Chicot Aquifer occurs at an elevation of -1,200 feet, the bottom of the Evangeline Aquifer at an elevation of -2,600 feet, the bottom of the Burkeville Confining System at an elevation of -5,000 feet, and the bottom of the Jasper Aquifer at an elevation of -8,000 feet.

Sediment thickness increases from west to east toward the Gulf of Mexico. Thickness maps for the aquifers and the confining unit indicate a maximum sediment thickness of up to 1,200 feet for the Chicot Aquifer, 2,800 feet for the Evangeline Aquifer, 1,600 feet for the Burkeville Confining System, and 3,200 feet for the Jasper Aquifer (Figures 5-8, 5-9, 5-10, and 5-11). The aquifers and confining unit thicken downdip toward the Gulf of Mexico (Figure 5-12). However, the aquifers show less variation in thicknesses along the north-south direction (Baker, 1979), perhaps indicating that sediment source areas have not considerably changed during sediment deposition.

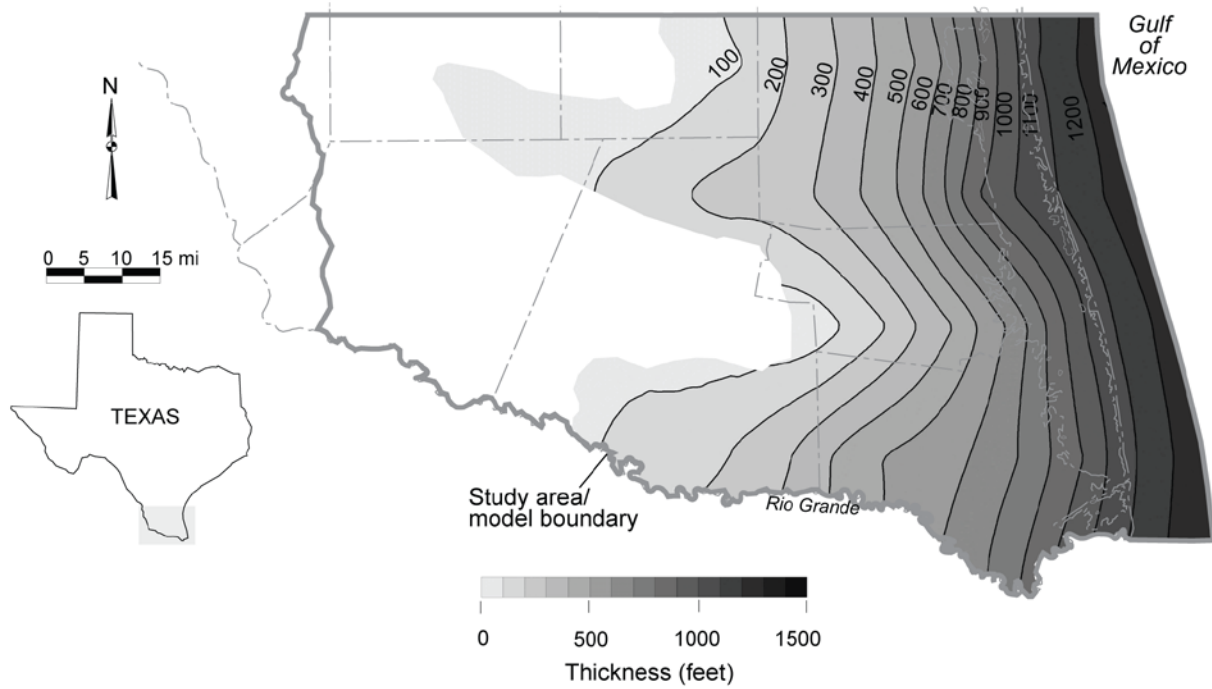


Figure 5-8. Thickness of the Chicot Aquifer (mi = miles).

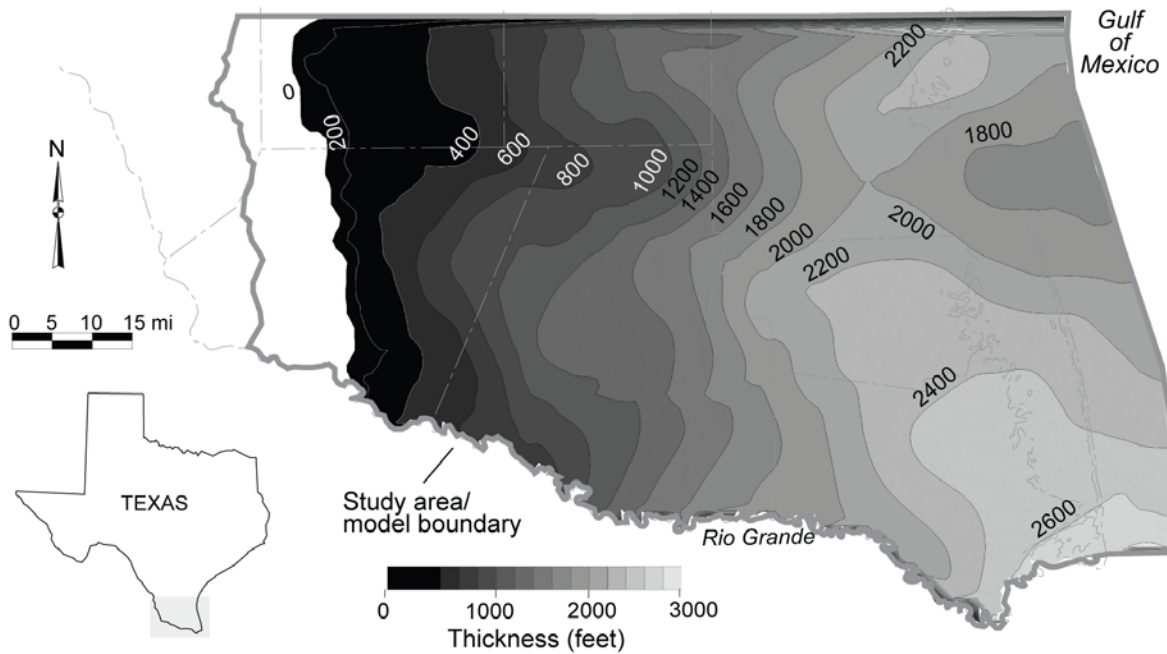


Figure 5-9. Thickness of the Evangeline Aquifer (mi = miles).

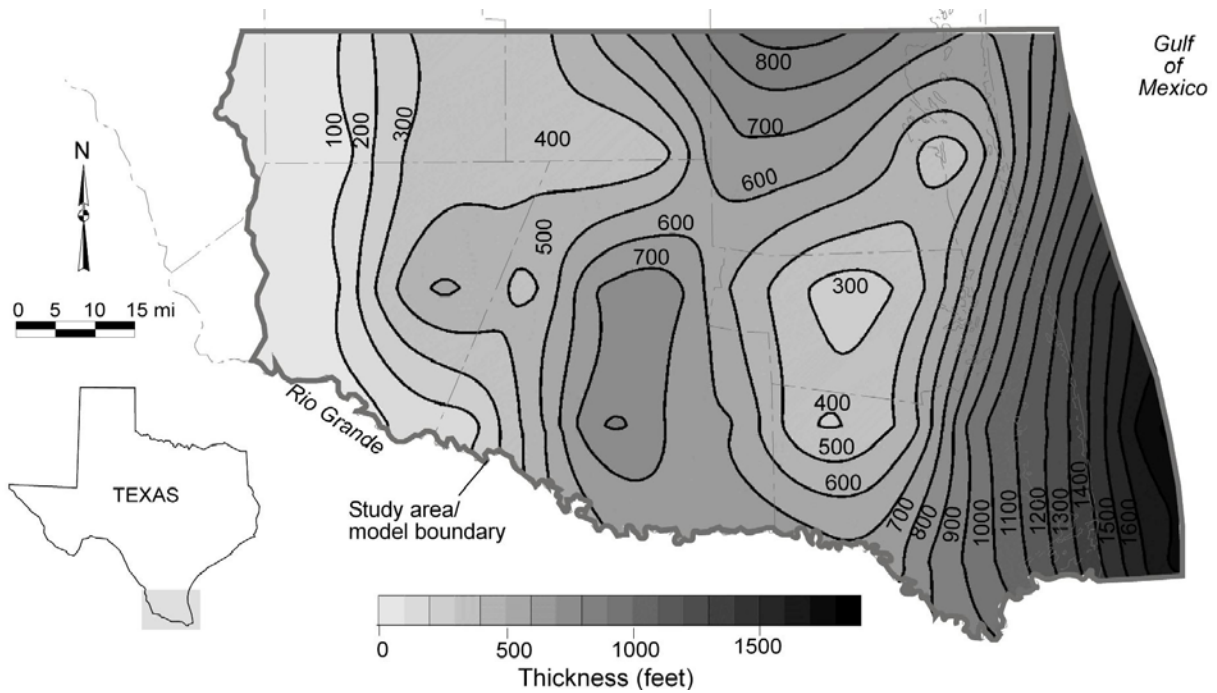


Figure 5-10. Thickness of the Burkeville Confining System (mi = miles).

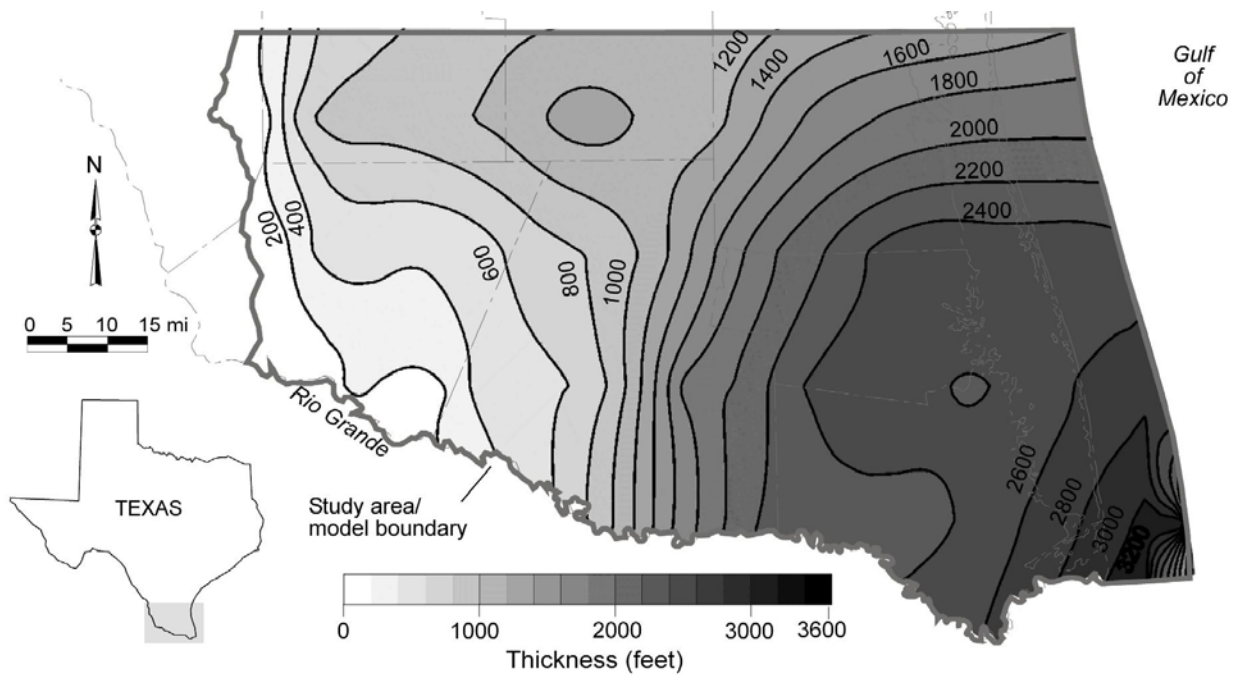


Figure 5-11. Thickness of the Jasper Aquifer (mi = miles).

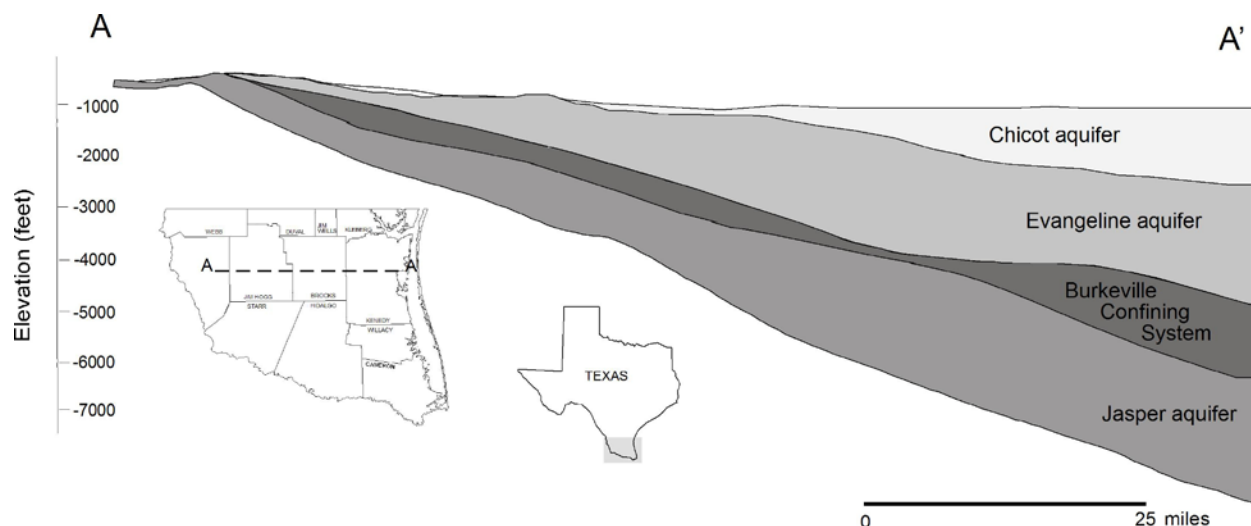


Figure 5-12. An east-west cross section showing geometry and stratigraphic distribution of the aquifers along A-A'.

5.3 Water levels and regional groundwater flow

Water levels in wells reflect the height of the groundwater above some datum such as mean sea level. Water level maps can be used to help determine groundwater flow directions based on the orientation of water level contours. In an unconfined aquifer, the water level is the upper surface of the groundwater—the water table—where its pressure is equal to atmospheric pressure. In confined aquifers, where the aquifer is overlain by material that is much less permeable, water in the aquifer has a higher pressure than the atmosphere; therefore, hydraulic head in the aquifer has a higher elevation than the upper elevation of the aquifer. Groundwater flows from higher water level elevations (high pressure or hydraulic head) to lower water level elevations (low pressure or hydraulic head). Groundwater moves when adequate hydraulic head is available to force water through the pore spaces of the aquifer materials. The hydraulic gradient and hydraulic conductivity determine how much water can flow through the aquifer.

We compiled water level measurements from TWDB's water well database and developed a generalized water level map for the Chicot and Evangeline aquifers representing conditions between 1930 and 1980. However, there was insufficient information for producing water level maps for the Burkeville Confining System and the Jasper Aquifer for this time period. We used the period from 1930 to 1980 because water levels were relatively uniform during this time (Figure 5-13). Using this 50-year time period also allowed us to maximize the number of water level measurements to create the map. Most of the wells completed in the Chicot Aquifer are located in the south close to or along the Rio Grande, closely matching areas where the Chicot Aquifer outcrops (Figure 5-14). Wells completed in the Evangeline Aquifer are mainly located in the west and north central areas of Starr and Hidalgo counties (Figures 5-15 and 5-16).

The water level surface in the study area generally follows the region's topography, with water level elevations being lower where ground-surface elevations are low and higher where the

ground surface elevations are higher in the west and the northwest. The maximum water level elevation (522 feet) occurs in the northwest part of Jim Hogg and Starr counties where the Bordas Escarpment arises. Water level elevations from the Bordas Escarpment (522 feet) sharply decrease toward central Hidalgo and Brooks counties (50 feet). Water level elevations then gradually decrease to nearly sea level in central Cameron, Willacy, and Kenedy counties. Depth to water in the Chicot Aquifer is 20 to 40 feet except in northern Brooks County where depth to water is 60 to 70 feet. Depth to water in the Evangeline Aquifer is up to 200 feet in Starr County but occurs at depths of 20 to 60 feet in the rest of the study area.

Water level maps of the Chicot Aquifer indicate that regional groundwater flow is from the west to the east toward the Gulf of Mexico (Figure 5-14). In southern Starr and southwestern Hidalgo counties, water flows toward and likely into the Rio Grande. Water level contours past central Hidalgo County become much broader near the coast. In southern Hidalgo County, water level contours bend upstream and downstream along different stretches of the Rio Grande, indicating streamflow gains and losses, respectively.

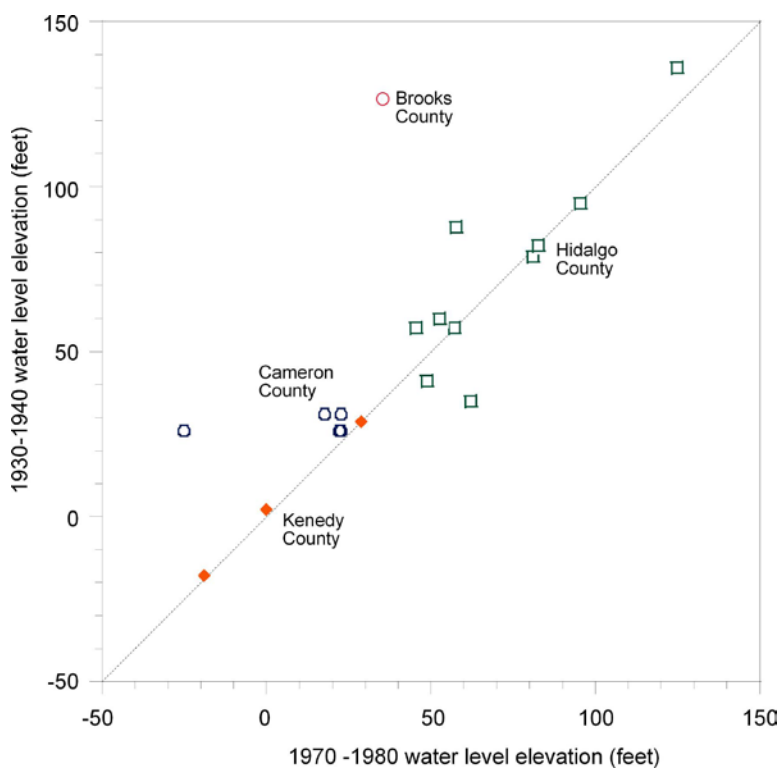


Figure 5-13. Comparison of water level elevations from wells in the study area for different time periods.

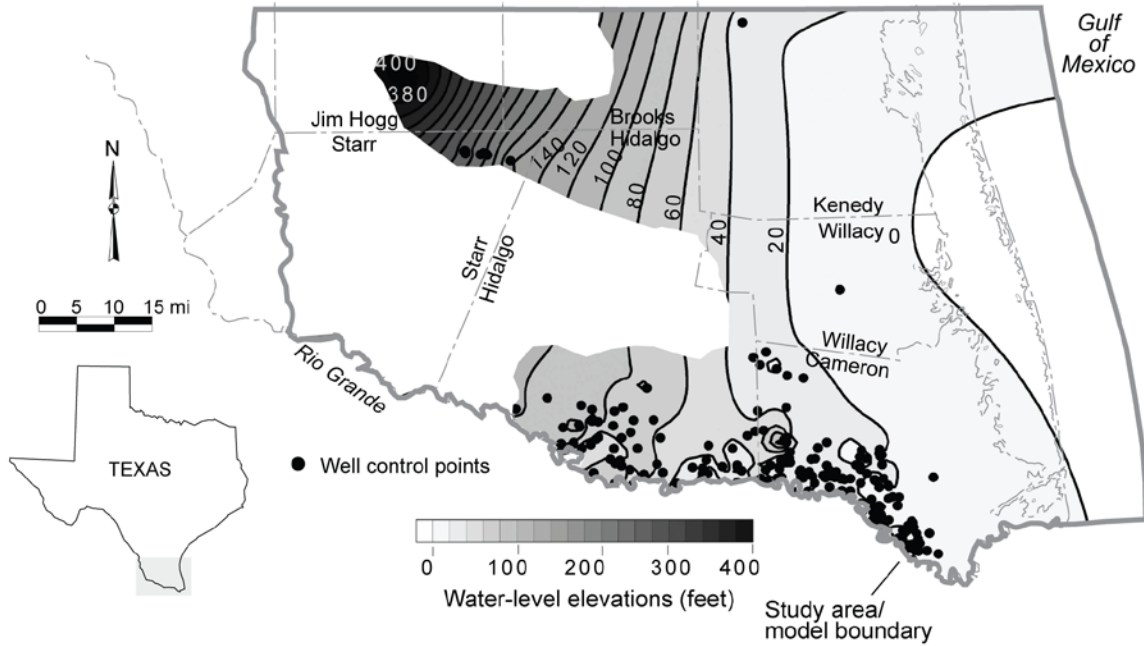


Figure 5-14. Water level elevations in the Chicot Aquifer (includes water level measurements from 1930 to 1980; mi = miles).

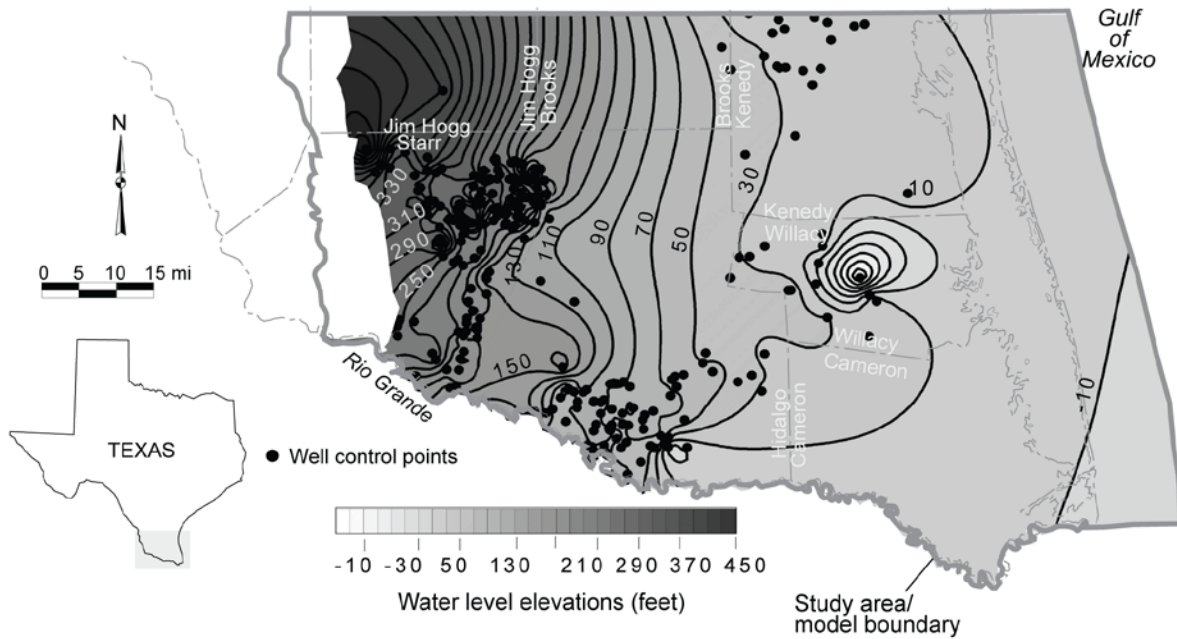


Figure 5-15. Water level elevations in the Evangeline Aquifer (includes water level measurements from 1930 to 1980; mi = miles).

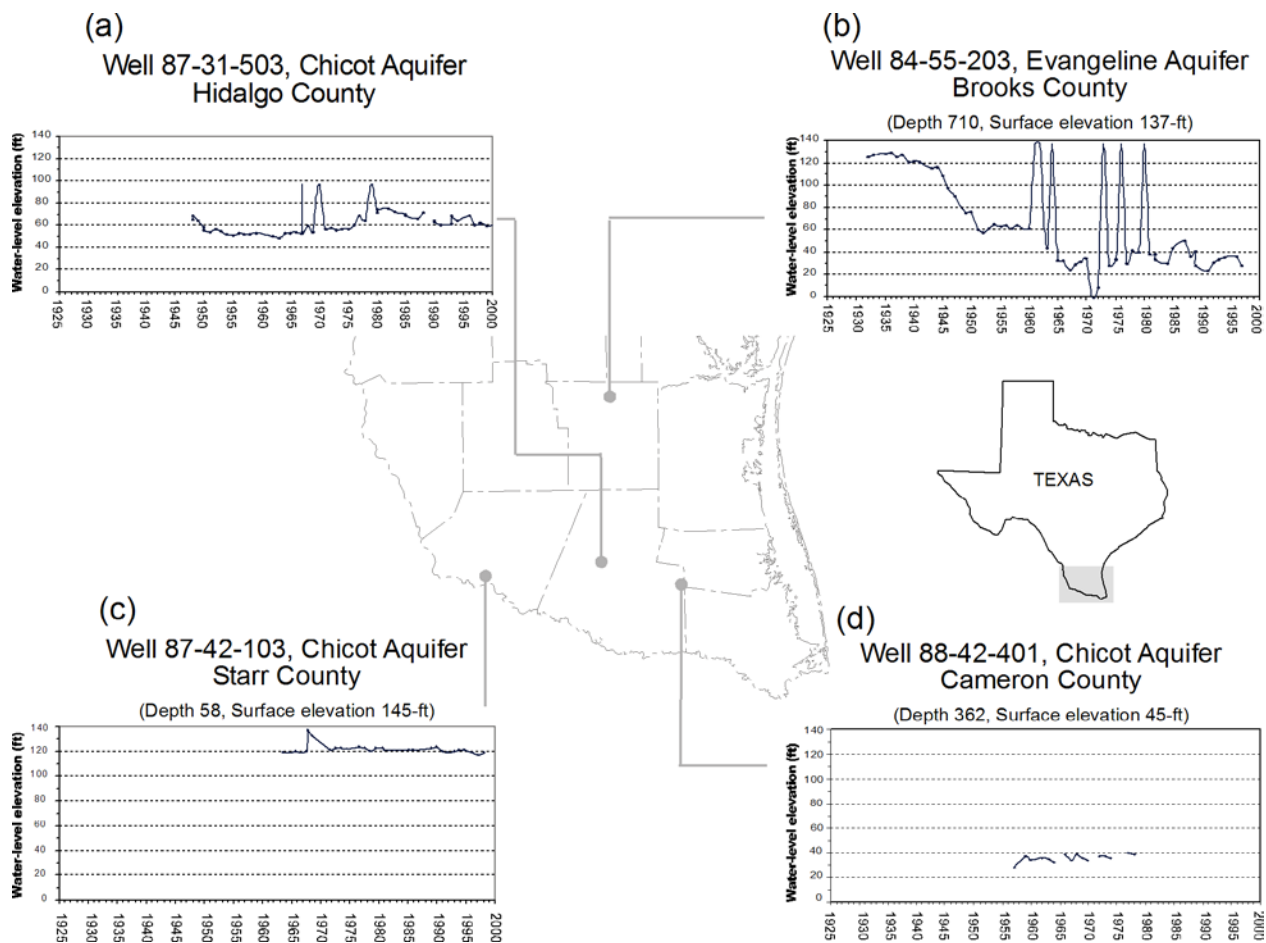


Figure 5-16. Hydrographs for wells (a) 87-31-601, (b) 88-02-403, (c) 88-34-101, and (d) 88-26-303 in the Chicot and Evangeline aquifers (mi = miles; ft = feet).

Water level maps of the Evangeline Aquifer also indicate regional groundwater flow from west to east toward the Gulf of Mexico (Figure 5-15). The hydraulic gradient is much steeper in Starr County and flattens considerably near the Starr-Hidalgo county line. The steeper gradient is probably due to a drop in the topographic elevations from the Bordas Escarpment toward the plain and the low-permeability sediments in the updip part of the aquifer that resist groundwater flow. In southwestern Hidalgo County, water levels show that groundwater is discharging to the Rio Grande.

Water levels in the Chicot and the Evangeline aquifers appear somewhat similar in values and spatial distribution except for Starr County where the values are higher in the Evangeline Aquifer (Figures 5-14 and 5-15). This similarity in water levels may indicate there is considerable hydraulic connection regionally between the two aquifers for most of the study area even though the aquifers have numerous clay lenses that may locally compartmentalize them. Water levels in the Chicot Aquifer and in the few wells completed in the alluvium are also similar.

Hydrographs show water level fluctuations in wells due to seasonal changes in recharge and groundwater pumping. Water levels generally increase during the winter and the spring months when most recharge to the aquifer occurs. Groundwater pumping lowers water levels in well hydrographs more than would otherwise occur naturally.

We examined several hydrographs from the study area, many of which show that water levels have remained relatively unchanged, with slight increases from 1970 to 1980 (Figures 5-16 and 5-17). This trend is more discernible over much of the model area where we have historical water level information from the 1930s to the 1980s (Figure 5-17). In parts of Brooks and Cameron counties, the water levels locally declined by 40 to 60 feet during the 1950s drought of record (Figure 5-16). These local water level declines were more common in the irrigated areas where there were larger concentrations of wells (Baker and Dale, 1961). However, Myers and Dale (1967) reported that water levels rapidly recover when the seasonal irrigation period was over.

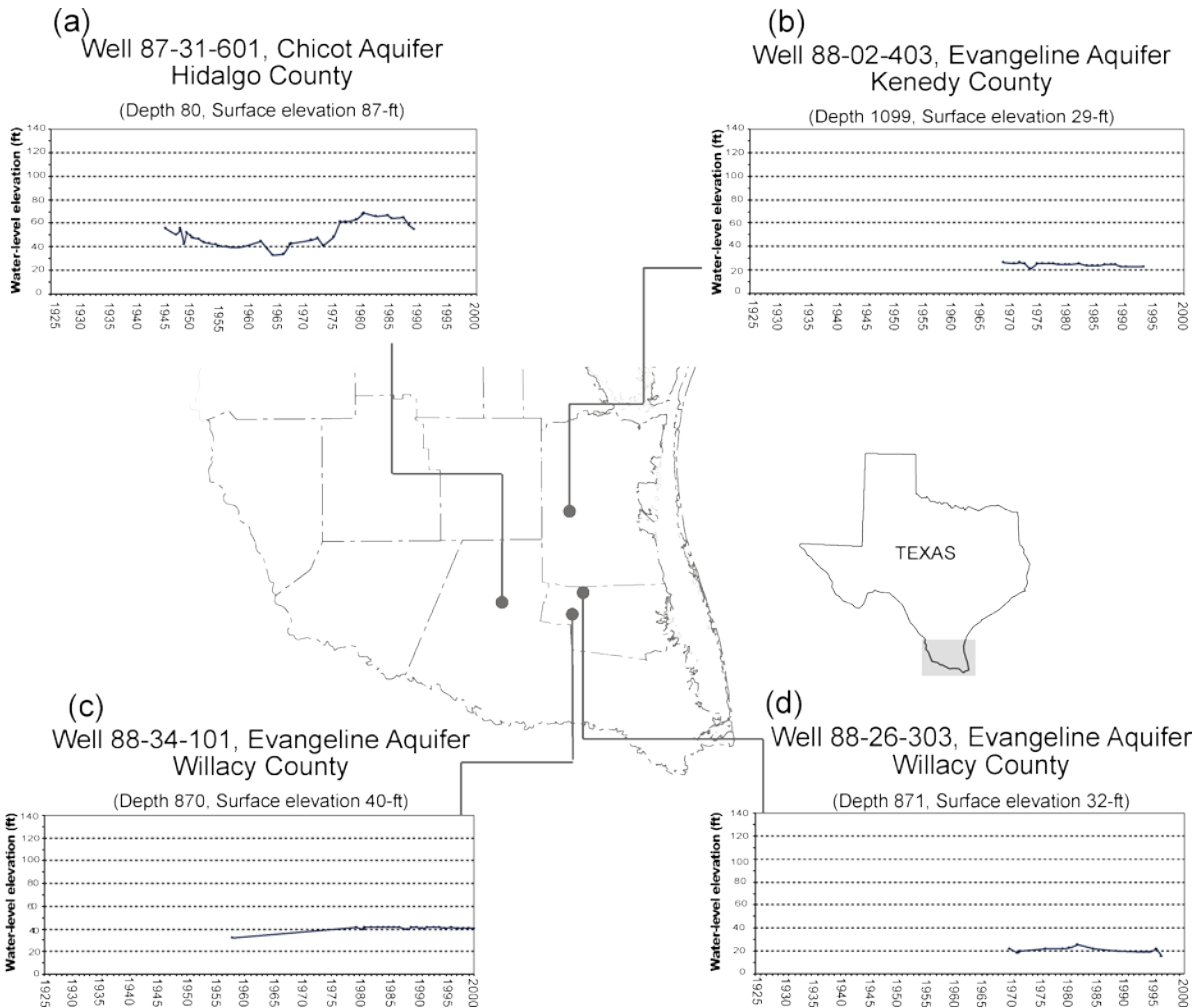


Figure 5-17. Hydrographs for wells (a) 87-31-601, (b) 88-02-403, (c) 88-34-101, and (d) 88-26-303 in the Chicot and Evangeline aquifers (mi = miles; ft = feet).

5.4 Rivers, streams, lakes, and canals

The study area includes two major drainage basins, a major river, a number of minor streams, several lakes and resacas, and a network of irrigation canals.

The two major drainage basins that traverse the study area and funnel surface water toward the Gulf of Mexico are the Rio Grande and the Nueces-Rio Grande basins (Figure 5-18). The Rio Grande Basin extends from southern Colorado through New Mexico, Texas, and Mexico to the Gulf of Mexico, with a combined watershed of 355,500 square miles. The Texas portion of the watershed is about 54,000 square miles (TCB, 2000). The Pecos and the Devils rivers are the main tributaries of the Rio Grande in Texas that eventually flows into Amistad Reservoir. The easternmost tributary from the upland plain joins the Rio Grande 10 miles west of Mission. The Mission Ridge prevents drainage from the upland reaching the Rio Grande. In Mexico, the Rio Conchos, Rio Salado, and the Rio San Juan are the largest tributaries of the Rio Grande.

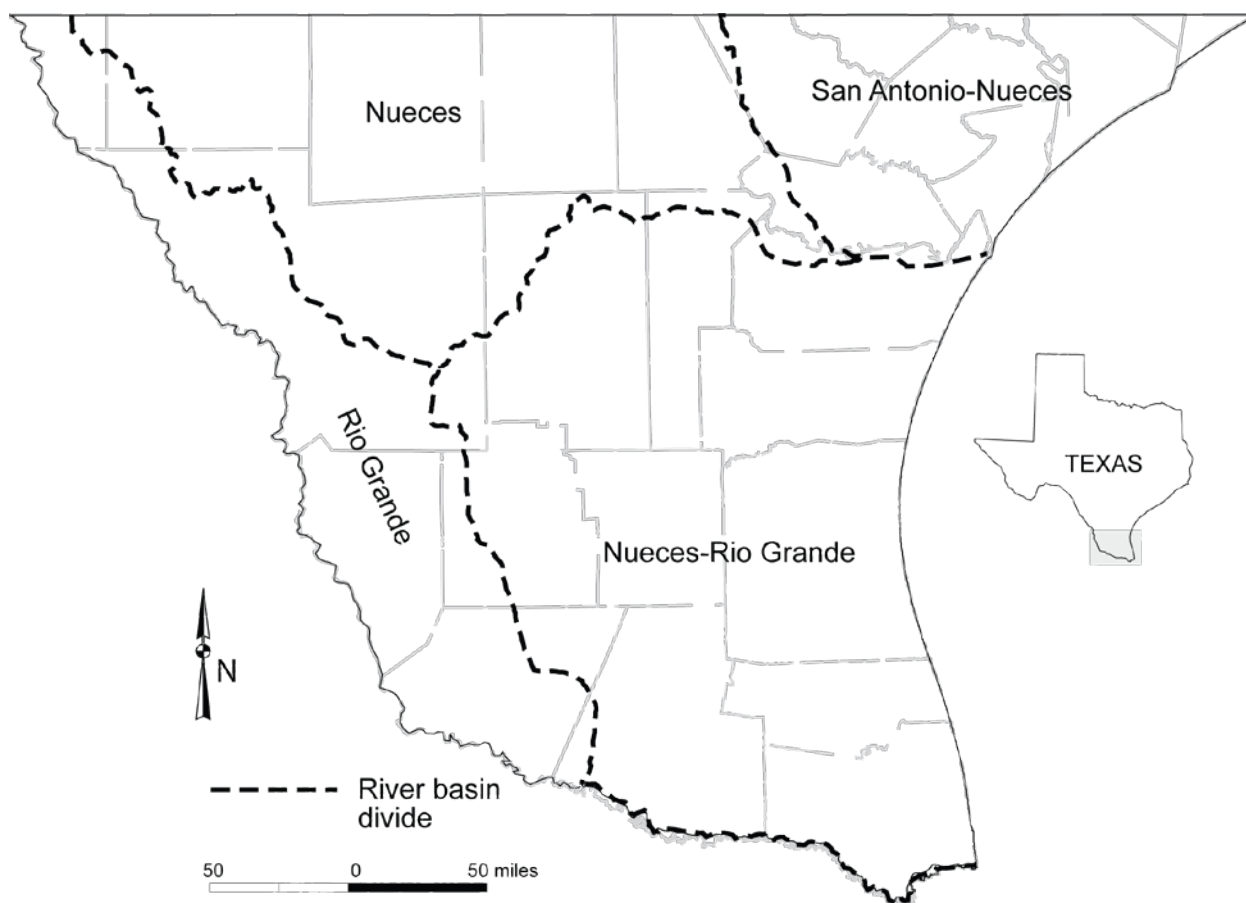


Figure 5-18. River basins in the study area. The Nueces, Rio Grande, and San Antonio-Nueces river basins extend outside the study area.

The Nueces-Rio Grande Basin is bounded on the north by the Nueces River Basin, on the west and south by the Rio Grande Basin. The Nueces-Rio Grande Basin has a drainage area of 10,442 square miles and drains to the Laguna Madre estuary (TCB, 2000). The main floodway, Arroyo Colorado, and the resacas are located within this drainage basin.

The Rio Grande forms the international boundary between the United States and Mexico along a distance of 1,250 river miles. Historic annual streamflow measured at three gages along the Rio Grande indicate that streamflow is variable and ranges from over 6,000,000 acre-feet per year to nearly nothing (Figure 5-19). Flow in the river declines steadily downstream, particularly in the streamgage down river of Brownsville where the Rio Grande nearly ceased to flow during the drought of 2000 to 2001. Average annual flow (1960 to 1997) from the Rio Grande to the Gulf of Mexico is 0.74 million acre-feet (TCB, 2000).

In addition to the Rio Grande, numerous small channels and intermittent streams cross the study area. Most of these channels and streams arise from the upland areas in the west and form tributaries to the Rio Grande. The Arroyo Colorado is an ancient channel of the Rio Grande originating north of Hidalgo County and eventually emptying into Laguna Madre through a network of abandoned distributary channels known as resacas.

Daily flow in the Arroyo Colorado is primarily comprised of irrigation return flows, storm water runoff from urban areas, treated wastewater discharges from the municipalities, groundwater base flow, and locally generated runoff. During major flood events, water from the Rio Grande is also diverted into parts of the Arroyo Colorado (TCB, 2000). Streamflow measured at three river gages indicates that as much as 1,100,000 acre-feet per year can flow through the arroyo (Figure 5-20). However, flow measured since the 1970s has been much lower (less than 200,000 acre-feet per year). Resacas of the arroyo are normally full due to irrigation return flows and diversions from the Rio Grande.

The study area has ten lakes, five reservoirs, and two lagoons (Figure 5-21). The lakes occur naturally in shallow depressions and vary in width from a few hundred feet to several miles. They are mostly located between the eastern half of the study area in central Hidalgo and Brooks counties and the coast. These lakes are: (1) Lake Edinburg in south central Hidalgo County, (2) La Sal Del Ray in northeastern Hidalgo County, (3) La Loya Lake in southwestern Hidalgo County, (4) Campacuas Lake in eastern Hidalgo County, (5) Cross Lake in Cameron County, (6) La Sal Vieja in western Willacy County, (7) Rosita Lake in southern Kenedy County, (8) Cayo Soledad in central Kenedy County, (9) Le Cayos de la Mula along the Brooks-Kenedy county line, and (10) San Martin Lake near the coast in southeastern Cameron County. Many of the lakes are intermittent and are dry during the summer. If drought conditions persist for extended periods, some of these lakes may cease to exist. We could only find information for the three lakes discussed below.

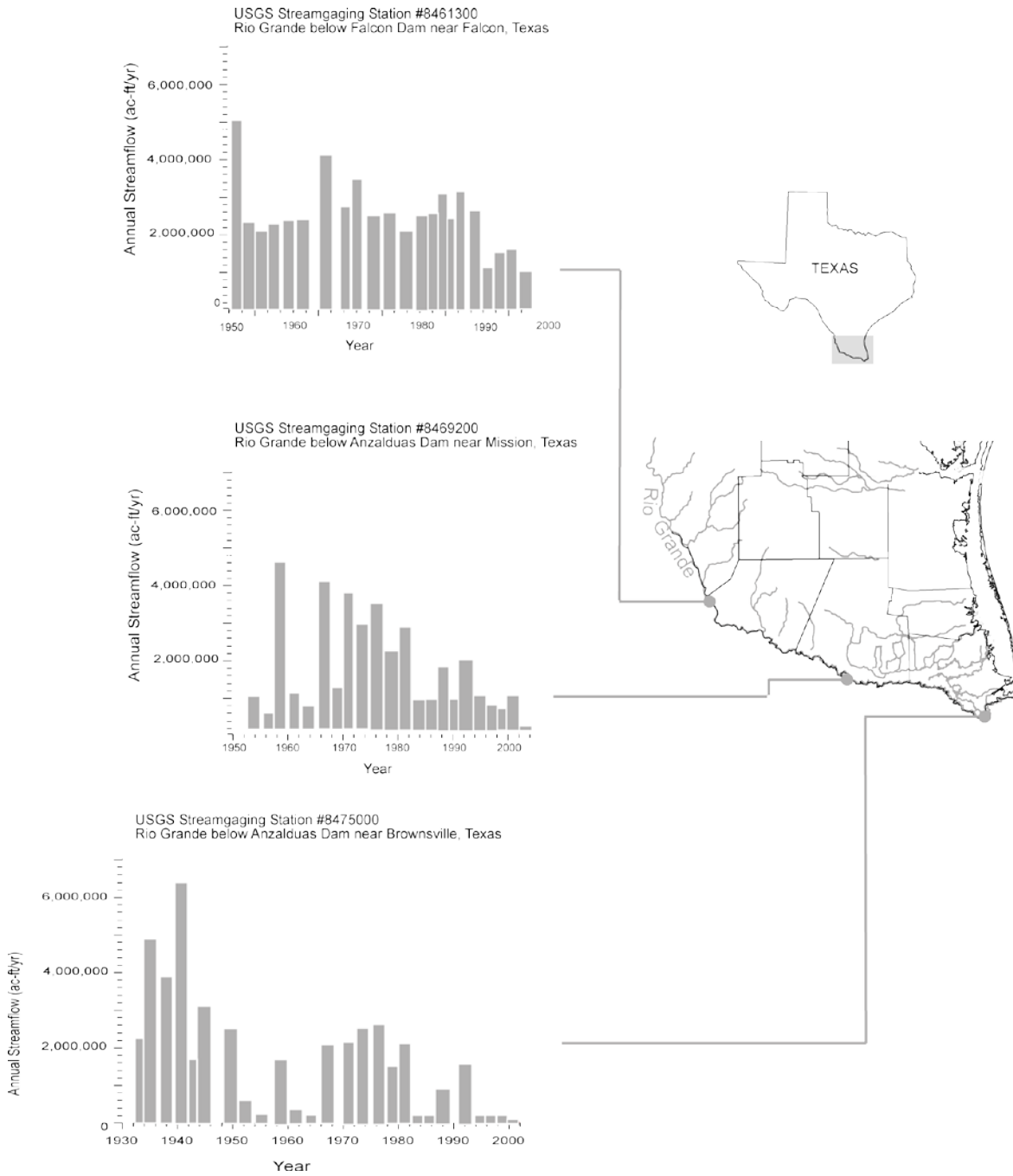


Figure 5-19. Historical streamflow data from three river gages on the Rio Grande. Note that flow decreased considerably after 1995 (ac-ft/yr = acre-feet per year; USGS = U.S. Geological Survey).

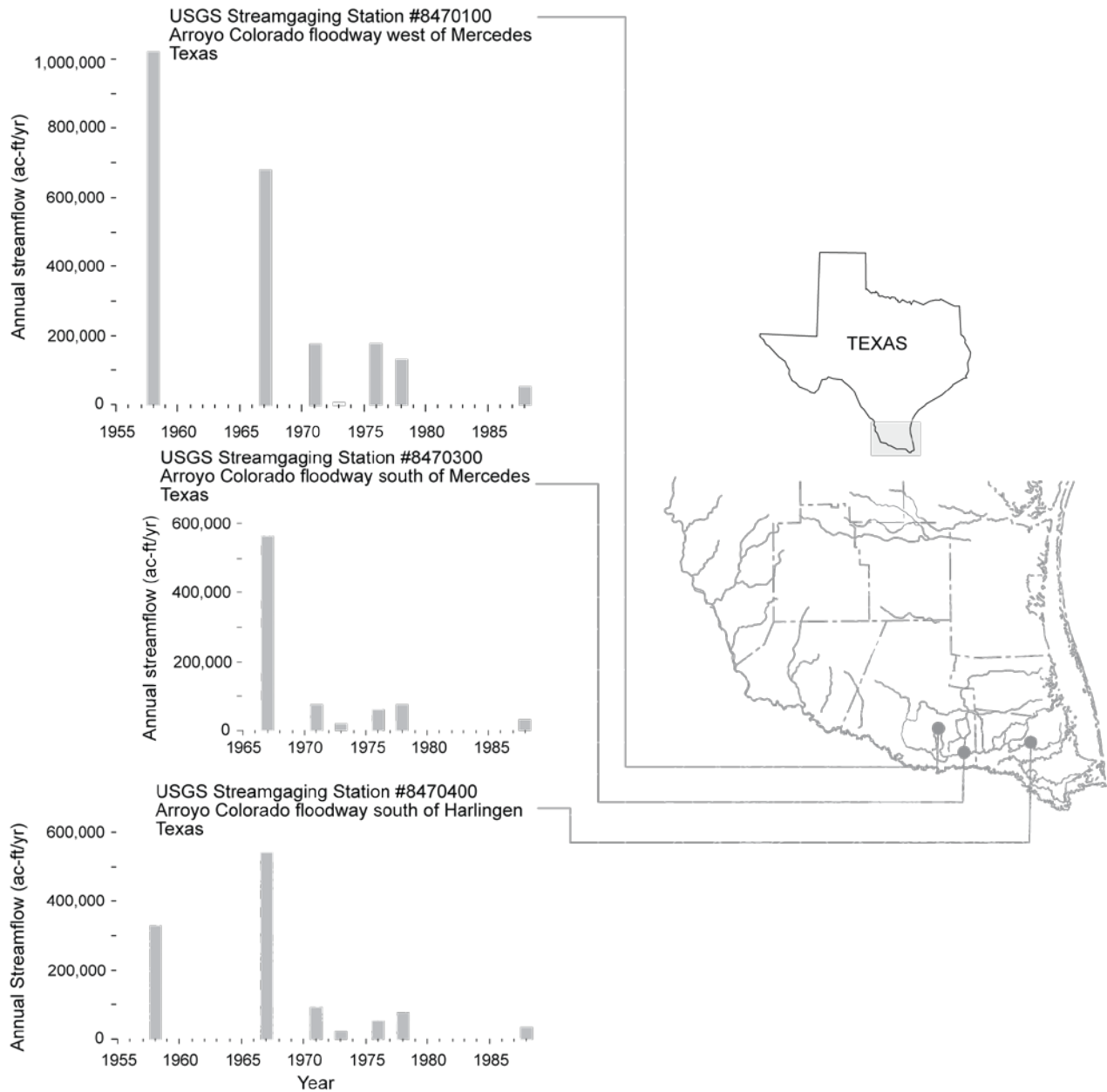


Figure 5-20. Historical annual streamflow from river gages installed on the Arroyo Colorado. Note differences in flow before and after 1970 (ac-ft/yr = acre-feet per year; USGS = U.S. Geological Survey).



Figure 5-21. Lakes and water supply reservoirs in the study area (mi = miles).

Discovered by the Spanish Conquistadors, La Sal del Ray Lake is a large salt lake located 22 miles north of Edinburg. Salt from the nearby mines was transported overseas to Spain and her colonies and westward into Mexico. The banks of the lake turn white from high concentrations of salt.

La Sal Vieja consists of two natural salt lakes—the east and west lakes. Brine from oil and gas wells and a paper mill were routinely discharged into the lakes (Robertson and others, 1992). Both lakes are closed basins in an area of high evaporation leading to the accumulation of contaminants.

Lake Campacuas lies near the north floodway and is part of the delta system of resacas and arroyos that drain floodwaters from the Rio Grande into the Gulf of Mexico. It is about 2 miles long and is 700 feet wide at its broadest point.

Five man-made reservoirs store water supplies off channel to the Rio Grande. The reservoirs are (1) Loma Alta Reservoir in southern Cameron County, (2) Monte Alto Reservoir in northwest Hidalgo County, (3) Valley Acres Reservoir in eastern Hidalgo County, (4) Adams Garden Reservoir, and (5) Willacy Reservoir in southeastern Cameron County (Figure 5-21).

Loma Alta Reservoir (Loma Alta Lake) has a storage capacity of 26,500 acre-feet, a surface of 2,490 acre-feet, and an elevation of 18 feet. It is surrounded by flat to rolling terrain and is

surfaced by dark, commonly calcareous clays that support mesquite, grasses, and cacti. Monte Alto Reservoir is an off-channel storage reservoir to the Rio Grande. It has a storage capacity of 25,000 acre-feet, a surface area of 2,371 acres, and an elevation of 56.5 feet. Water is diverted from the Rio Grande in Cameron County by a gravity canal system. From this main canal, water is diverted to another canal—known as Mesteñas Canal—for distribution to irrigation or to a pumping plant that lifts surplus water to the reservoir for storage. When needed for irrigation, the water is released and flows back to the Mesteñas Canal for distribution.

Valley Acres Reservoir is an off-channel storage reservoir to the Rio Grande, with a storage capacity of 7,840 acre-feet, a surface area of 906 acre, and an elevation of 62 feet. Adams Garden Reservoir and the Willacy Reservoir are also off-channel storage reservoirs to the Rio Grande but with low storage capacities (less than 5,000 acre-feet). There are two main lagoons along the coast: Laguna Madre and Laguna Atascosa. Laguna Madre is the only lagoon in the nation that is saltier than the ocean. It extends inland from the Gulf of Mexico as a gently sloping area containing short grasses, mesquite trees, thorny brush, and prickly pear cactus (UCS, undated). Since no major rivers flow into Laguna Madre, its salt content is quite high, with an average concentration of about 35,000 parts per million. This salinity increases to 45,000 parts per million in the lower part of Laguna Madre and during periods of hot, dry weather. The average water depth is about 2.5 feet with some areas reaching a depth of 5 feet. Variable depths and salinity support different types of seagrasses, hyper-saline marshes, algal flats, and lomas. Tidal currents in the lagoon are weak, circulation is sluggish, and residence times of water masses are long (UCS, undated).

Laguna Atascosa is a 69,500-acre saltwater lake in the southwestern region of the Laguna Atascosa National Wildlife Refuge located 3 miles west of Laguna Madre (The Handbook of Texas Online, 2002). Laguna Atascosa is 4 to 5 feet deep at its deepest. Needle Island is at its center, and Cayo Atascosa serves as an outlet into Laguna Madre. The surrounding terrain is flat to rolling and is surfaced by soils ranging from dark calcareous clay to mottled organic-rich mud with concentrations of shell. Mesquite, grasses, and cacti grow in the area.

Several diversions are used to remove water from the Rio Grande for water supply and flood control. The maximum average annual diversions during 1960 to 1997 occurred below the Anzalduas Dam between McAllen and Brownsville (0.76 million acre-feet on the United States side and 0.95 million acre-feet on the Mexico side of Rio Grande [TCB, 2000]). The resacas in Cameron County (Resaca Quates, Resaca Fresnos, Resaca De Los, and Resaca Del Ran) have average annual diversions of 225 acre-feet for municipal use and 13,684 acre-feet for irrigation use (TCB, 2000). These diversions upstream are probably partly responsible for a considerably reduced flow downstream, particularly in Cameron County.

A complex network of canals, pipelines, and resacas are used to convey water to the irrigated areas in Hidalgo, Cameron, and Willacy counties. The main distribution network consists of a total of 797.9 miles of canals, 123.4 miles of pipelines, and 76 miles of resacas. In addition, secondary and tertiary networks (laterals) consist of a total of 429 miles of canals and 973 miles of pipelines. In all, there are 549 miles of concrete-lined canals and 615 miles of unlined canals. Concrete-lined canals have extremely high seepage loss rates (90 to 1,220 acre-feet per mile per year) due to use of improper materials and poor maintenance. Unlined canals have much lower

seepage rate (54 to 1,037 acre-feet per mile per year), mainly controlled by the soil type beneath the canals (Fipps, 2001).

5.5 Recharge

Recharge to the aquifers occurs from (1) rainfall that falls on the outcrop, (2) surface water that discharges from the Rio Grande and Arroyo Colorado, and (3) irrigation return flows. Water not consumed by plants through transpiration or drained by streams from surface runoff infiltrates into the subsurface and eventually reaches the water table. The hydraulic conductivity of the soil largely controls infiltration. The soils in the Lower Rio Grande Valley have varying hydraulic conductivities, ranging from 0.06 inches per year to 6.0 inches per year (USSCS, 1972, 1977, 1981, 1982). The flood plain deposits (silt and mud) of the Chicot Aquifer covering parts of Cameron County and local areas around the Rio Grande in Hidalgo County may provide less recharge except where sands representing the ancient channels crop out. The Goliad Sands, where not calcified, provide the best route for recharge. Additional recharge may potentially reach the groundwater from excess application of irrigation water through agricultural drainage tiles, leakage from canals, and floodways (McCoy, 1990).

Several investigators have estimated recharge rates for the Gulf Coast Aquifer (Groschen 1985; Ryder, 1988; Dutton and Richter, 1990; Hay, 1999; Harden and Associates, 2002; Table 5-1). These recharge rates vary considerably as model areas selected for simulation have varied (1) hydraulic conductivity, (2) rainfall distribution, (3) evapotranspiration rates, (4) groundwater-surface water interaction, (5) model grid sizes, and (6) occurrences of caliches in the outcrop areas.

Groschen (1985) estimated an average recharge rate of 0.06 inches per year for the Evangeline Aquifer covering San Patricio to Jim Hogg counties. He postulated that most of the water flowing into the Evangeline Aquifer originated as cross-formational flow from the Jasper Aquifer beneath because (1) the area is marked by a precipitation deficit of 18 to 28 inches (average annual precipitation minus potential evapotranspiration), (2) most of the outcrop of the Goliad Formation is extensively cemented by caliche that prevents direct recharge from rainfall, and (3) there was no relationship between water levels in wells and rainfall events, even during the drought of record (Sayre, 1937).

Ryder (1988) estimated a maximum recharge of 6 inches per year in the outcrop areas of the upper Gulf Coast with most of it occurring over small areas of topographic highs. He used an average recharge rate of 0.74 inches per year to calibrate the model. Calibrated recharge values ranged from 0 to 4 inches per year for the Goliad Sand in the southern Gulf Coast, 0 to 2 inches per year for the alluvium in southern Cameron County, and no recharge for the remainder of the outcrop of the Chicot Aquifer over most of Cameron, Hidalgo, and Willacy counties. Ryder (1988) modeled recharge using a constant head boundary.

Table 5-1. Recharge estimates of the Gulf Coast Aquifer from previous modeling studies.

Source	Recharge rate (in/yr)	Study area	Recharge method
Groschen (1985)	0.06	San Patricio to Jim Hogg counties	Constant head
Ryder (1988)	0 to 6	Texas Gulf Coast	Specified head, top layer of the model
Dutton and Richter (1990)	0.1 to 0.4	Matagorda and Wharton counties	Head-dependent flux boundary, top layer of the model
Noble and others (1996)	6	Harris, Montgomery, and Walker counties	Isotopes
Hay (1999)	0.078	Navidad River to Willacy County	Constant head
Harden and Associates (2001)	0.1 to 0.2	Brownsville and vicinity	Used maximum potential recharge (3 inches) and MODFLOW's River Package
Kasmarek and Strom (2002)	0.89	A number of counties in the upper Gulf Coast with focus on Harris and Galveston counties	Specified head, top layer of the model
This study (2003)	0.09 to 0.15	Lower Rio Grande Valley	Calibrated recharge as a percent of distributed rainfall

in/yr = inches per year

Dutton and Richter (1990) estimated a recharge rate of 0.1 to 0.4 inches per year for simulating the Chicot and the Evangeline aquifers in Matagorda, Wharton, and Colorado counties, with the highest recharge occurring in the outcrop to the west and nearly no recharge down dip in Wharton and Matagorda counties. They used a head-dependent flux boundary in the uppermost active model cells with the leakance or the boundary conductance assigned to the cells forming the driving force for the flow system. The heads in the cells were adopted from Ryder's (1988) model.

Noble and others (1996) used tritium to estimate recharge into the Chicot and the Evangeline aquifers. They estimated an average recharge of 6 inches per year in the Chicot and Evangeline outcrops of the Upper Gulf Coast, using the deepest penetration (80 feet) of tritium isotopes. This higher recharge rate is the upper bound of average recharge for 1953 to 1990 and accounts for total recharge captured by the entire flow system unlike groundwater models that often miss the shallow flow system due to larger grid sizes of the model.

Harden and Associates (2002) estimated a net recharge (total recharge minus groundwater evapotranspiration) of 0.1 to 0.2 inches per year for simulating the alluvium aquifer near Brownsville. The top layer of the four-layered model was clay and was used as a confining water table layer. They assigned total annual recharge of up to 3 inches. However, MODFLOW's evapotranspiration package used in the model removed much of this infiltrated water resulting in a much lower net recharge (Bob Harden, personal communication, 2003).

We compiled precipitation data from 1930 to 1980 to develop the mean annual rainfall map using all available rainfall gages in the area (Figures 5-22 and 5-23). We chose this 50-year period because water levels in most of the aquifers showed no significant fluctuation throughout the period. In addition, it provided the maximum number of rain gages required to produce a precipitation map of the model area. We then contoured mean rainfall data at the rainfall gages using linear kriging (Figure 5-22).

Water level information from the Chicot and Evangeline aquifers suggest that the Rio Grande is a losing stream in the southwestern portion of Hidalgo County. Vandertulip and others (1964) estimated streamflow losses by taking the difference between the amount of water released from the reservoirs upstream and the amount of water received at the point of diversions. They calculated streamflow losses during periods of water release for the years 1954 to 1957 and 1960 to 1963. They reported that water loss per mile of reach ranges from $1.85 \times 10^{-4}Q$ to $3.9 \times 10^{-5}Q$ where Q is streamflow. Using daily streamflow information from the International Boundary Water Commission Web site, we found that average streamflow below the Falcon Dam for the years 1960 to 1963 was about 1.02×10^6 acre-feet per year. Using this average streamflow value and water loss information from Vandertulip and others (1964), we estimated water loss per mile of the river reaches along sections of the Rio Grande. Water loss along the river reaches of the Rio Grande is highest in southern Hidalgo County (461 acre feet per year per mile) and sharply declines downstream past Hidalgo County (30 acre-feet per year per mile). Therefore, the Rio Grande provides a considerable amount of water for recharging the aquifers in the Lower Rio Grande Valley. However, these estimates are likely to fluctuate depending on rainfall rates, river

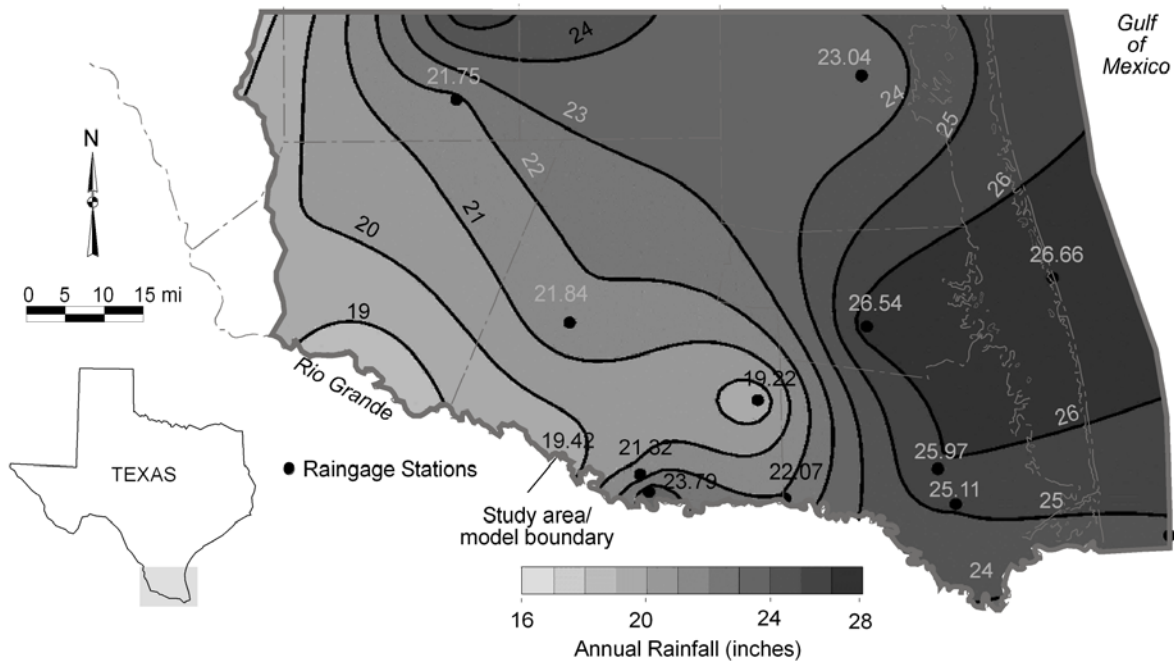


Figure 5-22. Average annual precipitation for the period 1930 to 1980. Black dots show locations of the rain gages within the model area and corresponding average annual precipitation values at each of these stations (mi = miles).

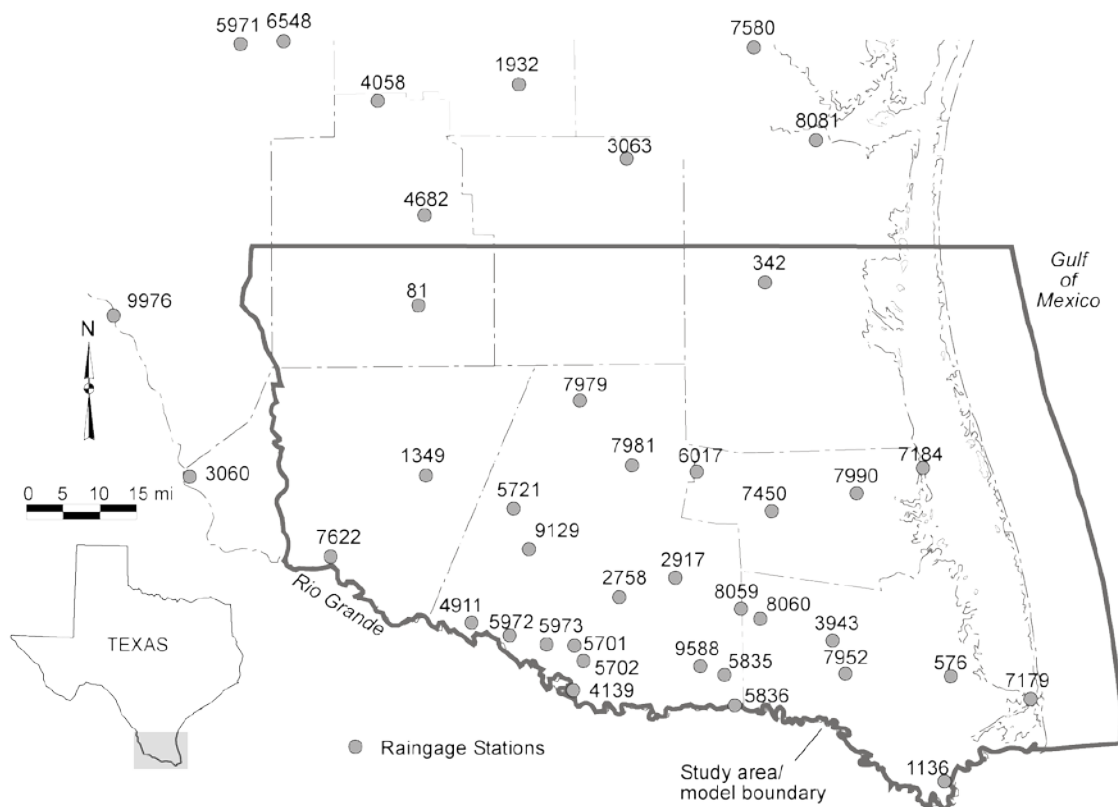


Figure 5-23. Rain gage locations in the study area and vicinity. Dots show rain gage locations, and the labels are the station numbers (mi = miles).

stage, and levels of interactions between the surface water in the Rio Grande and the groundwater in the adjacent aquifers.

Using a reservoir operations model, R.J. Brandes Company (1999) estimated the extent of water losses along the lower Rio Grande and within the irrigation district water delivery systems. They reported that on average 20 percent of the water may be lost if seepage, evaporation, and other losses from canals, pipelines, and reservoirs are considered. For 2000, they estimated that the total loss could amount to as much as 31,302 acre-feet per year (TCB, 2000).

We were unable to find information on streamflow losses for the Arroyo Colorado. The arroyo sustains flow from treated wastewater discharges, irrigation return flow, storm water runoff, and flood flows. Since the arroyo lies near the coast, streamflows and stream stages could potentially be sensitive in switching the arroyo from a net gaining to a net losing stream.

Most of the water from the arroyo is used for irrigation, and the remaining water in the arroyo naturally flows to Laguna Madre. Irrigation return water may also allow additional recharge into the aquifers of the Lower Rio Grande Valley. Where groundwater is withdrawn for irrigation in outcrop areas, a considerable amount of irrigation water can potentially return to the aquifer by downward percolation. Jorgensen (1975) estimated that as much as 30 percent of the irrigation water pumped from the aquifer in the Katy area has returned to the Chicot Aquifer.

Estimates of canal loss for the irrigation areas in the Lower Rio Grande Valley are sparse except for four studies (TBWE, 1946; Vandertulip and others, 1964; R. J. Brandes Company, 1999; Fipps, 2001). Leakage from the canals depends on a number of factors including (1) nature of the soil, (2) age of the canal, (3) flow of water in the canal, (4) canal depth and velocity, (5) relationship between wetted perimeter and discharge, and (6) temperature of the water and soil. In addition, canal loss appears to vary widely depending on whether laterals, resacas, unlined canals, or lined canals were measured and the methodology used to estimate the loss rates. Rate of loss based on the soils alone was estimated to range from 0.20 feet per day for clay to 1.50 feet per day for sandy loam.

From inflow-outflow tests on the resacas, a low estimate of net loss was found (0.004 feet per day) due to the sealing effect of natural silt deposits, the proximity of sea level (TBWE, 1946), or to low flow in the canal (Rantz and others, 1982).

Canals lined with gunite show a loss of 0.12 feet per day. Leakage in concrete canals presumably occurs through contraction cracks and expansion joints, with a net loss ranging from 0.08 to 0.3 feet per day. Cylinder tests have also been used to measure canal loss where cylinders of 24 inches in length were driven into the sloping banks or bottom of the channel and filled with water. Results from 40 cylinder tests produced an average seepage loss of 0.03 feet per day (TBWE, 1946).

Fipps (2001) estimated canal loss using ponding tests. In ponding tests, a section of the canal is blocked off at each end and filled with water at a level slightly higher than flows during the irrigation season (Rohwer, 1948). As the water level declines, the time is recorded and a seepage rate is determined after correcting for temperature and evaporation. Fipps (2001) reported that the unlined canals have seepage rates ranging from 54 to 1,037 acre-feet per mile per year and the concrete-lined canals have seepage rates ranging from 90 to 1,220 acre-feet per mile per year. However, these values may not represent actual leakage into the groundwater as the gates and the valves could have been leaking, and some of the water could have been lost to the ditches and the perched water table (Guy Fipps, personal communication, 2001).

5.6 *Hydraulic properties*

The ease with which water can move through pore spaces or fractures in the sediments and how much water the sediments can store is controlled by its hydraulic properties. For example, water can flow more easily through coarser sediments—such as sand and gravel—than finer sediments—such as silt and shale. Hydraulic conductivity depends on the intrinsic permeability of the sediments and on the degree of water saturation. Transmissivity, a product of hydraulic conductivity and aquifer thickness, describes the ability of an aquifer to transmit water through its entire thickness. If hydraulic conductivity is uniform from point to point, an aquifer is considered homogeneous. If hydraulic conductivity is not uniform, an aquifer is considered heterogeneous. Trending heterogeneity results from sediment accumulations in specific depositional environments (seaward to beach), and layered heterogeneity develops when beds with high and low permeability occur together (Freeze and Cherry, 1979).

The Chicot and the Evangeline aquifers show considerable variations in well yields over a short distance primarily due to the occurrences of trending heterogeneity. For example, ancient river courses containing narrow sand and gravel deposits produce high yields, but floodplain deposits on the banks containing silt and mud may produce no water at all.

Although the Gulf Coast Aquifer has been extensively pumped, it is difficult to predict yield from the aquifer. This uncertainty in estimating yield is due to the unpredictability in determining the distribution of sand-shale content, pore-fill cements, depositional facies, and compaction from the overlying sediments. Transmissivity ranges from 3,000 to 18,000 square feet per day and 3,000 to 15,000 square feet per day in the Chicot and Evangeline aquifers, respectively (Meyer and Carr, 1979). In a later report, Carr and others (1985) also found similar transmissivity values (3,000 to 25,000 square feet per day and 3,000 to 12,000 square feet per day in the Chicot and the Evangeline aquifers, respectively).

Ryder (1988) assumed that interbedded clays in a layer do not contribute to horizontal flow; therefore, he only calculated transmissivity for the sand portion of the layer (transmissivity = hydraulic conductivity × sand ratio × layer thickness). He found maximum sand-to-shale ratios of 0.88 to 0.99 for the aquifers with a minimum ratio of 0.02 to 0.18. The confining units have sand ratios of 0.21 to 0.41 with a minimum ratio of zero. He assigned a constant hydraulic conductivity of 170 feet per day to the Holocene-upper Pleistocene permeable zone (upper Chicot Aquifer), 20 feet per day to the lower Pleistocene-upper Pliocene permeable zone (lower Chicot Aquifer), 60 feet per day to the lower Pliocene-upper Miocene permeable zone (Evangeline Aquifer), and 80 feet per day to the middle Miocene permeable zone (Jasper Aquifer) to calibrate his predevelopment model. He showed that sands with a high sand-to-shale ratio can still have a low hydraulic conductivity.

Prudic (1990) examined 1,500 aquifer test analyses and more than 5,000 specific-capacity tests for the entire Gulf Coast Aquifer extending from Texas to Louisiana. He found that the hydraulic conductivity is highly variable, ranging from 1 to 1,000 feet per day in the Gulf Coast Aquifer. Geometric mean for hydraulic conductivity was 55 feet per day from pumping tests and 71 feet per day from specific-capacity tests. He noted that hydraulic conductivity is more dependent on the depth to the middle of the screened interval than the sand bed thickness. He also observed that hydraulic conductivity decreased as a function of depth.

In Matagorda and Wharton counties, Dutton and Richter (1990) reported measured hydraulic conductivity values that ranged from 17 to 528 feet per day in the upper Chicot Aquifer, 6 to 204 feet per day in the lower Chicot Aquifer, and 9 to 47 feet per day in the Evangeline Aquifer. However, the calibrated hydraulic conductivity values in their model were considerably lower and range from 0.13 to 22 feet per day (mean of 7 feet per day), 0.79 to 440 feet per day (mean of 23 feet per day), and 0.15 to 358 feet per day (mean of 5 feet per day) for the upper Chicot, lower Chicot, and the Evangeline aquifers, respectively.

Hay (1999) assigned much lower hydraulic conductivity values to calibrate his model than what was previously used in the Gulf Coast Aquifer (0.9 to 2.9 feet per day for the Upper Chicot Aquifer, 0.9 to 3.5 feet per day for the lower Chicot Aquifer, 0.4 to 7 feet per day for the Evangeline Aquifer, and 0.1 to 1 feet per day for the Jasper Aquifer). The model was verified

using water levels and pumpage data for 1985. A lower hydraulic conductivity required a lower annual recharge rate of 0.078 inches.

Vertical hydraulic conductivity in a sand aquifer is primarily controlled by low-permeability clay lenses contained within a sand sequence. Estimated vertical hydraulic conductivity is highly variable (10^{-7} to 1 feet per day) in the Gulf Coast Aquifer (Jorgensen, 1975). Carr and others (1985) found that calibrated vertical hydraulic conductivities for the Chicot and the Evangeline aquifers in the Houston area ranged from 1.2×10^{-5} to 4.6×10^{-3} feet per day. In later studies, calibrated vertical hydraulic conductivities for the Chicot and the Evangeline aquifers in the Houston area were also found to be about the same (3.2×10^{-5} to 4.6×10^{-3} feet per day) (Carr and others, 1985). In a regional study of the entire Gulf Coast Aquifer, Ryder (1988) calibrated vertical hydraulic conductivities that range from 1×10^{-5} feet per day for a confining unit and 1×10^{-2} feet per day for the four aquifers and permeable zones. In a more localized study of Matagorda and Wharton counties, Dutton and Richter (1990) used calibrated vertical hydraulic conductivity values of 1.05×10^{-4} to 6.76×10^{-1} feet per day (mean of 4.75×10^{-3} feet per day) for the upper Chicot Aquifer, 7.94×10^{-5} to 2.30×10^{-1} feet per day (mean of 2.38×10^{-3} feet per day) for the lower Chicot Aquifer, and 2.27×10^{-5} to 2.63×10^{-1} feet per day (mean = 5.58×10^{-4} feet per day) for the Evangeline Aquifer. In a more recent investigation of the Chicot and the Evangeline aquifers in the Houston area, Kasmarek and Strom (2002) used a vertical hydraulic conductivity of 1×10^{-3} feet per day to estimate leakance (vertical hydraulic conductivity divided by the clay thickness) which ranged from 2×10^{-7} to 1×10^{-4} feet per day.

Storativity describes the capacity of an aquifer to transfer water to and from storage (Anderson and Woessner, 1992). The capacity of an aquifer to transfer water can be described by the following parameters: specific storage, storage coefficient, and specific yield. Specific storage is equal to the volume of water released from storage within a unit volume of porous material per unit decline in hydraulic head. The storage coefficient is the product of specific storage and aquifer thickness and represents the volume of water released per unit area per unit decline in hydraulic head. Specific yield is the volume of water released by gravity drainage per unit area of the aquifer per unit decline in water level (Anderson and Woessner, 1992). In confined aquifers, storativity is controlled by the compression of the water and the porous medium. In unconfined aquifers, storativity approximates the effective porosity of the aquifer material.

The storativity of the Chicot Aquifer ranges from 0.0004 to 0.1 (Carr and others, 1985; Meyer and Carr, 1979). Dutton and Richter (1990) reported a slightly higher range of storativity values in the Chicot Aquifer in Matagorda and Wharton counties (3.11×10^{-2} to 2.39×10^{-1}). The storativity values of the Evangeline Aquifer range from 0.0005 to about 0.1 (Carr and others, 1985). Meyer and Carr (1979) reported storativity values that range from 0.001 to 0.01 in the unconfined areas and 0.0004 to 0.001 in the confined areas of the Evangeline Aquifer. Dutton and Richter (1990) reported a much lower range of storativity for the Evangeline Aquifer in Matagorda and Wharton counties (6.28×10^{-6} to 8.89×10^{-1}).

To evaluate the hydraulic properties of our study area, we collected pumping test and specific-capacity information, used specific-capacity information to estimate transmissivity values, and summarized the values using statistics.

We were only able to find 12 transmissivity values from pumping tests in three general locations in Cameron, Brooks, and Starr counties. We compiled a total of 797 specific-capacity tests (720 from well files at the Texas Commission on Environmental Quality) and 77 tests from the TWDB groundwater database. Most of these specific-capacity tests were completed in the Chicot and the Evangeline aquifers (Table 5-2, Figure 5-24). We only considered specific-capacity tests for wells completed in a single aquifer and not those screened through multiple aquifers.

Table 5-2. Hydraulic conductivities of the Chicot, Evangeline, and Jasper aquifers from the Lower Rio Grande Valley (units in feet per day).

Estimated from TCEQ specific-capacity data

	K_{cht}	K_{cht+evgl}	K_{evgl}	K_{evgl+burk}	K_{burk}	K_{burk+jasp}	K_{cat}	K_{all}
n	237	38	415	17	5	5	-	717
p₂₅	11.	5.4	1.7	1.1	0.18	0.15	-	4.0
p₅₀	20.	13.	9.5	3.1	1.1	0.31	-	13.
p₇₅	79.	33.	21.	4.2	2.4	1.3	-	27.
x_g	27.	12.	6.6	2.8	0.82	0.50	-	10.
s²	0.37	0.57	0.58	0.22	0.48	0.40	-	0.61

Estimated from TWDB specific-capacity data

	K_{cht}	K_{cht+evgl}	K_{evgl}	K_{evgl+burk}	K_{burk}	K_{burk+jasp}	K_{cat}	K_{all}
n	60	-	10	-	-	-	7	77
p₂₅	12.	-	10.	-	-	-	1.3	9.3
p₅₀	20.	-	11.	-	-	-	1.4	16.
p₇₅	72.	-	14.	-	-	-	1.8	49.
x_g	21.	-	12.	-	-	-	2.0	15.
s²	0.92	-	0.03	-	-	-	0.33	0.83

Estimated from TWDB pumping test data

	K_{cht}	K_{cht+evgl}	K_{evgl}	K_{evgl+burk}	K_{burk}	K_{burk+jasp}	K_{cat}	K_{all}
n	6	-	5	-	-	-	-	11
p₂₅	330.	-	33.	-	-	-	-	52.
p₅₀	770.	-	50.	-	-	-	-	200.
p₇₅	920.	-	54.	-	-	-	-	770.
x_g	530	-	43.	-	-	-	-	170.
s²	1.28	-	1.27	-	-	-	-	0.39

values rounded to two significant figures

- K_{cht} - Hydraulic conductivity for the Chicot Aquifer (ft/d)
- K_{cht+evgl} - Hydraulic conductivity for the Chicot and Evangeline aquifers (ft/d)
- K_{evgl} - Hydraulic conductivity for the Evangeline Aquifer (ft/d)
- K_{evgl+burk} - Hydraulic conductivity for the Evangeline Aquifer and Burkeville Confining System (ft/d)
- K_{burke} - Hydraulic conductivity for the Burkeville Confining System (ft/d)
- K_{burk+jasp} - Hydraulic conductivity for the Burkeville Confining System and Jasper Aquifer (ft/d)
- K_{all} - Hydraulic conductivity for all of the aquifers pooled together (ft/d)
- n - Number of data points
- p₂₅ - 25th percentile (ft/d)
- p₅₀ - 50th percentile (ft/d)
- p₇₅ - 75th percentile (ft/d)
- x_g - Geometric mean (ft/d)
- s² - Variance (log[ft/d])²

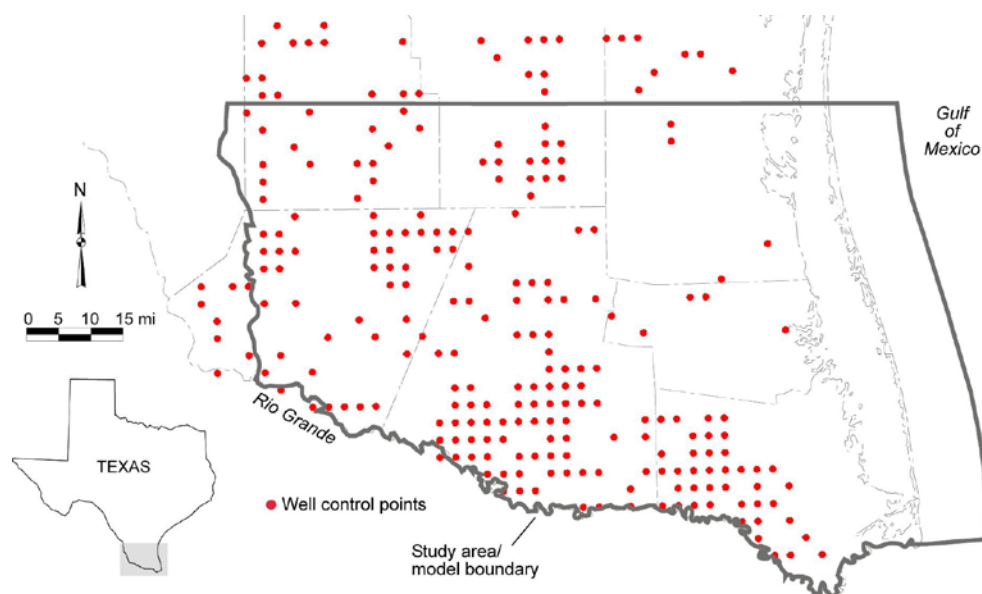


Figure 5-24. Specific-capacity and pumping test locations (indicated by red dots). The occurrences of the locations in apparent grids are caused by averaging the specific-capacity values on a 2½ minute quadrangle and placing the average value at the center of the grid. The average specific capacity was considered representative for that grid as no geographic coordinates were present for this information.

To estimate transmissivity using specific-capacity information, we used an analytical technique (Theis, 1963). Based on the analyses of specific-capacity and pumping tests, we observed that the hydraulic conductivity of the Gulf Coast Aquifer in the Lower Rio Grande Valley is nearly log-normally distributed (Figure 5-25). Hydraulic conductivity from specific-capacity tests for the Gulf Coast Aquifer has a geometric mean of 11 feet per day (Texas Commission on Environmental Quality data, 720 data points) to 15 feet per day (TWDB data, 77 data points; Table 5-2). The geometric mean of hydraulic conductivity from these two combined sources is 18 feet per day for the Chicot Aquifer and 3 feet per day for the Evangeline Aquifer. Pumping tests result in higher hydraulic conductivity values in the Rio Grande Alluvium section of the Chicot Aquifer.

We used a semivariogram to determine spatial correlation of hydraulic conductivity. A semivariogram is a measure of the spatial correlation of a parameter. Samples taken close together are typically more similar than samples separated by larger distances. The semivariogram represents this change in variance with increasing separation distance. When we used a spherical theoretical semivariogram to fit the experimental variogram (Clark, 1979; McCuen and Snyder, 1986) for our samples, we observed a range of 65,000 feet, a nugget of 0.2, and a sill of 0.25 for the Chicot Aquifer and a range of 50,000 feet, a nugget of 0, and a sill of 0.5 for the Evangeline Aquifer (Figure 5-26). Sill defines the variance; range is the distance at which the variogram reaches the sill; and nugget is caused by errors in the data due to measurement value, location assigned, or lack of data. We suspect that the poor-to-moderate spatial correlation

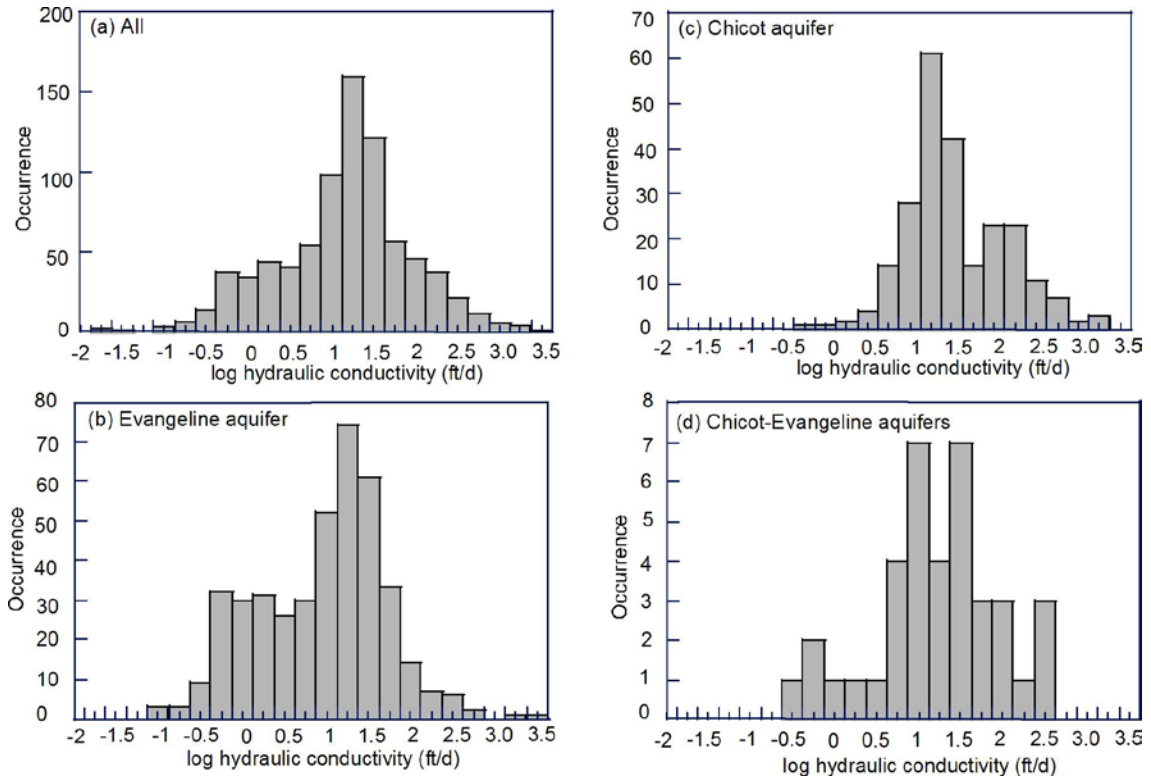


Figure 5-25. Histograms of measured hydraulic conductivity for (a) all tests and tests from the (b) Evangeline Aquifer, (c) Chicot Aquifer, and (d) wells completed in both the Chicot and the Evangeline aquifers (ft/d = feet per day).

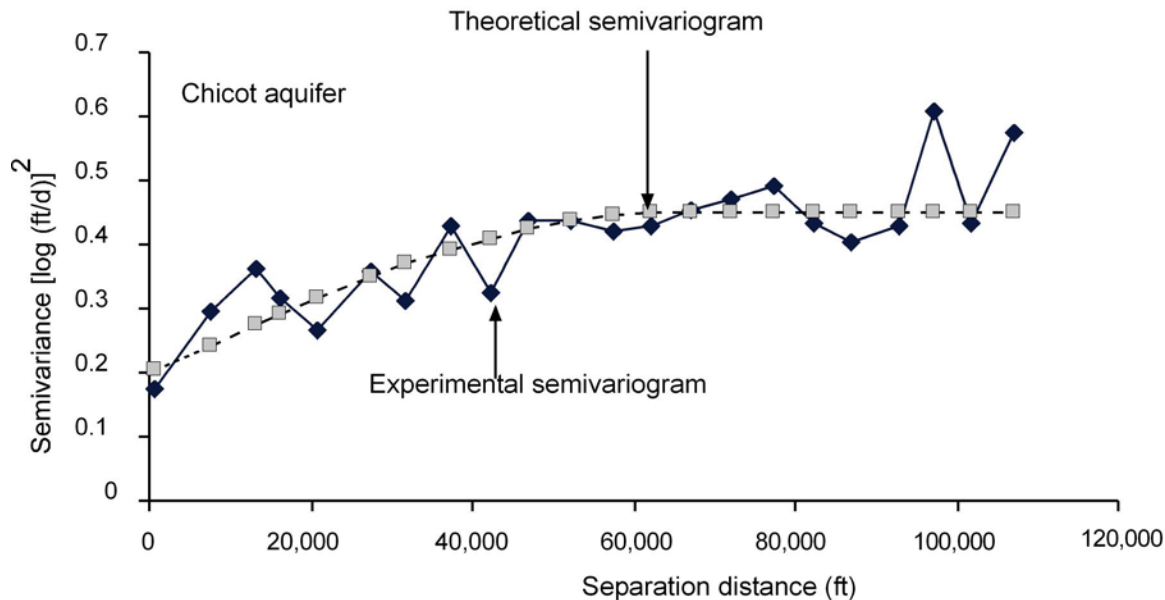
of hydraulic conductivity is primarily controlled by heterogeneity of the aquifer material commonly encountered in a fluvial-deltaic depositional sequence. We used the values obtained from the semivariogram analyses to generate a kriged distribution of hydraulic conductivity (Figures 5-27 and 5-28).

5.7 Discharge

Most of the natural groundwater discharge in the area is by flow to rivers, resacas, and the gulf, and by evapotranspiration (particularly by phreatophytes). A substantial amount of discharge also occurs artificially by groundwater pumping.

The Rio Grande, the main river in the Lower Rio Grande Valley, flows south from Colorado through New Mexico and most of west and south Texas to discharge into the Gulf of Mexico. The Amistad and Falcon reservoirs built upstream of the study area primarily control the flow in the Rio Grande. The Rio Grande switches from a net gaining stream in Starr County to a losing stream in central Hidalgo County then switches back to a gaining stream near Brownsville. Although the gain-loss characteristics of the Rio Grande in the Lower Rio Grande Valley are apparent from groundwater level information, we could not find any discharge values in the literature. Numerous resacas, including Arroyo Colorado, that are relict channels of the Rio

(a)



(b)

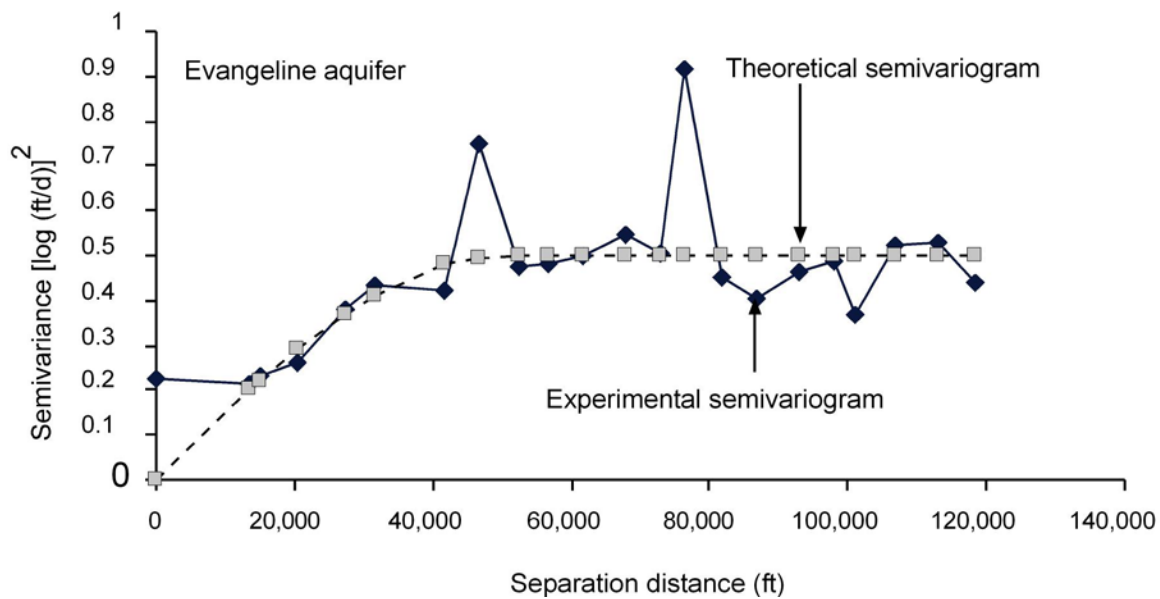


Figure 5-26. Experimental and theoretical semivariograms for (a) the Chicot Aquifer and (b) the Evangeline Aquifer (ft = feet; ft/d = feet per day).

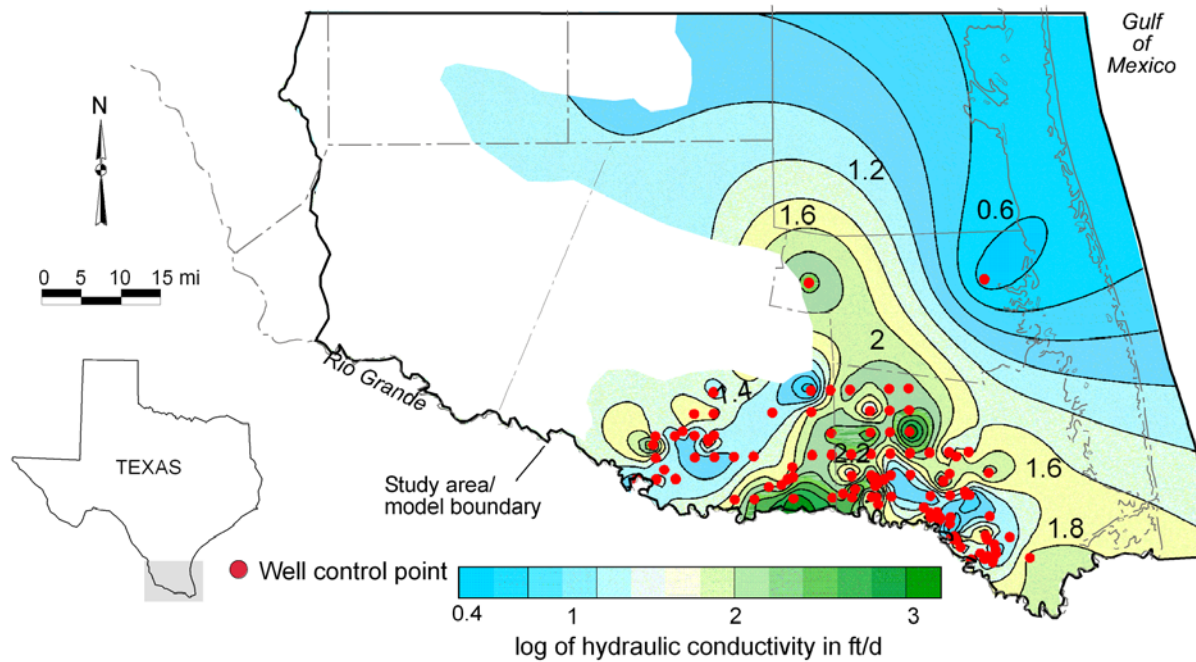


Figure 5-27. Kriged distribution of hydraulic conductivity in the Chicot Aquifer. Each contour interval is 0.2 in log values (ft/d = feet per day).

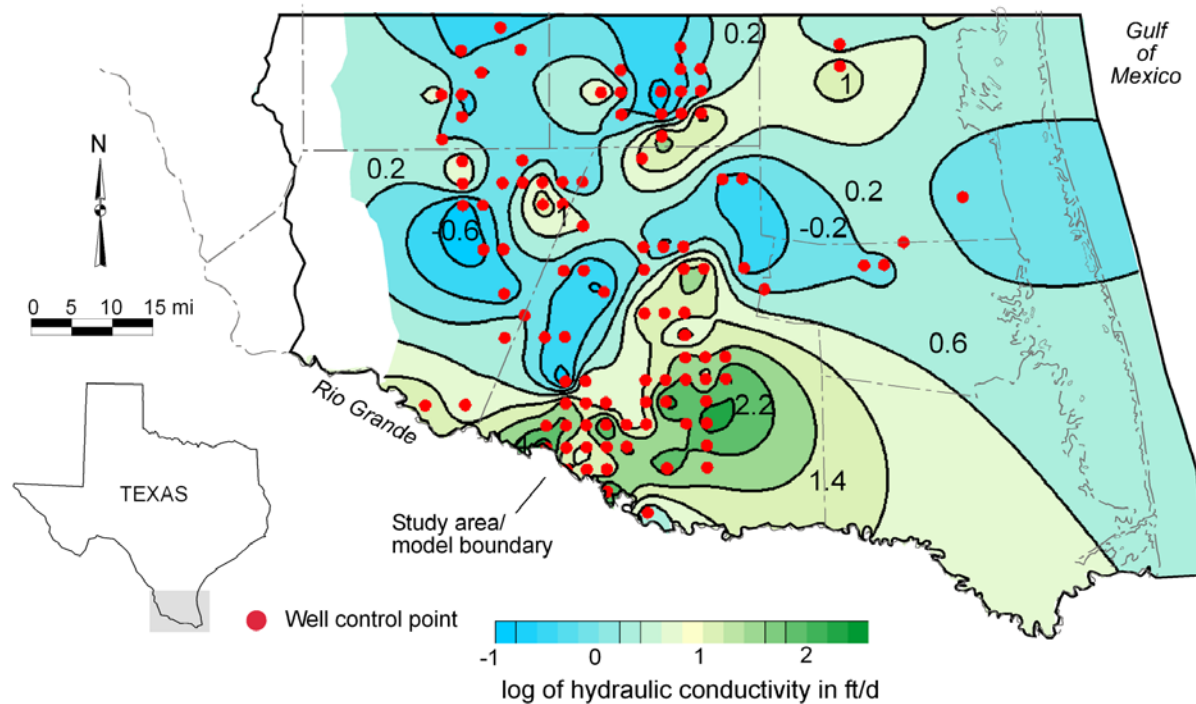


Figure 5-28. Kriged distribution of measured hydraulic conductivity in the Evangeline Aquifer. Each contour interval is 0.4 in log values (mi = miles; ft/d = feet per day).

Grande may receive nominal groundwater discharge since the water table lies 20 to 30 feet below ground surface and the resacas flow through shallow depressions.

Evaporation is the process by which liquid water is converted to water vapor and removed from evaporating surfaces, such as lakes, rivers, soils, and vegetation. Transpiration is vaporization of liquid water through stomata—the small openings in the leaf through which gases and water vapor pass (Allen and others, 1998). Both processes largely depend on soil radiation, air temperature, air humidity, and wind. The water content of the soil and its ability to conduct water to the roots also determine the transpiration rate. Plant types, plant development, and environment also control transpiration rate. When first planted, 100 percent of the evapotranspiration in a field comes from evaporation. However, in a fully-grown crop, more than 90 percent of the evapotranspiration comes from transpiration (Allen and others, 1998). If the saturated groundwater table is at or near the surface, crop transpiration could potentially constitute a large percentage of transpiration.

Relatively little information exists on water use by native vegetation as compared to crops. In the western United States, 80 percent of the irrigation water is lost to phreatophytes such as cattail, tules, willows, saltcedar, and mesquite (Borrelli and others, 1998). Saltcedar (*Tamarix pentandra*) is one of the most widespread and heavy users of water (Van Hylckma, 1970; Gay and Hartman; 1982; Weeks and others, 1987). Gay and Hartman (1982) report measured evapotranspiration to be 68 inches near Blythe, California, for a dense grove of saltcedar underlain by a 10-foot deep water table. Water use by mesquite for a normal season is estimated at 95 percent of the precipitation (Carlson and others, 1990). The transpiration rate is 44 percent greater in riparian (water table less than 5 feet) areas than transpiration rates in nonriparian areas (Cuoma and others, 1992).

Prior to clearing the land for farming, the primary discharge from the aquifers in the Lower Rio Grande Valley mainly occurred through evapotranspiration. Baker and Dale (1961) noted that a heavy growth of mesquite trees and brush in the area could have consumed as much as 3 acre-feet per acre per year. They further indicated that clearing land resulted in a substantial rise in the water table until it was near surface in some localities, causing direct evaporation and local accumulation of salts in the shallow groundwater.

Evapotranspiration losses from oak trees may amount to about 7,000 acre-feet per acre per year or about 6 million gallons per day in Jackson County, Texas (Baker, 1965). These estimates were based on maximum seasonal transpiration rates of 8 to 10 inches per acre for pine and hickory and 10 inches per acre for oak trees, assuming 60 year-old, even-aged, full-stocked stands (Raber, 1937). In parts of the irrigated areas in Cameron and southern Hidalgo counties, clearing the land of phreatophytes and applying irrigation water has caused groundwater to rise close to the land surface and water log soils (Wood and others, 1963).

The vegetation in the Lower Rio Grande Valley includes mesquite, live oak, marsh grass, salt cedar, and crops (Figure 5-29). Mesquite roots are considered the longest of any desert plant and can reach up to 160 feet deep in search of the water table (Phillips, 1963). Plants from arid environments or from environments with a long, dry season show the deepest rooting habits (Canadell and others, 1996). The downward growth of the roots is mainly limited by stratified

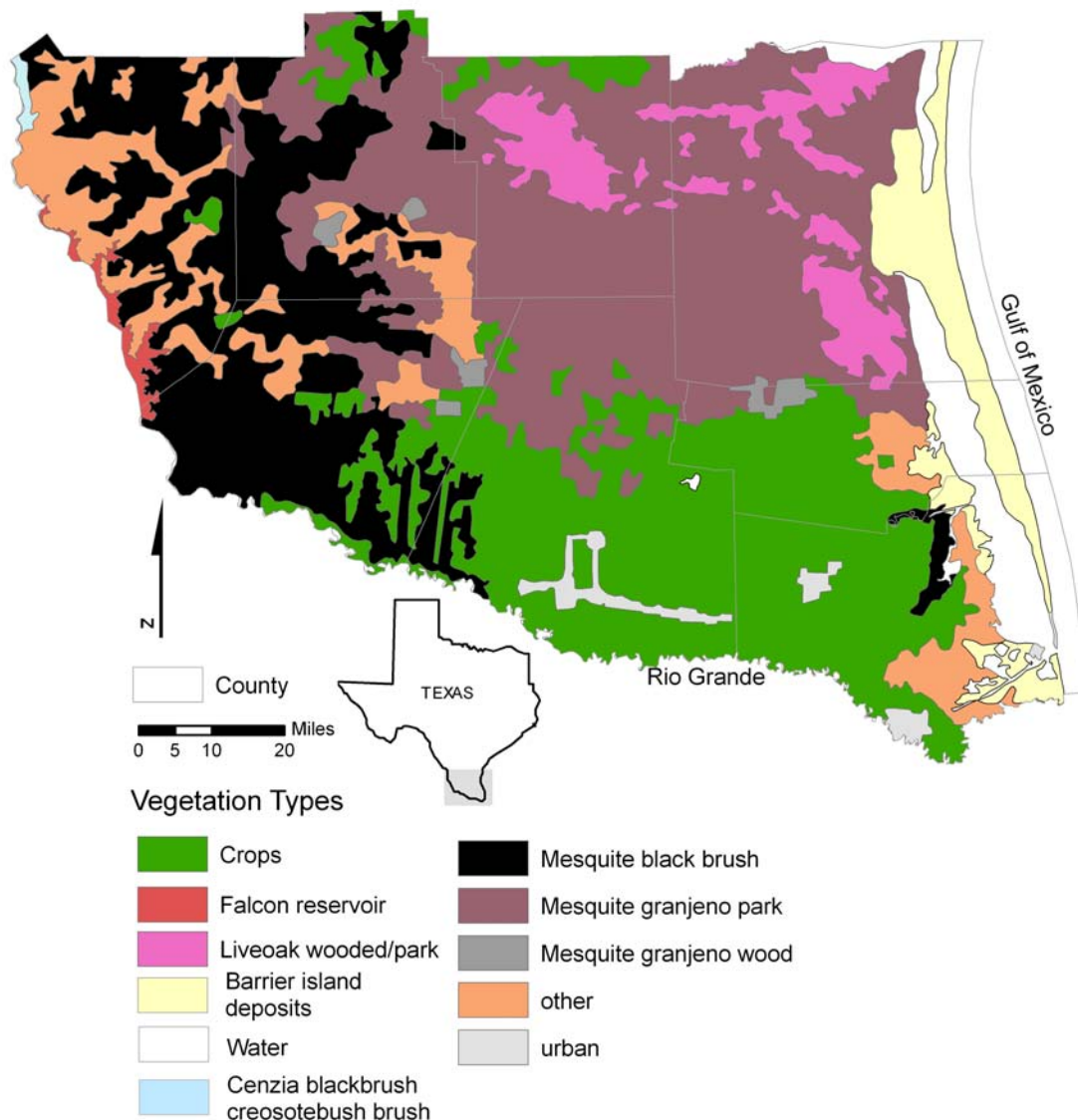


Figure 5-29. Vegetation types in the study area (data from Frye and others, 1984).

layers of shale and clay and depth to the water table (Dennis and others, 1978). Others report that these tap roots can even penetrate through rocky soils and hard pans (Canadell and others, 1996). Water extracted during the wet season comes from shallow layers but, as the shallow layers dry, there is a progressive shift toward deeper water (Gardner, 1983). Mesquite can consume significant quantities of water. Gatewood and others (1950) estimate water loss for mesquite to be 2.19 feet per year. However, evapotranspiration rates fluctuate considerably based on plant density, plant age, depth to water table, and precipitation rates.

Various crops grown in Hidalgo and Cameron counties may also potentially tap the water table. The main crops produced in the Lower Rio Grande Valley include corn, cotton, peanuts, sorghum, soybeans, and winter wheat. The growing season for these crops ranges from 118 to

206 days. Annual evapotranspiration for these crops ranges from 22 inches for sorghum to 34 inches for soybeans (Borrelli and others, 1998). Crop evapotranspiration is an important component of the hydrologic cycle as a whole, but it may not affect groundwater as water levels in the irrigated areas lie at depths of 20 to 30 feet below ground surface. These crops have shallow roots suggesting that they are sustained by applied irrigation water.

Historical groundwater pumpage information in the Lower Rio Grande Valley can be found in several county groundwater assessment reports (Dale, 1952; Baker and Dale, 1961; Myers and Dale, 1967; Shafer and Baker, 1973). Groundwater demand fluctuates considerably from year to year depending on surface water availability from the Rio Grande, temperature extremes, and rainfall conditions in the Lower Rio Grande Valley (Baker and Dale, 1961). During times of adequate surface water supply, many of the large wells are not used, making an accurate estimation of groundwater usage difficult. However, more recent pumpage information from 1980 to 2000 and predictive pumpage information from 2000 to 2050 are reported in the TWDB water use survey database and Regions M and N water plans (TCB, 2000).

The Evangeline Aquifer that crops out over two-thirds of Starr County provides most of Starr County's groundwater needs (Dale, 1952). About 300 primarily domestic and stock wells drilled during the 1950s pumped groundwater from the aquifer with well yields of up to 500 gallons per minute (Dale, 1952). In the alluvium aquifer in Starr County, the yields fluctuate widely and may range from 45 up to 1,200 gallons per minute (Dale, 1952; Baker and Dale, 1961). Some of the wells in the alluvium aquifer located as far as 2 miles from the Rio Grande dry up with the lowering of stages of the Rio Grande (Dale, 1952).

The Jasper Aquifer in northeastern Starr County produces considerable groundwater for irrigation and the oil industry. The wells have a maximum yield of up to 600 gallons per minute with an average well yield of 125 gallons per minute. Well depths range from 665 to 1,050 feet (Baker and Dale, 1961).

The Goliad Sand, Lissie Formation, Beaumont Clay, and the alluvium in southeastern Starr, southern Hidalgo, and western Cameron counties host numerous irrigation, domestic, and public supply wells. Maximum reported yield from these units was 2,900 gallons per minute with an average yield of 300 gallons per minute. Most of the groundwater in Brooks County comes from wells completed in the Goliad Sand that range in depth from 100 to 900 feet (Myers and Dale, 1967). Most of the groundwater in Kenedy County pumped from the Evangeline Aquifer is used for domestic and livestock purposes (Shafer and Baker, 1973). Shafer and Baker (1973) estimate that up to 13 million acre-feet of fresh water could potentially be stored in the Goliad Sand to a depth of 2,000 feet assuming a sand porosity of 30 percent.

The total annual demand for water in the Lower Rio Grande Valley area in 2000 was about 1,800,000 acre-feet under normal rainfall conditions. Even during the drought years, three-fourths of the total demand was available from surface water in the Rio Grande (TCB, 2000). For our study area, we estimated pumping for 1980 to 1999 based on the TWDB water use survey database (Figure 5-30, Tables 5-3 and 5-4). As 1999 pumping data was the most complete data set, we extrapolated this data to 2000. We estimated domestic pumping based on population

density distribution for 1990 and 2000. For historical domestic pumping, we used the 1990 population density cover, and we used 2000 population density cover for distributing domestic pumping through 2050 (Figures 5-31 and 5-32; Table 5-5). Irrigation and livestock pumping was distributed based on 1994 land use covers. We estimated predictive pumping based on drought-of-record demands reported by the regional water planning groups.

Annual pumpage data (1980 to 1999) by county and pumping categories (municipal, manufacturing, irrigation, domestic, and livestock) indicate that most of the groundwater withdrawal occurs from Hidalgo, Cameron, and Brooks counties (Figure 5-33, Tables 5-3 and 5-4). Groundwater pumping is the highest for irrigation followed by domestic, municipal, manufacturing, and livestock categories. Considerable fluctuation occurs in pumping from year to year due to occasional drought conditions that diminish surface water supplies, requiring existing users to switch to groundwater sources. Total groundwater pumping for 1980 was at 13,982 acre-feet per year and increased to 33,697 acre-feet per year in 1991. Groundwater pumping decreased to 24,288 acre-feet per year in 1999 (Figure 5-30).

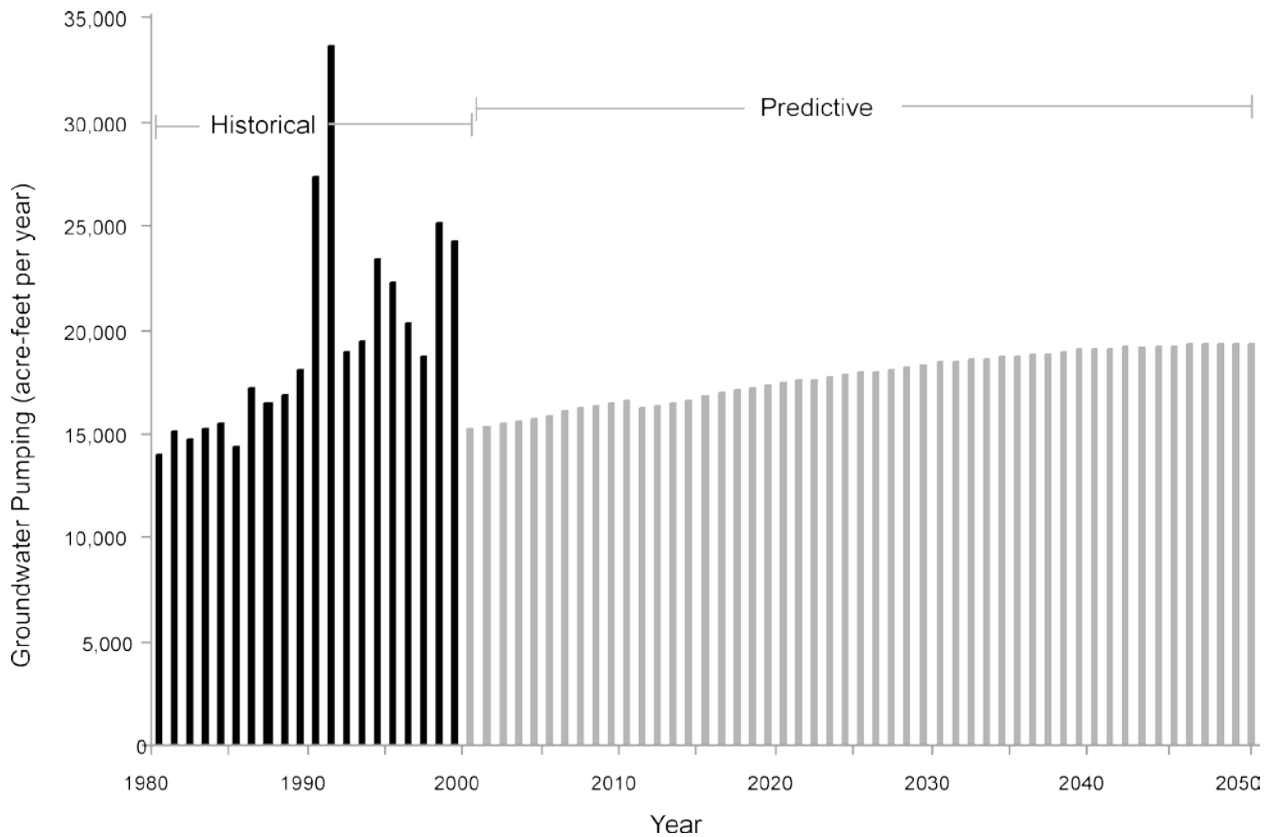


Figure 5-30. Total groundwater withdrawal from the Chicot and the Evangeline aquifers in the study area. Values for 1980 to 1999 are based on TWDB water use survey information. Values for 2000, 2010, 2020, 2030, 2040, and 2050 are estimated based on drought-of-record demands by the regional water planning groups in the area for their 2002 regional water plans. Note groundwater pumping values reflect pumping assigned only to active cells within the model area.

Table 5-3. Rates of groundwater withdrawal (in acre-feet per year) from the Chicot Aquifer within the total county areas of the modeled aquifer (1980 to 1999).

Municipal

County	1980	1981	1982	1983	1984	1985	1986	1987	1988	1989	1990
Brooks	0	0	0	0	0	0	0	0	0	0	0
Cameron	0	0	0	0	0	0	0	0	0	0	0
Hidalgo	909	1,484	755	731	648	623	1,419	878	1,287	964	757
Jim Hogg	0	0	0	0	0	0	0	0	0	0	0
Kenedy	0	0	0	0	0	0	0	0	0	0	0
Starr	0	0	0	0	0	0	0	0	0	0	0
Willacy	0	0	0	0	0	0	0	0	0	0	0

County	1991	1992	1993	1994	1995	1996	1997	1998	1999
Brooks	0	0	0	0	0	0	0	0	0
Cameron	0	190	6	288	410	466	511	416	320
Hidalgo	897	876	939	1,405	1,524	1,959	1,978	2,093	2,073
Jim Hogg	0	0	0	0	0	0	0	0	0
Kenedy	0	0	0	0	0	0	0	0	0
Starr	0	0	0	0	0	0	0	0	0
Willacy	0	0	0	0	0	0	0	0	0

Manufacturing

County	1980	1981	1982	1983	1984	1985	1986	1987	1988	1989	1990
Brooks	0	0	0	0	0	0	0	0	0	0	0
Cameron	55	43	40	49	0	0	0	25	37	37	42
Hidalgo	608	584	521	536	476	599	1,329	1,211	1,232	1,416	1,819
Jim Hogg	0	0	0	0	0	0	0	0	0	0	0
Kenedy	0	0	0	0	0	0	0	0	0	0	0
Starr	142	145	142	0	0	0	0	0	0	0	0
Willacy	0	0	0	0	0	0	0	0	0	0	0

County	1991	1992	1993	1994	1995	1996	1997	1998	1999
Brooks	0	0	0	0	0	0	0	0	0
Cameron	41	38	31	1	0	0	0	8	8
Hidalgo	1,230	1,103	984	1,093	1,167	2,190	2,705	3,119	2,971
Jim Hogg	0	0	0	0	0	0	0	0	0
Kenedy	0	0	0	0	0	0	0	0	0
Starr	0	0	0	0	0	0	0	0	0
Willacy	0	0	0	0	0	0	0	0	0

Irrigation

County	1980	1981	1982	1983	1984	1985	1986	1987	1988	1989	1990
Brooks	0	0	0	0	0	0	0	0	0	0	0
Cameron	251	250	249	248	247	277	284	291	298	305	569
Hidalgo	8,368	8,334	8,299	8,264	8,229	9,259	9,485	9,712	9,939	10,165	18,972
Jim Hogg	0	0	0	0	0	0	0	0	0	0	0
Kenedy	0	0	0	0	0	0	0	0	0	0	0
Starr	0	125	250	375	500	597	573	549	524	500	434
Willacy	0	0	0	0	0	0	0	0	0	0	0

Table 5-3. Continued

County	1991	1992	1993	1994	1995	1996	1997	1998	1999
Brooks	0	0	0	0	0	0	0	0	0
Cameron	552	230	360	415	369	227	161	0	0
Hidalgo	18,407	7,680	12,007	13,851	12,296	7,567	5,377	11,107	11,495
Jim Hogg	0	0	0	0	0	0	0	0	0
Kenedy	0	0	0	0	0	0	0	0	0
Starr	6,597	2,850	362	300	473	434	456	873	628
Willacy	0	0	0	0	0	0	0	0	0

<i>Domestic</i>											
County	1980	1981	1982	1983	1984	1985	1986	1987	1988	1989	1990
Brooks	0	0	0	0	0	0	0	0	0	0	0
Cameron	496	839	1,181	1,524	1,866	773	1,308	1,488	1,252	2,195	2,184
Hidalgo	1,876	2,336	2,796	3,255	3,715	2,446	3,101	2,886	2,546	3,023	3,530
Jim Hogg	0	0	0	0	0	0	0	0	0	0	0
Kenedy	0	0	0	0	0	0	0	0	0	0	0
Starr	14	123	233	343	452	364	661	648	576	338	430
Willacy	196	149	102	55	8	1	2	1	1	1	1

County	1991	1992	1993	1994	1995	1996	1997	1998	1999
Brooks	0	0	0	0	0	0	0	0	0
Cameron	2,058	1,825	1,667	1,922	1,778	2,448	2,993	2,440	1,874
Hidalgo	3,824	3,662	3,312	4,857	5,308	5,412	4,775	5,053	5,004
Jim Hogg	0	0	0	0	0	0	0	0	0
Kenedy	0	0	0	0	0	0	0	0	0
Starr	463	328	180	336	398	413	317	198	202
Willacy	0	0	0	0	0	0	0	0	0

<i>Livestock</i>											
County	1980	1981	1982	1983	1984	1985	1986	1987	1988	1989	1990
Brooks	0	0	0	0	0	0	0	0	0	0	0
Cameron	455	368	282	196	110	102	92	104	76	78	89
Hidalgo	9	8	7	7	6	5	24	5	20	21	22
Jim Hogg	0	0	0	0	0	0	0	0	0	0	0
Kenedy	0	0	0	0	0	0	0	0	0	0	0
Starr	3	3	3	3	3	4	3	3	3	3	3
Willacy	4	4	5	5	5	5	3	3	4	4	4

County	1991	1992	1993	1994	1995	1996	1997	1998	1999
Brooks	0	0	0	0	0	0	0	0	0
Cameron	92	146	144	91	102	92	110	88	127
Hidalgo	22	17	17	18	19	18	18	15	17
Jim Hogg	0	0	0	0	0	0	0	0	0
Kenedy	0	0	0	0	0	0	0	0	0
Starr	3	2	2	2	2	3	2	9	1
Willacy	4	3	3	2	2	3	3	3	3

Table 5-4. Rate of groundwater withdrawal (in acre-feet per year) from the Evangeline Aquifer within the county areas of the modeled aquifer (1980–1999).

Municipal

County	1980	1981	1982	1983	1984	1985	1986	1987	1988	1989
Brooks	872	880	922	1,030	1,043	882	1,089	653	749	1,050
Cameron	0	0	0	0	0	0	0	0	0	0
Hidalgo	0	0	0	0	0	0	0	0	0	0
Jim Hogg	0	0	0	0	0	0	0	0	0	0
Kenedy	23	22	20	20	20	21	23	24	24	24
Starr	0	0	0	0	0	0	0	0	0	0
Willacy	29	0	0	0	0	0	0	0	0	0

County	1991	1992	1993	1994	1995	1996	1997	1998	1999
Brooks	784	918	872	1,046	1,181	1,285	2,210	2,258	2,258
Cameron	0	0	0	0	0	0	0	0	0
Hidalgo	0	0	0	0	0	0	0	0	0
Jim Hogg	0	0	0	0	0	0	0	0	0
Kenedy	26	26	23	26	26	27	27	27	28
Starr	0	0	0	0	0	0	0	0	0
Willacy	0	0	29	0	0	0	0	0	0

Manufacturing

County	1980	1981	1982	1983	1984	1985	1986	1987	1988	1989
Brooks	202	186	186	179	158	158	159	36	159	20
Cameron	0	0	0	0	0	0	0	0	0	0
Hidalgo	0	0	0	0	19	22	0	0	0	0
Jim Hogg	0	0	0	85	81	119	119	133	118	12
Kenedy	6	6	6	6	6	6	6	6	5	4
Starr	226	264	268	271	291	282	253	392	362	105
Willacy	0	0	0	0	0	0	0	0	0	0

County	1991	1992	1993	1994	1995	1996	1997	1998	1999
Brooks	14	14	9	2	2	0	0	127	127
Cameron	0	0	0	0	0	0	0	0	0
Hidalgo	2	1	2	1	9	1,137	453	522	498
Jim Hogg	0	0	0	0	0	0	0	0	0
Kenedy	4	1	1	0	0	0	0	1	1
Starr	131	131	7	8	8	136	0	239	239
Willacy	0	0	0	0	0	0	0	0	0

Irrigation

County	1980	1981	1982	1983	1984	1985	1986	1987	1988	1989
Brooks	301	260	218	177	136	251	501	501	501	282
Cameron	0	0	0	0	0	0	0	0	0	0
Hidalgo	380	378	376	375	373	420	0	0	0	461
Jim Hogg	0	0	0	0	0	0	0	0	0	0
Kenedy	0	0	0	0	0	0	0	0	0	0
Starr	0	0	0	0	0	0	0	0	0	0
Willacy	0	0	0	0	0	0	0	0	0	0

Table 5-4. Continued.

County	1991	1992	1993	1994	1995	1996	1997	1998	1999
Brooks	727	601	361	466	466	466	466	465	465
Cameron	0	0	0	0	0	0	0	0	0
Hidalgo	835	348	545	628	558	343	244	504	522
Jim Hogg	0	0	0	0	0	0	0	0	0
Kenedy	0	0	0	0	0	0	0	0	0
Starr	0	0	0	0	0	0	0	0	0
Willacy	0	0	0	0	0	0	0	0	0

<i>Domestic</i>										
County	1980	1981	1982	1983	1984	1985	1986	1987	1988	1989
Brooks	206	246	286	326	367	400	430	278	264	246
Cameron	0	0	0	0	0	0	0	0	0	0
Hidalgo	165	205	245	284	324	216	273	254	225	257
Jim Hogg	16	17	19	20	22	16	20	37	33	25
Kenedy	75	71	67	63	58	40	43	39	36	18
Starr	114	128	142	156	170	172	196	205	202	189
Willacy	284	216	148	80	12	2	3	1	1	1

County	1991	1992	1993	1994	1995	1996	1997	1998	1999
Brooks	254	259	259	267	262	258	261	267	267
Cameron	0	0	0	0	0	0	0	0	0
Hidalgo	603	577	522	765	849	853	753	796	789
Jim Hogg	121	146	121	115	101	132	53	836	598
Kenedy	12	11	11	21	12	20	38	37	40
Starr	269	270	272	285	194	198	201	126	129
Willacy	0	0	0	0	0	0	0	0	0

<i>Livestock</i>										
County	1980	1981	1982	1983	1984	1985	1986	1987	1988	1989
Brooks	97	92	88	83	78	70	80	82	85	84
Cameron	0	0	0	0	0	0	0	0	0	0
Hidalgo	146	134	123	111	99	87	404	83	331	344
Jim Hogg	40	39	39	38	37	35	29	27	29	29
Kenedy	125	119	112	105	98	82	86	98	104	103
Starr	48	47	47	47	47	48	50	45	45	47
Willacy	18	18	19	19	20	19	15	14	17	18

County	1991	1992	1993	1994	1995	1996	1997	1998	1999
Brooks	87	66	66	61	60	64	66	51	54
Cameron	0	0	0	0	0	0	0	0	0
Hidalgo	372	279	280	298	313	290	294	253	287
Jim Hogg	29	47	47	37	37	41	41	58	58
Kenedy	104	67	82	66	61	67	58	84	89
Starr	46	41	42	38	44	56	34	170	26
Willacy	19	14	14	11	12	13	13	15	12

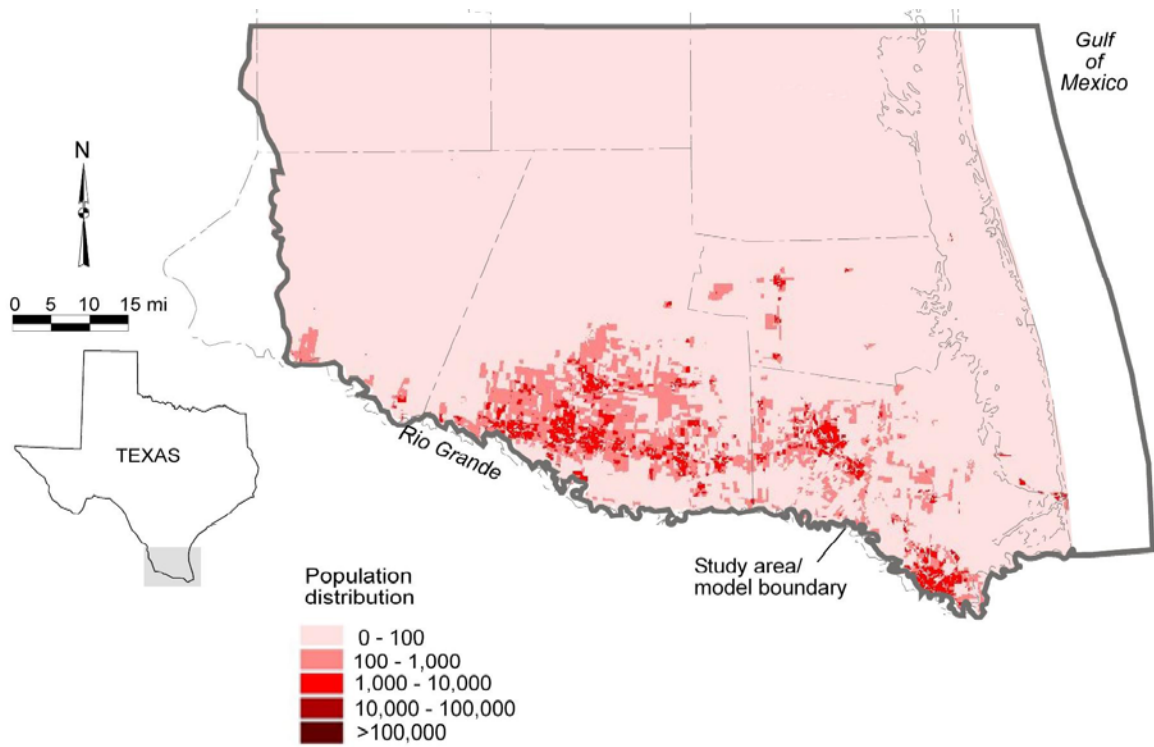


Figure 5-31. Map of population density for 1990 (data from the Texas State Data Center, txsdc.tamu.edu; mi = miles).

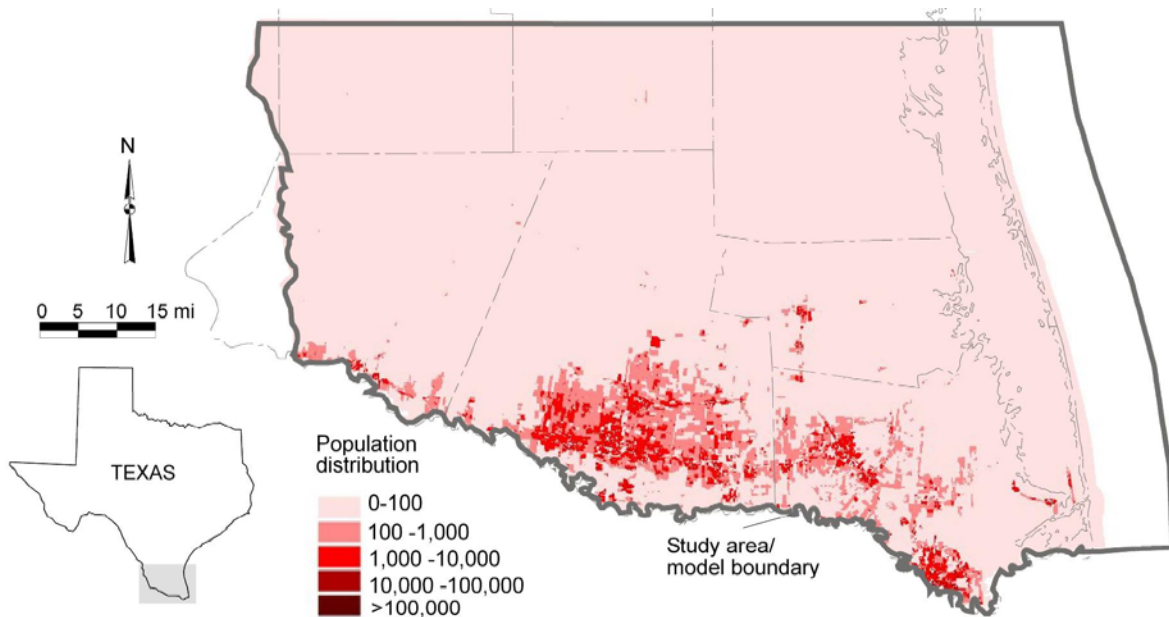


Figure 5-32. Map of population density for 2000 (data from the Texas State Data Center, txsdc.tamu.edu; mi = miles).

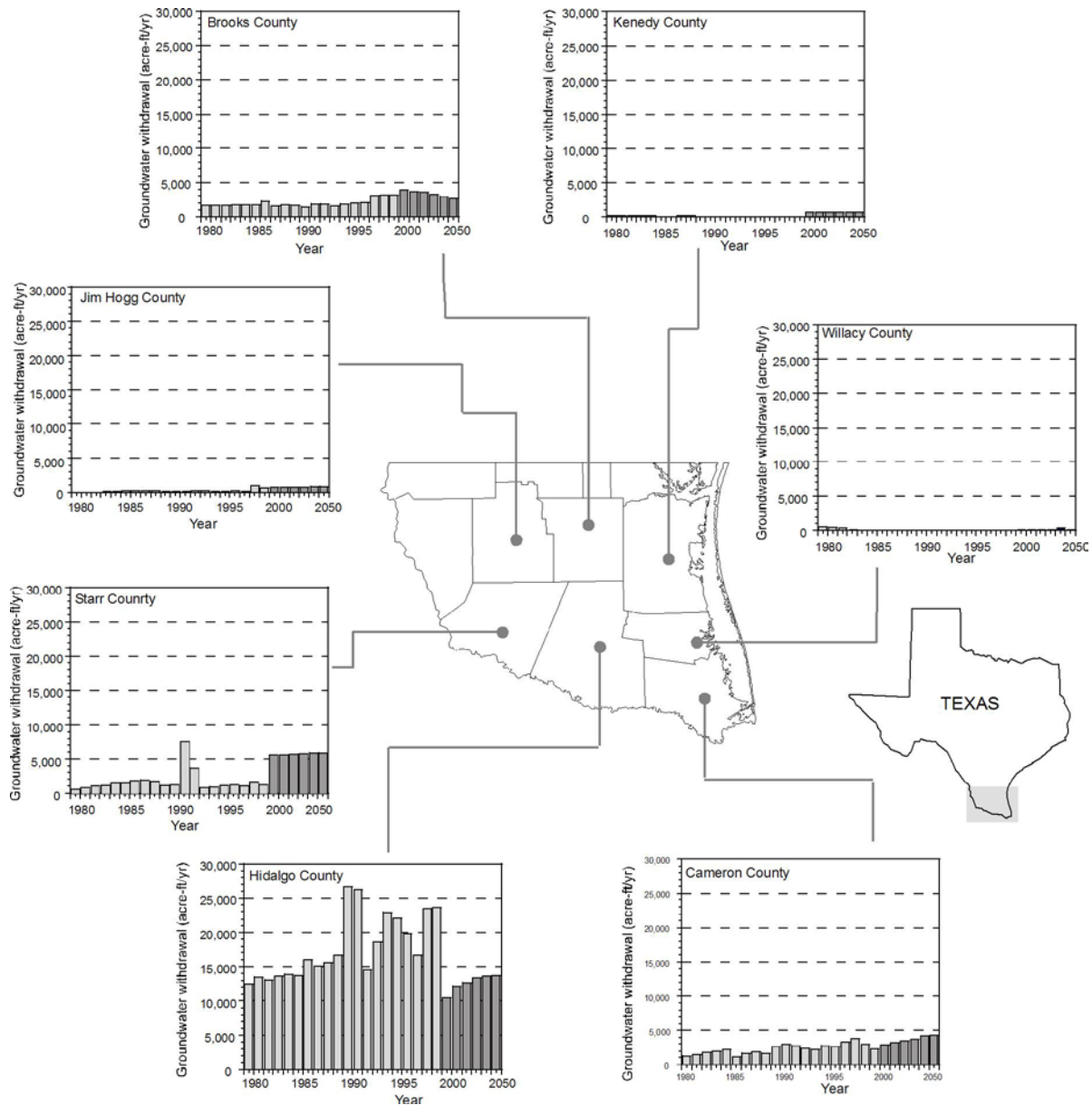


Figure 5-33. Total groundwater withdrawals from the Chicot and Evangeline aquifers for the counties covering the study area. Groundwater pumping values for 1980 to 1999 are based on the TWDB water use survey. Pumping values for 2000, 2010, 2020, 2030, 2040, and 2050 are estimated based on dry demands by the regional water planning groups in the area for their 2001 regional water plans (acre-ft/yr = acre-feet per year).

Table 5-5. Predictive total groundwater withdrawal estimates (in acre-feet per year) by (a) category and decade and by (b) county and decade within the model area.

(a)

Category	2000	2010	2020	2030	2040	2050
Domestic	6,937	7,728	8,612	8,847	9,423	9,581
Irrigation	8,816	8,805	8,796	8,786	8,777	8,768
Manufacturing	1,992	1,890	1,896	1,878	1,978	2,055
Municipal	6,055	6,577	7,050	7,568	7,444	7,337
Stock	2,647	2,647	2,647	2,647	2,647	2,647

(b)

County	2000	2010	2020	2030	2040	2050
Brooks	371	451	420	382	354	330
Cameron	2,712	2,712	3,023	3,207	3,702	3,858
Hidalgo	10,022	11,082	11,593	12,308	12,424	12,514
Jim Hogg	371	374	372	375	378	379
Kenedy	527	527	593	550	548	548
Starr	1,260	1,261	1,358	1,459	1,566	1,621
Willacy	145	144	134	133	133	134

6.0 Groundwater quality

Knowing groundwater quality is important for identifying sources of fresh water or water for desalination, and understanding water quality distribution characteristics in an aquifer can help define a groundwater flow system. For example, the presence of older saline groundwater may indicate a lack of circulation from recent recharge events and/or hydraulic compartmentalization, with significant implications for how aquifers are used. Although significant quantities of groundwater occur in the Gulf Coast Aquifer in sections where sands are dominant, much of this groundwater resource is not directly usable due to its moderate to high salinity. Groundwater is generally fresh in most of the outcrop but increases in salinity at depth and along flow paths toward the coast. Groundwater quality in the Gulf Coast Aquifer of the Lower Grande Valley is particularly important because of the (1) significant demand for good quality water, (2) supply of surface water resources that is often interrupted by droughts, and (3) aquifer heterogeneity that makes it difficult to discern the groundwater quality distribution trend. Understanding the water quality trend is of paramount importance in order to fully use the desalination potential of the aquifer. Because groundwater in the southern parts of the Gulf Coast Aquifer of the Lower Rio Grande Valley has not been excessively used, it may contain significant volumes of water that could be desalinated (TCB, 2000).

Several investigators have reported on the groundwater quality of the Lower Rio Grande Valley (Myers and Dale, 1967; Preston, 1983; Knape, 1984; McCoy, 1990; Paine and others, 2001; Chowdhury and Mace, 2002; Chowdhury and Mace, 2004b; Chowdhury and others, 2006). The best quality groundwater is found near the Rio Grande in the south. The overall quality progressively deteriorates in areas away from the Rio Grande. Groundwater quality also abruptly varies in closely spaced wells due to rapid facies changes and heterogeneity of the aquifer

materials. We describe below a summary of groundwater quality information on the southern parts of the Gulf Coast Aquifer in the Lower Rio Grande Valley.

Myers and Dale (1967) identified that the base of the fresh water rapidly varies across the valley. For example, the fresh water base lies at an elevation of about 50 feet near Falfurrias. Farther downdip in southern Kenedy County, the fresh water base lies at much greater depth, at an elevation of about -2,300 feet. In addition to groundwater salinization by natural processes, suspected oil field waters stored in unlined pits could be a source of groundwater salinization. Excessive salinity of these waters, ranging from 22,000 to 147,000 parts per million, suggests possible salinization of these aquifers from leakage of these unlined pits.

Preston (1983) suggested that groundwater quality deteriorates with distance from the Rio Grande and with depth. He observed that the groundwater could well be chemically stratified at different stratigraphic intervals (less than 75 feet, 75 to 150 feet, and 150 to 225 feet) in Brownsville and vicinity. He observed more mineralized water with high total dissolved solids values (5,000 to 37,500 parts per million) at depths of less than 75 feet. The intermediate total dissolved solids values (1,180 to 13,450 parts per million) occurred between 75 to 150 feet. The total dissolved solids slightly decrease (770 to 11,900 parts per million) at depths of 150 to 225 feet. He attributed the salinity at shallower depths to be caused by a number of factors, including seawater blown from the gulf, leaching of minerals deposited on the salt flats, and/or concentration of minerals caused by evaporation and plant usage.

Knape (1984) reported on the drainage well systems that were installed in the Lower Rio Grande Valley to help with the problems of raised water tables. Water tables are locally raised due to the presence of smectite clays that impede percolation of surface waters and result in perched water tables. Shallow water tables in these areas with high smectite further expose the water table to evaporation, thus increasing groundwater salinity. In order to address this water logging problem, the drainage lines installed are perforated, packed in gravel to aid percolation, and installed in parallel at a spacing of 75 to 225 feet and at a depth of 6 feet. The drainage lines lead to a central collector or drainage well that discharges into the ground.

McCoy (1990) compared the groundwater quality (commonly less than 3,000 milligrams per liter of total dissolved solids) with surface water from the Rio Grande (400 to 750 milligrams per liter of total dissolved solids). However, land areas that receive recharge from the Rio Grande have not been identified. McCoy (1990) observed that the alluvial and deltaic deposits and shallow sediments covering small areas in southern Hidalgo, southwestern Cameron, and north central Hidalgo County counties contain fresh water, indicating effects of local recharge.

Chemical stratification of the groundwater was further demonstrated using geophysical methods (Paine and others, 2001). They used airborne electromagnetic induction to identify groundwater resources and their quality in the Faysville and Stockholm areas of the Lower Rio Grande Valley. Electromagnetic methods measure electrical conductivity of the water—fresh water has low electrical conductivity, and saline water has high electrical conductivity. At high total dissolved solids, water quality dominates the conductivity signal, whereas at low total dissolved solids, sediment texture, porosity, and mineral composition dominate conductivity response. Based on this approach, Paine and others (2001) identified nine fresh to slightly saline areas in

the Faysville area and five fresh to moderately saline areas in the Stockholm area. Limited ground-based electromagnetic measurements at these sites also agreed with the conductivity values and spatial trends determined from the airborne method.

Chowdhury and Mace (2004b) used chemical and isotopic compositions to determine the origins of the groundwater across the Lower Rio Grande Valley. They suggested that multiple factors are responsible for salinity, including evaporation, halite dissolution, and cation exchanges of the dissolved calcium in the groundwater with sodium attached on clay surfaces. Based on the tritium and percentage of modern carbon distributions in the area, they suggested that the groundwater in the area consists of (1) remnant paleogroundwater in areas where the groundwater is stagnant because of interbedded clays that often compartmentalize the flow system and (2) modern groundwater in areas where coarser sediments allow adequate infiltration of modern recharge from precipitation and leakage of river water from the Rio Grande.

Chowdhury and others (2006) described hydrogeochemistry and sources of groundwater salinity in the Texas Gulf Coast. They suggested that the salinity differences in the groundwater are mainly controlled by lithologic compositions of the aquifer materials, evaporation, dissolution-precipitation reactions, and cation exchanges. Based on low bromide-to-chloride ratios, they suggested that part of the salinity could locally be contributed by dissolution of halite from salt domes and/or evaporite contained in the aquifer materials. They observed no significant trends in groundwater salinity changes due to a rise or decline in water levels.

All water quality data that we have examined for this study come from the TWDB groundwater quality database. We only included charge-balanced samples for our evaluation. We analyzed 300 groundwater samples for major ions derived mostly from the Chicot and the Evangeline aquifers.

Groundwater in the Lower Rio Grande Valley varies widely in composition from fresh to brine (198 to 37,752 milligrams per liter). Of the nearly 300 samples examined, we found that the Chicot Aquifer has 14 percent fresh, 48 percent slightly saline, and 33 percent moderately saline waters. The Evangeline Aquifer has 27 percent fresh, 65 percent slightly saline, and 6 percent moderately saline waters. However, more saline waters are encountered at depths of less than 600 feet (Figure 6-1). Groundwater in west Starr, south central Cameron, and central Willacy counties have the highest total dissolved solid values (Figure 6-2). Large areas in north central Brooks, northern Hidalgo, eastern Starr, and western Willacy counties have fresh to slightly saline water. We did not observe any trend in the distribution of the total dissolved solids either in the outcrop or in groundwater flowing deeper toward the discharge areas in the direction of the gulf (Figure 6-2). For example, some moderately saline water zones occur in southern Hidalgo County. However, fresh water zones appear farther downdip indicating multiple sources of recharge water.

The water quality data show that slightly saline to moderately saline water is more common at depths of less than 100 feet. Fresh water occurs more frequently at depths of 300 to 1,000 feet in both the Evangeline and Jasper aquifers in Brooks County and at depths of 100 to 300 feet along

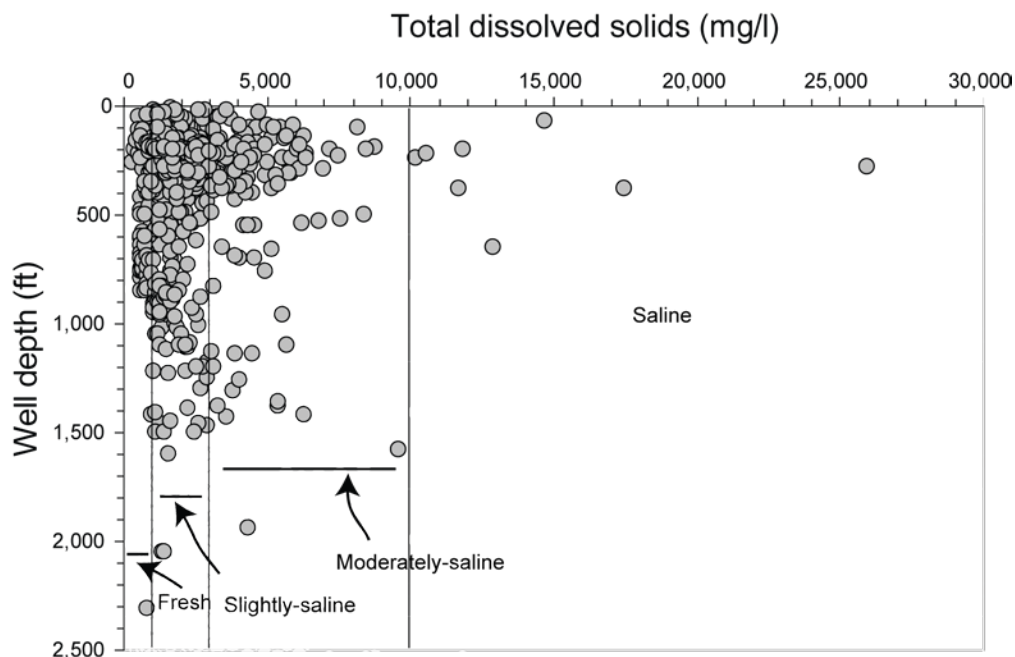


Figure 6-1. Total dissolved solids versus well depth in the study area. Note that some of the water with high total dissolved solids occurs at shallow depths (ft = feet, mg/l = milligrams per liter).

the Rio Grande in Hidalgo and Cameron counties. When total dissolved solids are plotted against well depth, there is no preferential occurrence except at shallow depth (Figure 6-1). This enrichment in salinity may partially be due to upward movement of more saline groundwater into the shallow aquifer and perhaps to leakage of irrigation water into the shallow subsurface.

Using the spatial distribution of the total dissolved solids, we estimated the volume of fresh to moderately saline water (0 to 3,000 milligrams per liter) present in the Chicot and the Evangeline aquifers. We identified areas that contain fresh to moderately saline water. We used the following assumptions: (1) total dissolved solids remain constant spatially and vertically for the entire thickness of the aquifer and (2) a drainable porosity of 0.15. Using the aquifer thickness, porosity, and geographic area, we estimated the volumes of fresh to moderately saline water. We estimated that about 39,000,000 acre-feet of fresh to moderately saline water occurs in the Chicot Aquifer and about 230,000,000 acre-feet of fresh to moderately saline water occurs in the Evangeline Aquifer. The quantity of fresh to moderately saline water reported represents only a small volume of the total groundwater present in these aquifers. In addition, since we considered the total thickness of the aquifer in our estimates, the volume of water fitting the water quality category may be overestimated as groundwater salinity deteriorates with increasing depth. In a detailed investigation of the brackish water resources (fresh to moderately saline) across the state, LBG-Guyton (2003) reported that the Gulf Coast Aquifer contains about 138,000,000 acre-

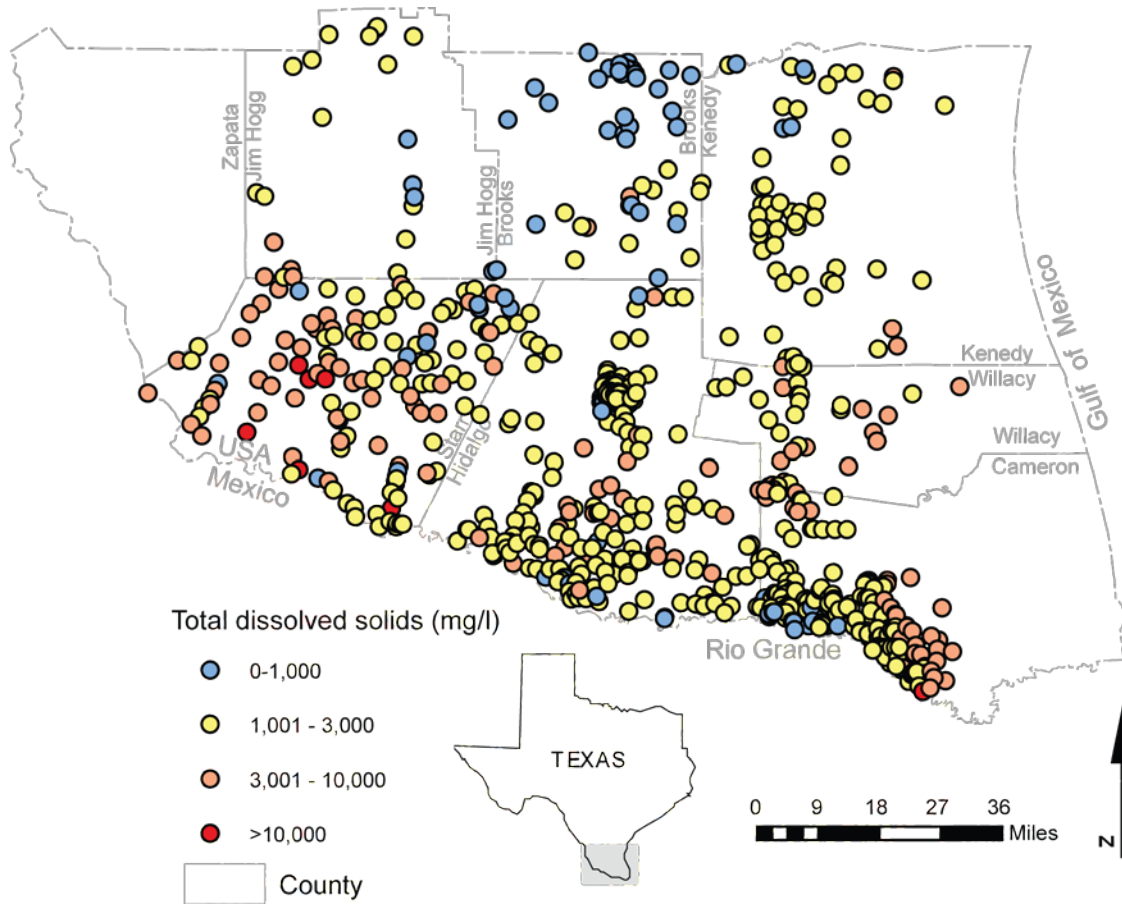


Figure 6-2. Distribution of total dissolved solids in the Chicot and Evangeline aquifers in the study area. Note that fresher water (less than 1,000 milligrams per liter of total dissolved solids) is present near the Rio Grande, in northern parts of Brooks County, and sporadically in other areas (mg/l = milligrams per liter).

feet of brackish water in Region N and 46,000,000 acre-feet of brackish water in Region M. However, these values are lower than what we presented in the previous paragraph mainly due to the inclusion of fresh water in the calculation. Estimated volumes were reported for fresh to moderately saline range due to the difficulty in separating the fresh water areas from moderately saline water areas. These estimates of fresh to moderately saline water are subject to change as better information becomes available on the lateral and vertical distribution of water quality. Our groundwater modeling results indicate that about 88,000 acre-feet of groundwater flows through the aquifer annually (see Section 11.2 Water budget). Comparing the total annual flux with the estimated volume of fresh to moderately saline water suggests that groundwater flows rather slowly throughout most of the aquifer (Chowdhury and Mace, 2004a). Therefore, it is likely that much of the groundwater may represent relatively older formation water.

7.0 Conceptual model of groundwater flow in the aquifer

A conceptual model is a description of our best understanding of the groundwater flow system (Figure 7-1). When rain falls on the outcrop areas of the aquifers, much of the water is lost through evapotranspiration or runs off into local streams to join the major rivers and eventually discharge into the Gulf of Mexico. A small percentage of the rainfall percolates through the soils to reach the water table in the aquifer below. Leakage through numerous canals may also locally funnel additional recharge to the aquifer. However, this portion of recharge in the shallow parts of the aquifer may not reach the groundwater table either due to the presence of clay lenses that make the water pond in perched portions of the aquifer or because water may just seep along irrigation drainage ditches that lie at lower elevations from the canals. Sections of the Rio Grande that lose water may also locally recharge the shallow aquifers, particularly in Hidalgo and Cameron counties.

The lithology in the outcrop areas may largely determine rates of infiltration into the aquifer. Unlike the Gulf Coast Aquifer in the northeast part of Texas, the Beaumont Clay in the Lower Rio Grande Valley is mainly composed of sand with lesser amounts of clay that may allow direct recharge from rainfall near the coast. Caliche-cemented areas of the aquifers, however, can hinder direct recharge from rainfall or resist groundwater flow across it. The presence of significant amounts of interbedded clays in the subsurface may also hydrologically compartmentalize the flow system locally, resulting in stagnating groundwater and/or diminished groundwater flow within and between the subjacent aquifers.

As waters flow from the recharge to the discharge areas, pressure differences force groundwater to move vertically upward resulting in groundwater discharge in the coastal areas. In addition, when groundwater reaches the coastline, it encounters the freshwater-saltwater interface that essentially acts as a no-flow boundary, causing water to move upward. Where the Burkeville Confining System is absent, all three aquifers are in direct hydraulic contact, allowing for increased vertical mixing of the waters. Where present, the Burkeville Confining System retards downward flow. A considerable volume of water that flows through the Evangeline Aquifer may move upwards into the Chicot Aquifer farther down dip.

Groundwater that flows through the Gulf Coast Aquifer discharges naturally through reaches of the Rio Grande and Arroyo Colorado. In parts of the Lower Rio Grande Valley, where there are phreatophytes and the water table is at a relatively shallow depth, considerable volumes of water may be extracted through transpiration. Agricultural lands occupy large areas of Cameron, Willacy, and Hidalgo counties. Most of these lands have annual crops with roots that do not penetrate to great depths. Given the limited depth of the root systems of these plants and the fact that they derive most of the water from irrigation, we have not considered their role, if any, in water loss from the groundwater table. Therefore, no evapotranspiration values were assigned for these areas where crops are being cultivated.

Most of the pumping in the Lower Rio Grande Valley is widely dispersed, although three major pumping areas lay along the Rio Grande in southwestern Starr and northern Brooks counties. Irrigation uses the largest volume of groundwater in the Lower Rio Grande Valley. In a wet year, when surface water is readily available, groundwater pumping can drop considerably. As a result, groundwater pumping fluctuates widely from year to year.

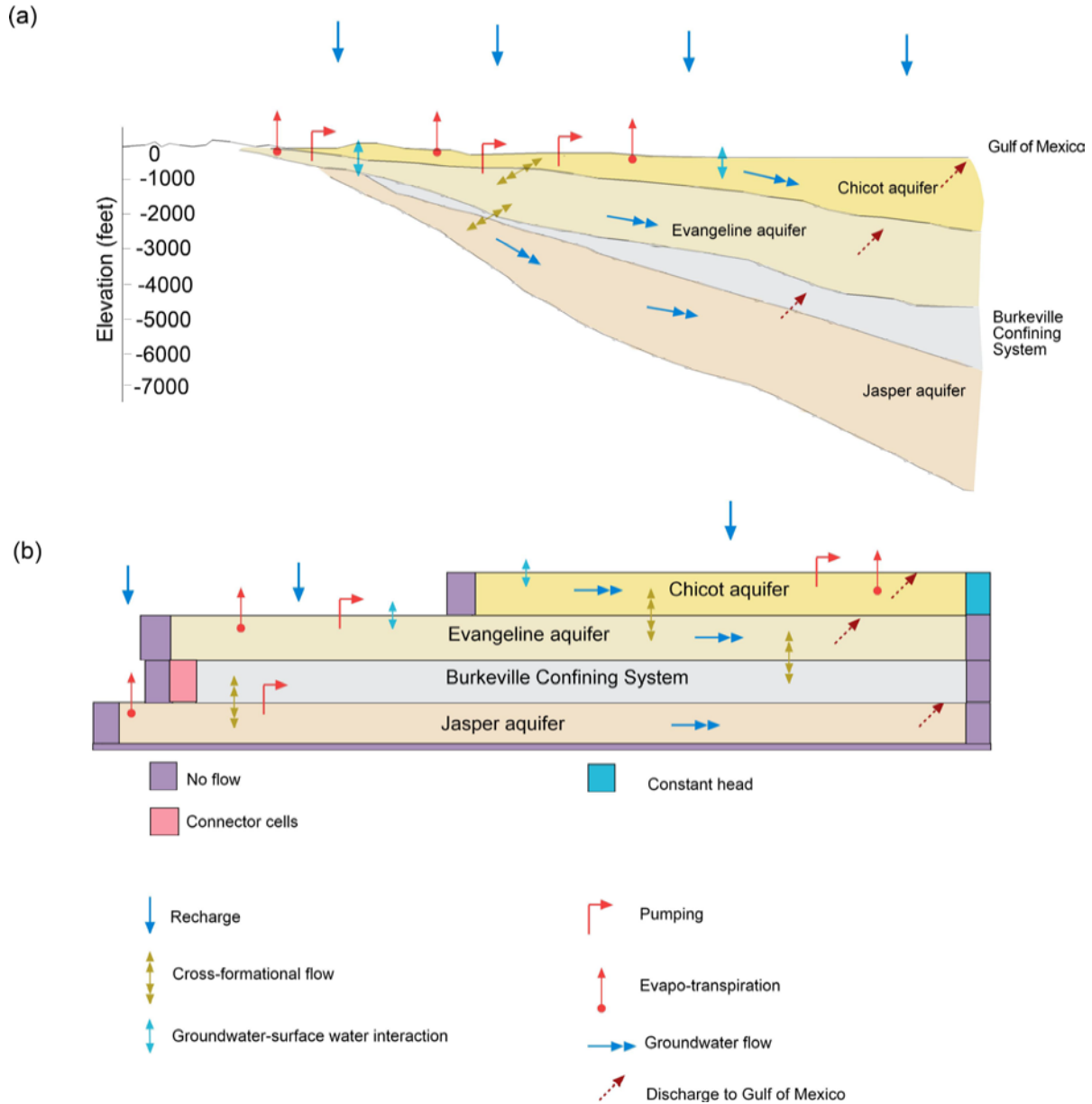


Figure 7-1. Conceptual model of the aquifer showing (a) recharge, discharge, and cross-formational flow between the layers along an east-west direction (see Figure 5-12 for position of cross section line) and (b) the numerical translation of the conceptualization for model simulation.

8.0 Model design

In the model design process, we assembled the different elements of the conceptual model into a form suitable for numerical modeling that would reproduce the groundwater flow system. During the design process, we selected the code and the processor, grid layout, time steps, boundary conditions, initial conditions, and preliminary values for hydraulic parameters and pumping.

8.1 Code and processor

We used MODFLOW-96 (Harbaugh and McDonald, 1996), a widely used modular finite-difference groundwater flow code written by the U.S. Geological Survey, to model groundwater flow in the Gulf Coast Aquifer of the Lower Rio Grande Valley. We chose MODFLOW-96 because it (1) can simulate the hydrogeologic processes necessary to model the Gulf Coast Aquifer, (2) is well documented (McDonald and Harbaugh, 1988) and widely used (Anderson and Woessner, 1992, p. xvi), (3) has a number of third-party pre- and post-processors available to make the model easy to use, and (4) is available through the public domain. To help us with loading information into the model and observing model results, we used Processing MODFLOW for Windows (PMWIN) version 5.0.54 (Chiang and Kinzelbach, 1998). Other pre- and post-processors should be able to read the source files for MODFLOW-96. We developed and ran the model on a Dell OptiPlex GX1p with a 450 MHz Pentium II Processor and 128 MB RAM running Windows 98.

8.2 Layers and grid

The lateral extent of the model mainly coincides with natural hydrologic boundaries, such as the outcrop limits of the Catahoula Sand or Tuff in the west, the Rio Grande in the south, and a groundwater flow line in the north. In the east, the model boundary was drawn at 10 miles offshore into the Gulf of Mexico. Based on the hydrostratigraphy and conceptual model, we designed the model to contain the Chicot, Evangeline, and Jasper aquifers. Layer 1 represents the Chicot Aquifer, layer 2 the Evangeline Aquifer, layer 3 the Burkeville Confining System, and layer 4 the Jasper Aquifer. We did not include the Anahuac Formation that underlies the Jasper Aquifer in the model because (1) it is not heavily used due to its poor water quality, (2) there is little information on it, (3) it is very thick (up to 5,000 feet), and (4) it has low hydraulic conductivity.

Each layer has 125 rows and 135 columns for a total of 67,500 cells in the model. All the cells have uniform lateral dimensions of 1 mile by 1 mile. We chose this cell size to be small enough to reflect the density of input data and the desired output detail and large enough for the model to be manageable. The uniform cell size allowed us to use spreadsheets and grid-based contouring programs to easily manipulate input data. Cell thickness depended on the elevation of the contacts between the different layers. The model had a total of 27,007 active cells: 4,952 active cells in layer 1; 7,250 active cells in layer 2; 7,280 active cells in layer 3; and 7,525 active cells in layer 4 (Figures 8-1, 8-2, 8-3, and 8-4).

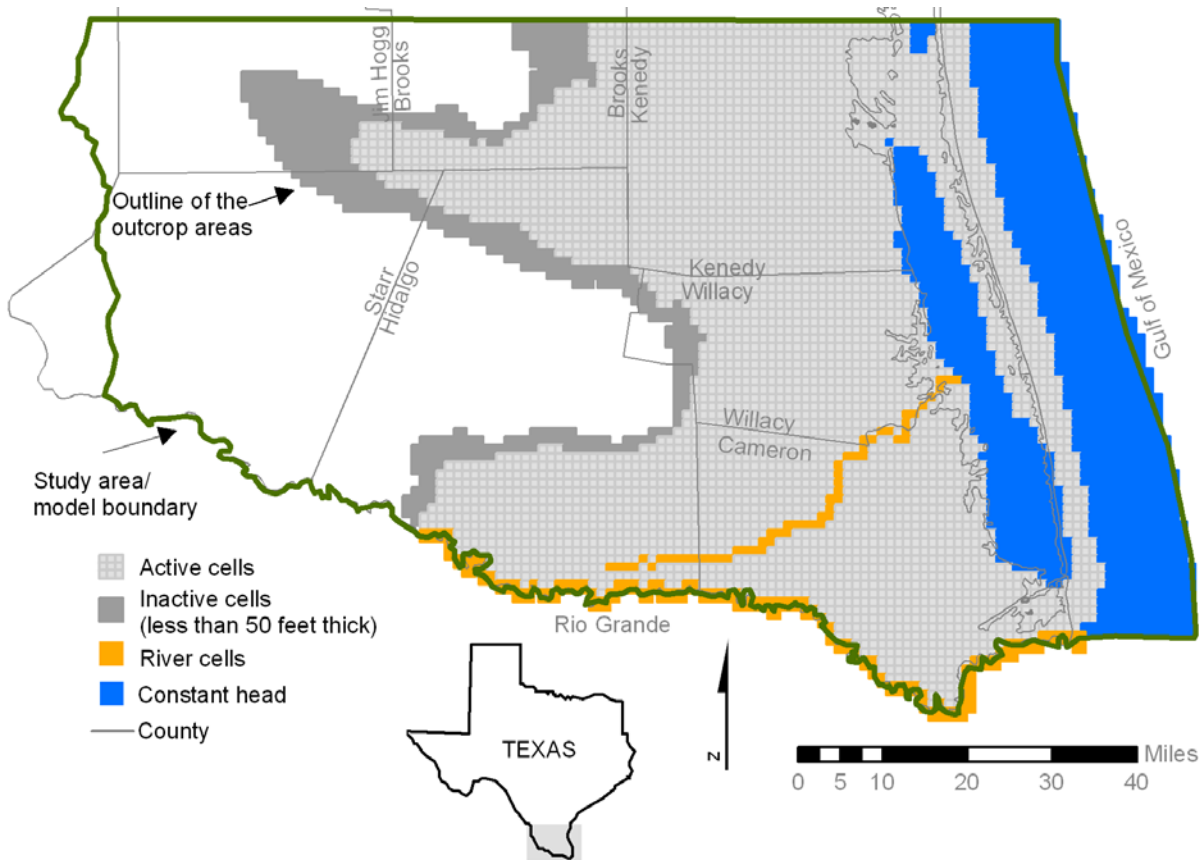


Figure 8-1. Active cells and boundary assignments in layer 1 of the model (Chicot Aquifer). Inactive cells noted on the map are cells with an aquifer thickness (land surface elevation minus the elevation of the bottom of the aquifer) less than 50 feet thick. We changed these cells from active to inactive to assist in stabilizing the model.

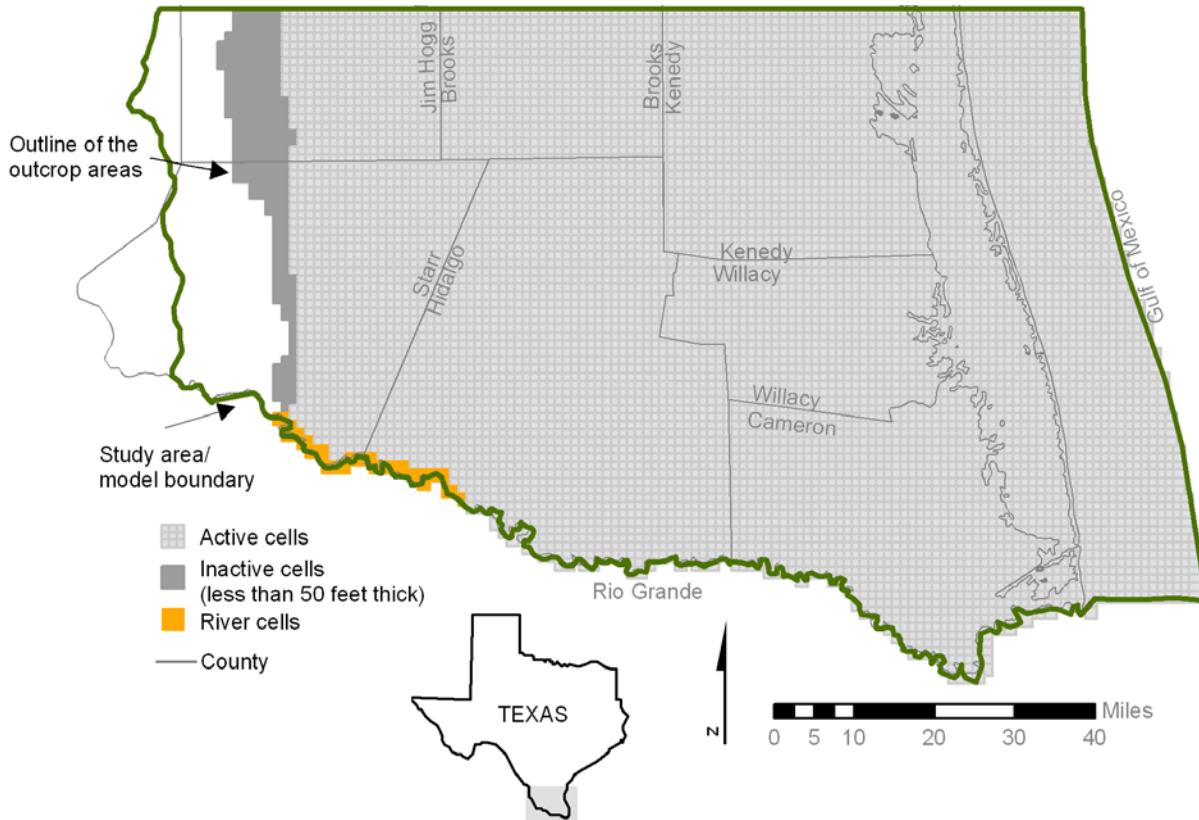


Figure 8-2. Active cells and boundary assignments in layer 2 of the model (Evangeline Aquifer). Inactive cells noted on the map are cells with an aquifer thickness (land surface elevation minus the elevation of the bottom of the aquifer) less than 50 feet thick. We changed these cells from active to inactive to assist in stabilizing the model.

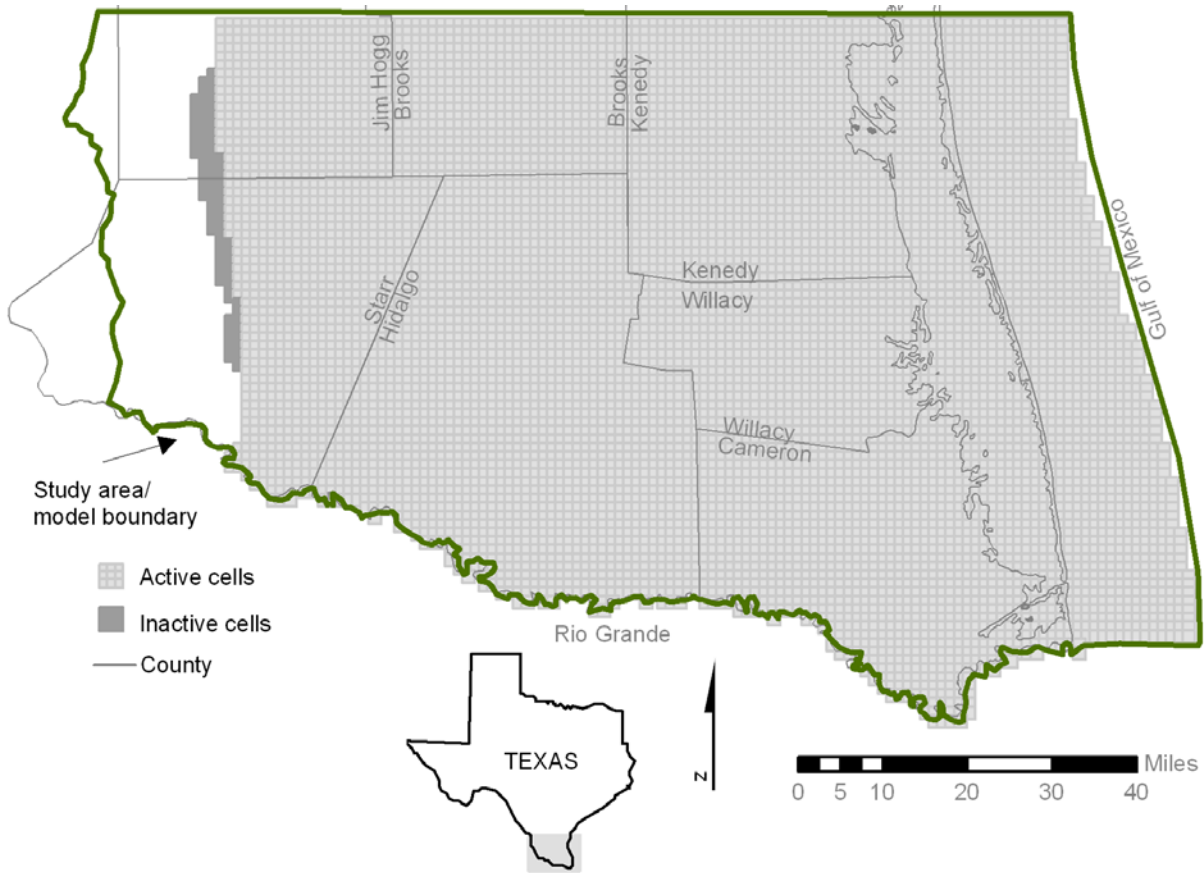


Figure 8-3. Active cells and boundary assignments in layer 3 of the model (Burkeville Confining System plus cells added to allow a hydraulic connection between the Jasper and Evangeline aquifers where the Burkeville Confining System has pinched out).

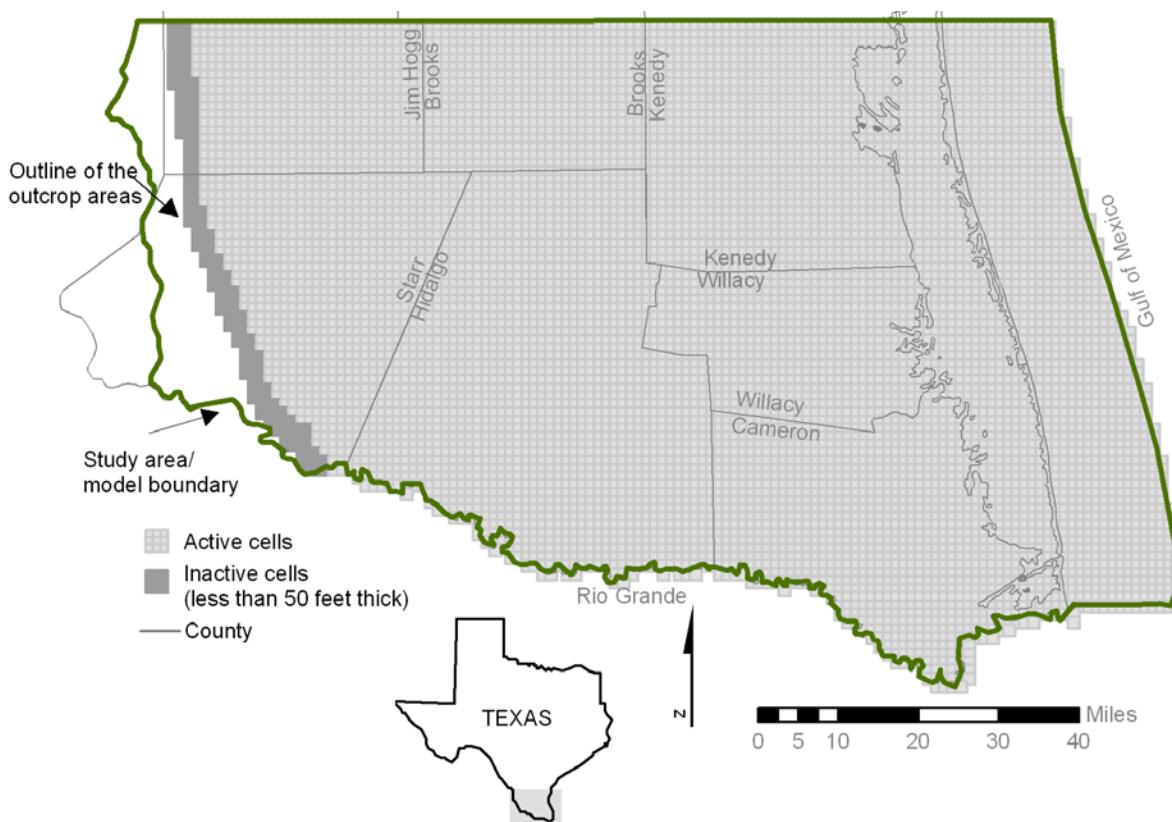


Figure 8-4. Active cells and boundary assignments in layer 4 of the model (Jasper Aquifer). Inactive cells noted on the map are cells with an aquifer thickness (land surface elevation minus the elevation of the bottom of the aquifer) less than 50 feet thick. We changed these cells from active to inactive to assist in stabilizing the model.

We assigned active and inactive cells using the lateral extent of the formations as indicated on the geology map (Figure 8-5). A cell was active if the aquifer covered more than 50 percent of the cell area. We assigned cells as inactive if the aquifer thickness was less than 50 feet, if the cell was south of the Rio Grande, and if the aquifer did not exist in the cell. We originally assigned the full extent of each aquifer as active; however, during calibration we needed to make active cells with aquifer thicknesses less than 50 feet inactive to stabilize the model. We included the dune sands in the northwestern part of the model area into the Chicot Aquifer because some shallow wells tap the dunes, and the bottom of these sands is not clearly known. We also included the alluvium near the Rio Grande with the Chicot Aquifer because we did not observe any differences in the water levels between wells completed in the alluvium and the Chicot Aquifer.

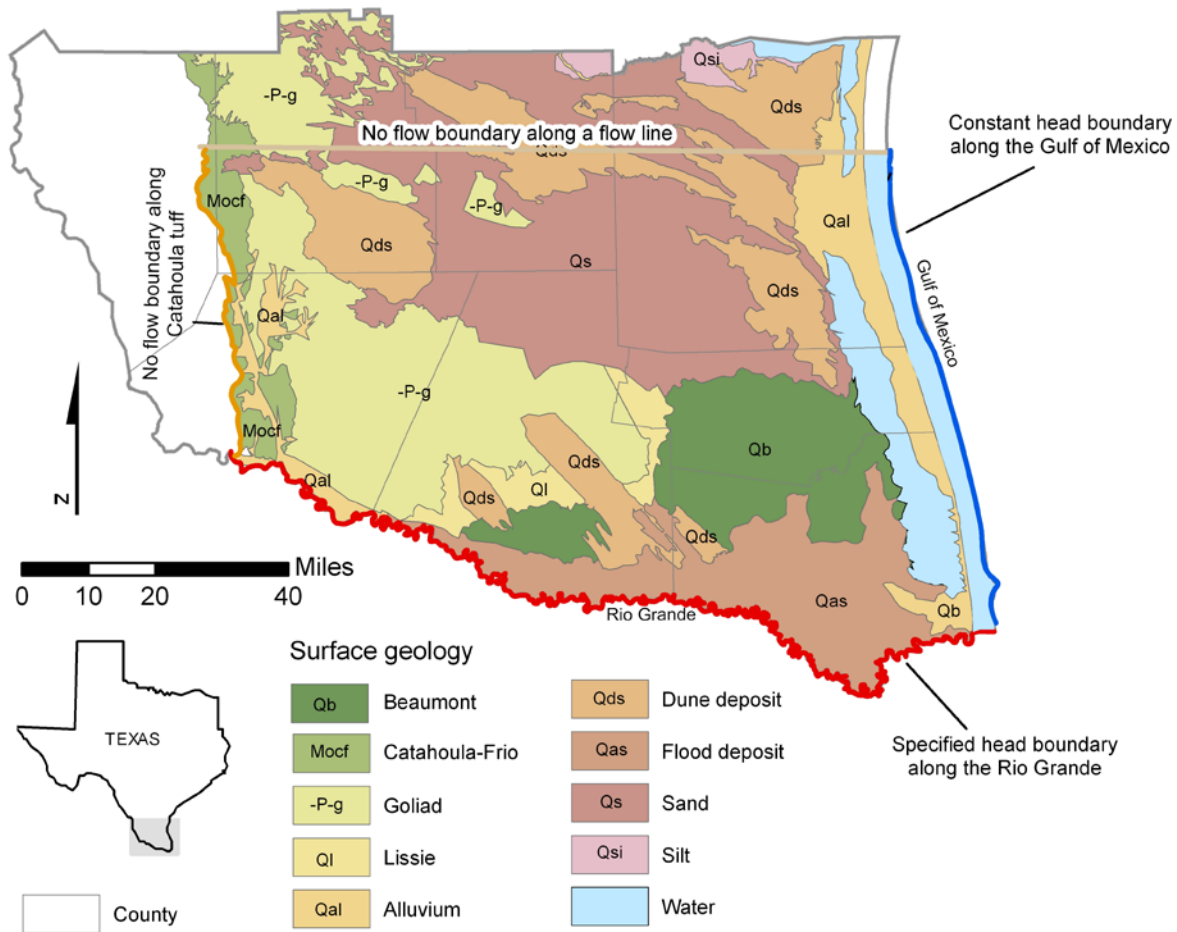


Figure 8-5. Surface geology of the study area along with model boundaries. The western boundary coincides with the outcrop limit of the Catahoula Tuff; the eastern boundary is 10 miles offshore in the Gulf of Mexico; the southern boundary is the Rio Grande; and the northern boundary follows a groundwater flow line.

The Burkeville Confining System pinches out in the subsurface in the study area. However, MODFLOW does not allow hydrostratigraphic units to pinch out (Anderson and Woessner, 1992). To allow hydraulic communication between the Burkeville Confining System, the Evangeline Aquifer, and the Jasper Aquifer in the pinch out area, we assigned a minimum thickness of 50 feet to the Burkeville Confining System and extended the bottom of the layer to the outcrop. We assigned hydraulic properties to the pinchout area based on hydraulic properties of the lower and the upper layers. Although this artificial assignment of minimum thickness introduces some error into the finite-difference approximation, the error is considered to be small (McDonald and Harbaugh, 1988, Anderson and Woessner, 1992, Eaton and Feinstein, 2002).

In some areas, abrupt thickening or thinning of the strata occurs over a short lateral distance that was probably caused by growth faulting. In the absence of any supporting documentation, we did not include these faults in the model.

8.3 *Model parameters*

We distributed model parameters, including (1) elevations of the top and bottom of the aquifers and the confining unit, (2) horizontal and vertical hydraulic conductivity, (3) recharge, (4) evapotranspiration, and (5) groundwater pumpage based on data described in chapter 5.

We assigned top and bottom elevations of the aquifers and the confining units using ArcInfo. The top of layer 1 (the Chicot Aquifer) is the land-surface elevation and the bottom is the same as that of the structure map of the Chicot Aquifer (Figure 5-2). The top of layer 2 (Evangeline Aquifer) uses the bottom of the Chicot Aquifer and the land-surface elevation where it is exposed. The base of layer 2 represents the bottom of the Goliad Sand (Figure 5-3). The top of layer 3 (Burkeville Confining System) uses the bottom of the Goliad Sand, as it entirely covers most of layer 3 except where it pinches out in the subsurface in the west. The base of layer 3 represents the bottom of the Burkeville Confining System (Figure 5-4). The top of layer 4 (Jasper Aquifer) was assigned using the bottom of the Burkeville Confining System where it is covered by layer 3 and the land-surface elevations where it is exposed to allow inclusions of the sands of the Catahoula Sand or Tuff. The bottom of layer 4 is the bottom of the Jasper Aquifer (Figure 5-5).

We assigned initial values of hydraulic conductivity to layer 1 and layer 2 based on our statistical interpretation (Figure 5-28). For layers 3 and 4, we assigned uniform hydraulic conductivity because there were too few data points to generate grids. We initially assigned vertical hydraulic conductivity to be one-tenth of the horizontal hydraulic conductivity. Lateral isotropy was initially assumed in each layer. We assigned uniform values of specific yield and specific storage in the layers. We assigned specific yield values of 0.001, 0.0005, and 0.01, for the Chicot, Evangeline, and Jasper aquifers, respectively, and 0.00001 for the Burkeville Confining System. We assigned specific storage values of 0.000001, 0.000001, and 0.00001 for the Chicot, Evangeline, and the Jasper aquifers, respectively and 0.00001 for the Burkeville Confining System.

Recharge was initially assigned in the model based on distributed mean annual rainfall for the period of 1930 to 1980. Recharge was then calibrated into the model as a uniform percent of rainfall. Given the large variability between the measured and estimated canal loss, we selected canal loss through the resacas (0.004 feet per day) to be representative of canal loss through all irrigation canals. This estimated loss of 0.004 feet per day converted to canal width of 30 feet was then assigned only to cells with irrigation canals. This estimated loss value was added to the estimated recharge. Our initial assumption was that leakage from the canals reaches the water table.

We used MODFLOW's evapotranspiration package to simulate transpiration by mesquite. It includes three parameters: elevation of the evapotranspiration surface, evapotranspiration extinction depth, and maximum evapotranspiration rate. We used the U.S. Geological Survey Digital Elevation Model as the elevation of the evapotranspiration surface and set the evapotranspiration extinction depth at 30 feet based on average depths of mesquite root systems. We used vegetation coverage to locate vegetation types and density (Figure 5-29). Mesquite is the dominant vegetation in the model area, with the highest density occurring in central Kenedy

and Jim Hogg counties. We applied three sets of multipliers (0.001, 0.0012, 0.0015) to the distributed rainfall grid to account for varying evapotranspiration rates to account for differences in the density of mesquite. Using these multipliers, we obtained evapotranspiration rates that ranged from 4.14×10^{-6} to 9.11×10^{-6} feet per day.

We used MODFLOW's River Package to simulate flow between the Chicot Aquifer and the Rio Grande. The River Package uses river surface elevation, river bottom elevation, and conductance of the river bed sediments. River surface elevation at different segments of the river was estimated from topographic maps and the U.S. Geological Survey Digital Elevation Model. River bottom elevation was set at 10 feet below the river head elevation. River bed conductance was estimated using the equation $(K \times L \times W) / M$ where K is the hydraulic conductivity, L is the length of the river, W is the width of the river, and M is the sediment thickness. In the calibration, we used a river bed conductance of about 100,000 feet per day, assuming a sediment thickness of 1 foot, an average river width of 10 feet, river length of 5,280 feet, and a hydraulic conductivity of 2 feet per day.

We distributed pumpage data into irrigation, domestic, manufacturing, municipal, and livestock categories (Tables 5-3 and 5-4). Irrigation pumpage data were available for 1980 and from 1984 through 1999. Pumpage data were linearly interpolated for the intervening years (1981, 1982, and 1983). Irrigation data were spatially distributed into model cells using the 1994 irrigation survey on irrigated portions of the county. The 1994 irrigation survey cover was intersected with the model grid that subdivides the original irrigated areas into polygons corresponding to model cells or parts of a model cell. Pumpage was then assigned to each model cell based on the area of the irrigated land within that cell relative to the total irrigated land in that county. Based on distribution of the aquifers, well completion records, and crop cultivation areas, we assigned the irrigation pumpage data in northern Hidalgo, Brooks, and Jim Hogg counties to the Evangeline Aquifer and irrigation pumpage in southern Hidalgo and Starr counties to the Chicot Aquifer.

Domestic pumpage was available by county and river basin for the years 1980 and 1984 through 1997. We interpolated data for the intervening years to account for the missing years. We spatially distributed the pumpage based on 1990 and 2000 census data, assuming that domestic pumpage is proportional to the population density in each census block. We intersected the population density cover with the model grid, excluding the urban areas (greater than 4,000 people per square mile). This intersection split the census blocks into polygons that could be attributed to model cells. The pumpage was then further distributed to the Chicot (Cameron, southern Hidalgo, southern Willacy, and southeast Starr counties) and Evangeline (eastern Jim Hogg, Brooks, Kenedy, Willacy, and northern Hidalgo counties) aquifers based on the spatial distribution of the two aquifers within the model area.

Manufacturing pumpage includes mining and power generation. If location data were absent, we attempted to determine approximate locations for the facility based on the mailing address or facility name present in the TWDB water use database. The municipal pumpage category was more complete than any of the other pumpage data sets in the TWDB water use database. Both the location and the aquifer assignment were derived directly from the database. Livestock pumpage was distributed based on the occurrence of rangeland within each county/basin.

Rangeland coverage was intersected with the model grid and the pumpage was assigned to each cell based on the relative area of rangeland in each cell.

Pumpage was assigned to individual cells within the model area. When more than one well was located within the same cell, the total pumpage was assigned to that cell. If aquifer information was missing in the pumpage database, the pumpage was similarly assigned to the Chicot Aquifer or the Evangeline Aquifer based on the aquifer that is pumped in the general location.

We assigned layer 1 as unconfined and layers 2, 3, and 4 as unconfined/confined. We allowed the model to calculate transmissivity and storativity based on saturated thickness. We used units of feet for length and days for time for all input data to the model. To solve the groundwater flow equation, we used the PCG2 solver with a convergence criterion of 0.01 ft.

9.0 Model boundaries

We assigned model boundaries for (1) recharge, (2) pumping, (3) rivers, (4) outer boundaries, and (5) initial conditions. We assigned initial values of recharge based on rainfall distribution as discussed in the section on recharge (Section 5.5). We applied pumping based on our pumping analyses as discussed in the section on discharge (Section 5.7). We used the River Package of MODFLOW that allows rivers to gain or lose water for simulating the Rio Grande.

To simulate the movement of the water out of the model and into the Gulf of Mexico, we assigned constant heads across 10 miles of an area offshore, including the area of Matagorda Bay, in layer 1. In the subsequent layers, we assigned a no-flow boundary in the east to allow upward vertical flow of water toward the discharge areas of the coastline. We used the interpreted water levels for 1980 as the initial head for the steady-state model.

We assigned a no-flow boundary to represent the bottom of the Jasper Aquifer and a no-flow boundary along the outcrop areas of the aquifers and the confining unit. We assigned constant head values for the lakes.

10.0 Modeling approach

Our approach for modeling the aquifer included three major steps: (1) calibrating a steady-state model, (2) calibrating a transient model, and (3) using the transient model to predict water levels over the next 50-year planning period. We first calibrated the steady-state model to establish stable boundary conditions and simulate static water levels under prepumping conditions. We selected 1980 for the steady-state calibration because water levels had remained nearly uniform between 1930 and 1980. We used the steady-state model to investigate (1) recharge rates, (2) hydraulic properties, (3) boundary conditions, (4) water budget, and (5) sensitivity of the different model parameters on the model results.

Our approach for calibrating the model was to match water levels under steady-state conditions and match seasonal water level changes under transient conditions. To calibrate the model, we primarily focused on the Chicot and the Evangeline aquifers, which contained the largest number

of well control points. We also checked the few water levels from the Burkeville Confining System and the Jasper Aquifer to ensure that the simulated water levels were reasonable.

We quantified the calibration or goodness of fit between the simulated and measured water level values using the mean error (ME), mean absolute error (MAE), and root mean square error (RMS):

$$ME = 1/n \sum_{i=1}^n (h_m - h_s)_i \quad (10.1)$$

$$MAE = 1/n \sum_{i=1}^n |(h_m - h_s)_i| \quad (10.2)$$

$$RMS = \left[1/n \sum_{i=1}^n (h_m - h_s)_i^2 \right]^{0.5} \quad (10.3)$$

where n is the number of calibration points, h_m is the measured hydraulic head, or water level, at any point i and h_s is the simulated hydraulic head, or water level, at the same point i .

Once we completed calibrating the steady-state model, we used the framework of the model as a starting point for transient modeling for the years 1981 to 2000. We chose these years because this period contained the most accurate and recent water use and water level information. We chose monthly time steps for the years 1988 to 1990 and 1994 to 1996 to test model response to recharge and pumping during drought transitions. Allowing for both annual and monthly time steps for the transient calibration led us to reproduce water level fluctuations under both dry and wet climatic conditions thus increasing confidence in the model. We calibrated the transient model by adjusting the storativity values to minimize the differences between simulated and measured water levels.

After we completed the transient calibration, we then used the model to predict water level conditions in response to pumping and drought over the next 50 years.

11.0 Steady-state model

Once we completed constructing the framework of the model and assembled the input data sets, our next step was to calibrate the steady-state model and then assess the sensitivity of the model to different hydrologic input parameters.

11.1 Calibration

We calibrated the steady-state model to mean annual winter water levels (1930 to 1980) in the Chicot and Evangeline aquifers because there was minimum pumping and negligible changes in the water levels in that season (Figure 5-13). Only five wells from the outcrop areas of the Jasper Aquifer had water level information to be included in model calibration.

To calibrate the model, we adjusted the various parameters to observe which one had the most effect on simulated water levels. Through this initial sensitivity analysis, we observed that the

horizontal hydraulic conductivity of layers 1 and 2, recharge rate, and evapotranspiration rate, most affected the model results. We also observed that the model calibration was not unique, particularly with respect to recharge rate, evapotranspiration rate, and hydraulic conductivity values.

We initially attempted to calibrate the model using distributed horizontal hydraulic conductivity for layers 1 and 2. However, we were only able to reproduce water levels at limited well locations. Water levels in numerous wells in the model were over- or underestimated, perhaps reflecting the poor spatial correlation between hydraulic conductivity values. We then assigned uniform geometric mean hydraulic conductivity for layers 1 and 2. We were able to better reproduce water levels with hydraulic conductivities that varied uniformly across the model area. However, the best-fit simulated water levels were produced using zoned horizontal hydraulic conductivity for layers 1 and 2 (Figures 11-1 and 11-2). We zoned the hydraulic conductivity into five to six smaller subzones while still honoring the distributed hydraulic conductivity values. It is probable that we had to use these hydraulic conductivity zones due to the presence of numerous clay/shale lenses within the aquifer that could potentially have resulted in hydrologic compartmentalization of some of the water-bearing units. For layer 3, we used a hydraulic conductivity value of 0.01 feet per day that was consistent with its abundant clay content and confining characteristics.

We assigned uniform recharge rates based on the distributed rainfall for calibrating the model. When we increased recharge through the floodplain/clay deposits in the south to account for presumed leakage through canal loss, we observed that the resulting water levels were too high in southern Hidalgo and Cameron counties even though measured hydraulic conductivity was used in calibration. This may indicate that any canal leakage occurring does not reach the saturated groundwater zone but discharges to nearby ditches at lower elevations or accumulates as perched groundwater eventually discharging into the Laguna Madre through Arroyo Colorado. Therefore, we assigned no additional recharge to the aquifer from canal losses.

Calibrated recharge ranges from 0.08 to 0.14 inches per year, which is 0.52 percent of the average annual rainfall for the years 1930 through 1980 (Figure 11-3). This recharge rate is lower than the recharge rates used in modeling the central (0.17 to 0.25 inches per year) (Chowdhury and others, 2004) and northern (0.32 to 0.43 inches per year) (Kasmarek and Robinson, 2004) parts of the Gulf Coast Aquifer. A slightly lower recharge rate in the southern part of the Gulf Coast Aquifer is more realistic due to higher evaporation and lower rainfall than the rest of the aquifer.

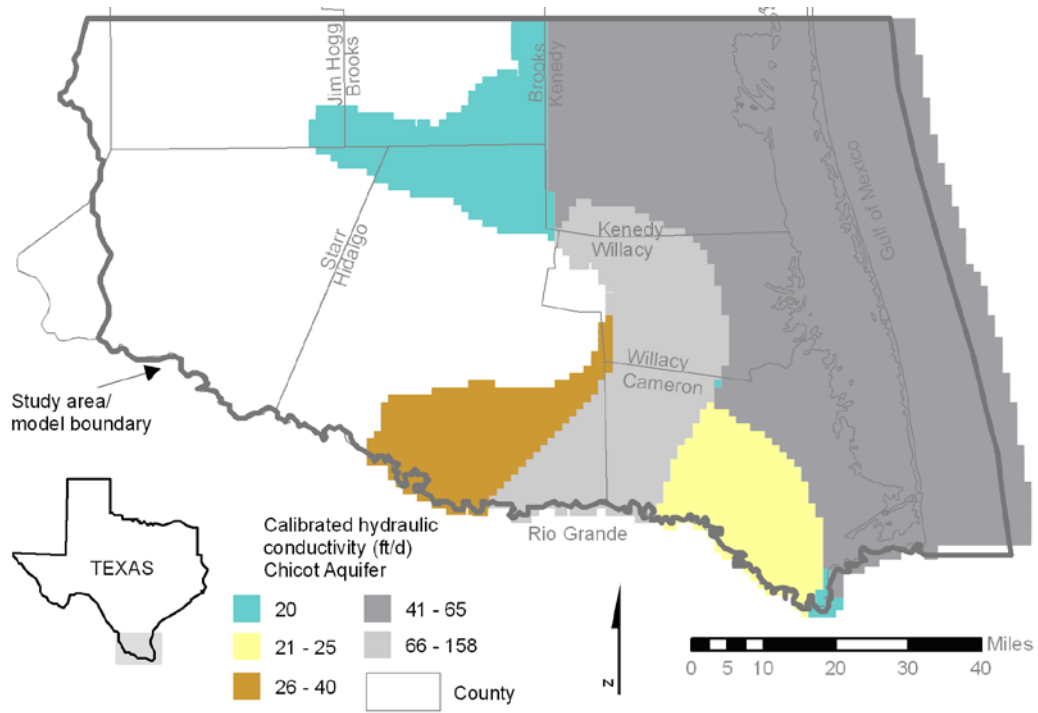


Figure 11-1. Calibrated hydraulic conductivity zones based on measured hydraulic conductivity values in the Chicot Aquifer (ft/d = feet per day).

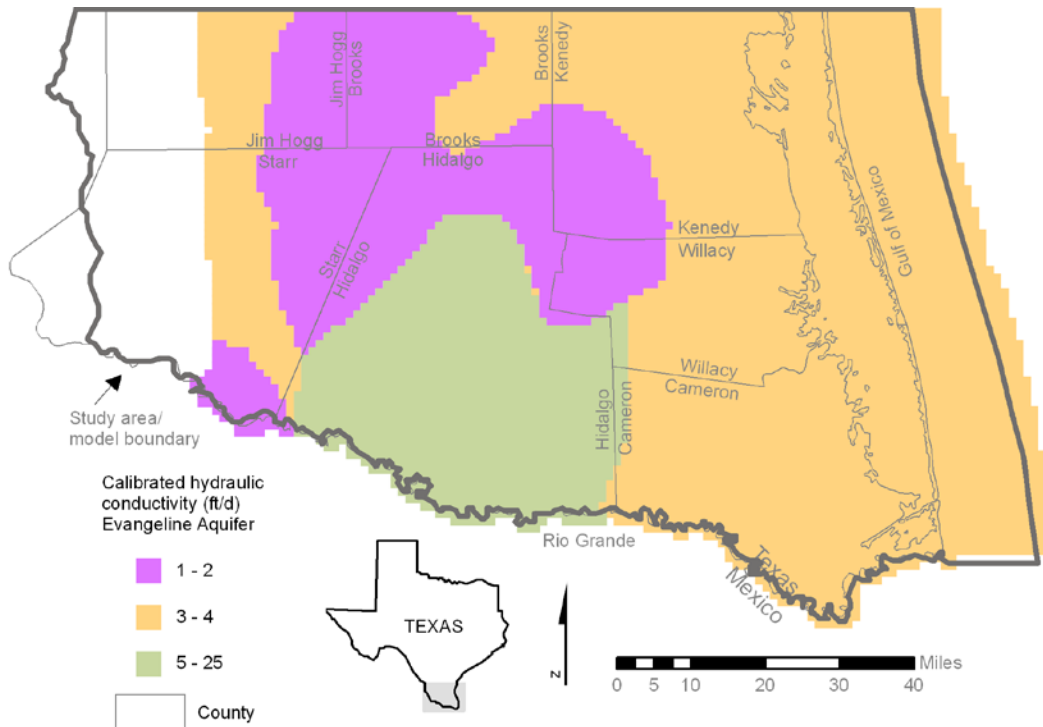


Figure 11.2. Calibrated hydraulic conductivity zones based on measured hydraulic conductivity values in the Evangeline Aquifer (ft/d = feet per day).

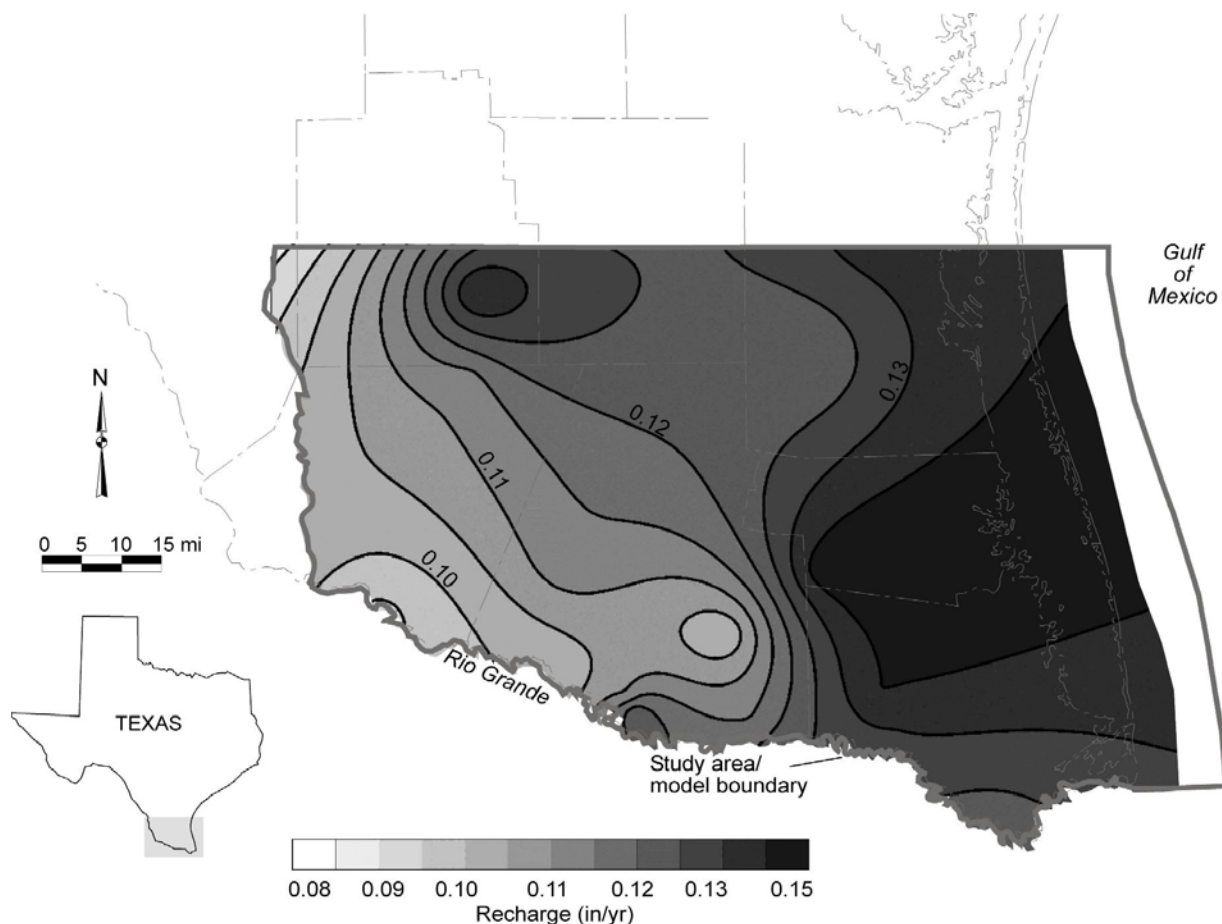


Figure 11-3. Spatial distribution of recharge used in calibrating the steady-state model (1980; mi = miles; in/yr = inches per year).

The maximum evapotranspiration rate was determined by trial and error during calibration (Figure 11-4). Groundwater extraction through evapotranspiration was assigned locally in areas where mesquite occurs. When we applied a higher percentage of evapotranspiration, it resulted in drying up model cells in the outcrop areas to the west and an increase in the root mean squared error. Given that the mean recharge is close to 0.5 percent of the mean annual rainfall, evapotranspiration could locally amount to as much as 19 to 29 percent of the recharge applied to calibrate the steady-state model.

During calibration, we noticed that a number of cells in the western edges of the outcrops went dry. We made these cells inactive after observing that the aquifers in this area are thin. The model is sensitive to water levels in the northwest portion of the model, perhaps because the steep gradient significantly controls volumes of water reaching the remainder of the model. We also noted that the model was very sensitive to the vertical hydraulic conductivity in the updip areas between the Burkeville Confining System and the Evangeline Aquifer. The extent of this hydraulic connection appeared to determine the water level elevations in the Evangeline Aquifer.

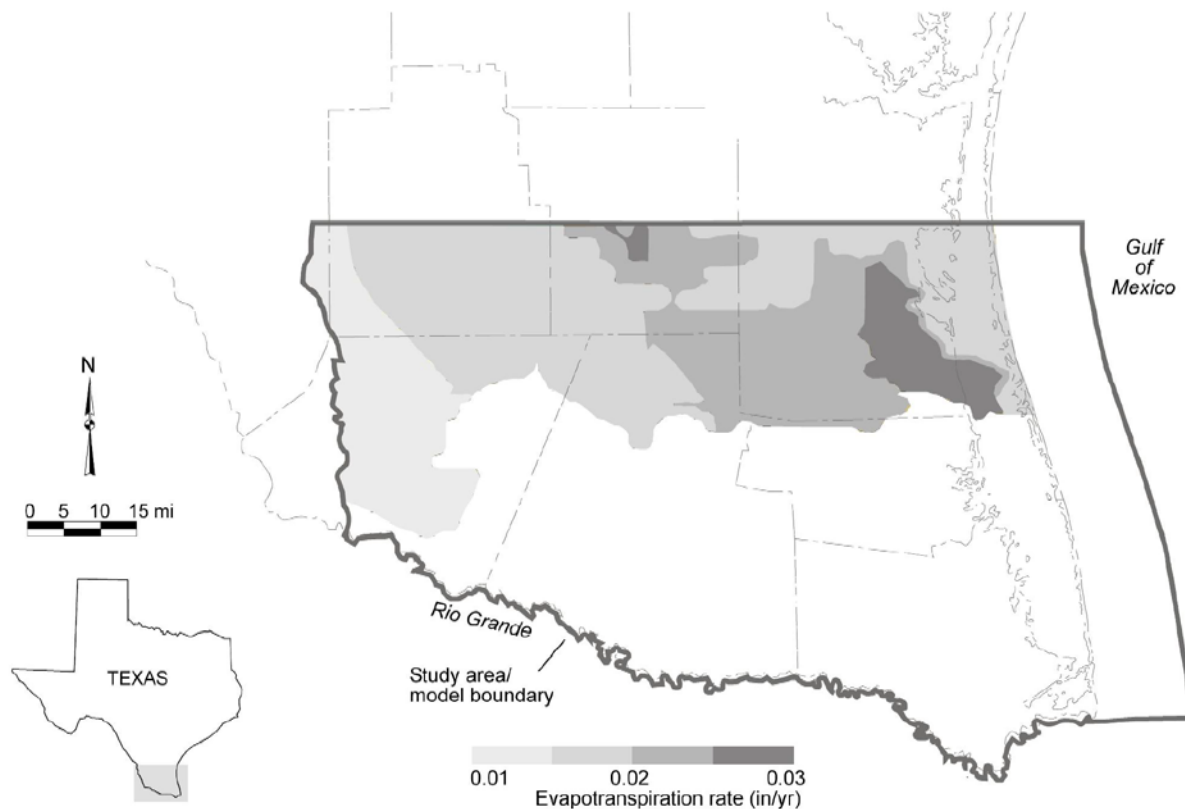


Figure 11-4. Spatial distribution of evapotranspiration values used to calibrate the steady-state model (mi = miles; in/yr = inches per year).

The calibrated model reasonably reproduces the spatial distribution of water levels in the Chicot, Evangeline, and the Jasper aquifers for the steady-state conditions of 1930 to 1980 (Figure 11-5). The mean error is 4.42 feet. The mean absolute error is 17.39 feet. The root mean squared error is 23 feet. The root mean squared error is about 4.4 percent of the hydraulic head drop (highest measured water level minus the lowest measured water level) across the model area well and is within the 10 percent error usually sought for model calibration. The model accurately replicates the interpreted flow directions toward the Gulf of Mexico and Rio Grande (Figures 11-6, 11-7, 11-8, and 11-9). Simulated water level contours that cross the Rio Grande locally bend upstream in southern Hidalgo and southwestern Cameron counties (Figures 11-6 and 11-7) and bend downstream along the remainder of the stretches as was observed in the measured water levels (Figure 5-14). River leakage into the aquifer is further supported by the occurrences of fresh groundwater in wells along the Rio Grande in these areas. The spatial distribution of water level residuals (differences in the simulated and the measured water levels) appears unbiased toward any specific location in the model area (Figures 11-10 and 11-11).

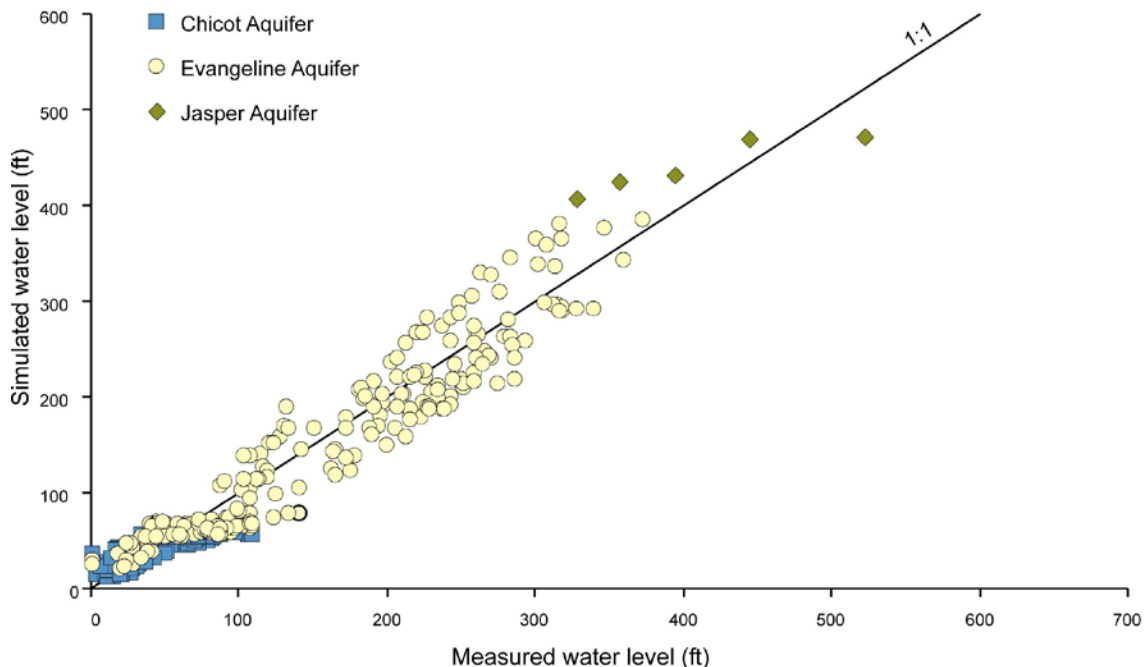


Figure 11-5. Comparison of simulated to measured water levels for the Chicot and the Evangeline aquifers for the 1980 steady-state model. The solid line is the 1:1 line where the simulated water level would exactly match the measured water level (ft = feet).

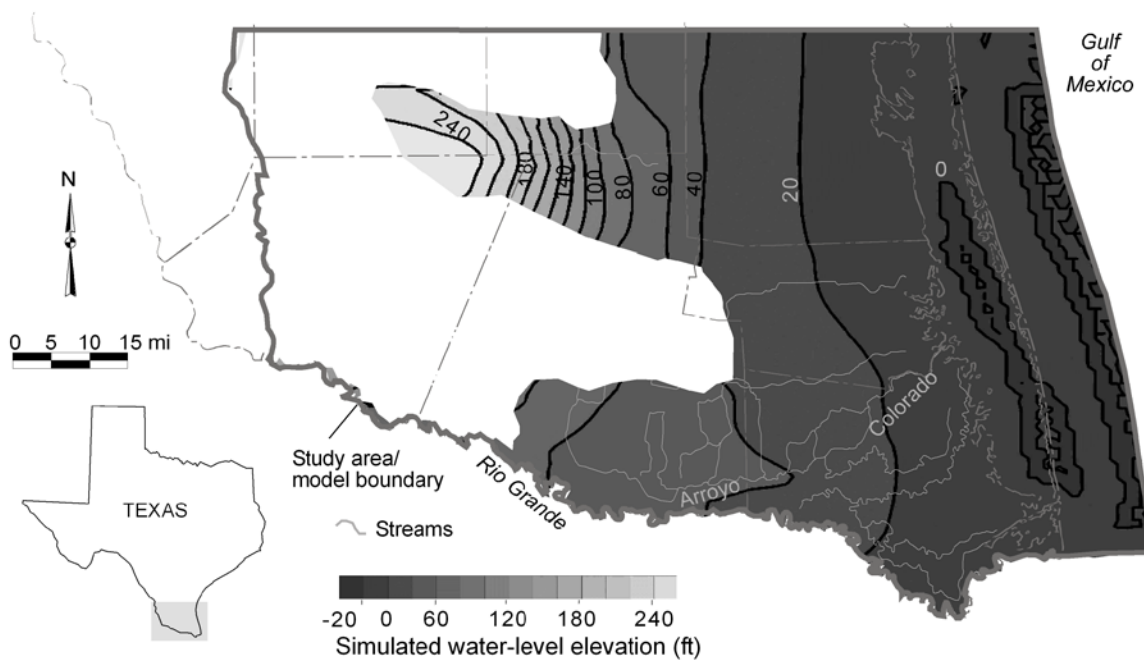


Figure 11-6. Simulated water levels in the Chicot Aquifer for the steady-state model (which represents conditions in 1980; mi = miles; ft = feet).

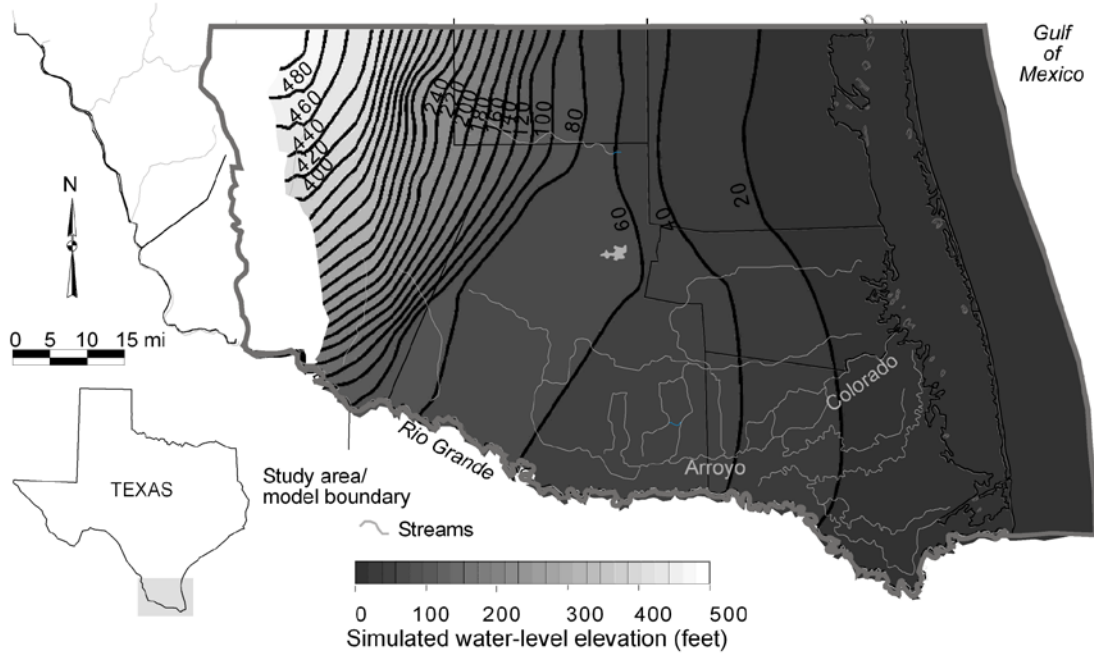


Figure 11-7. Simulated water levels in the Evangeline Aquifer for the steady-state model (which represents conditions in 1980; mi = miles).

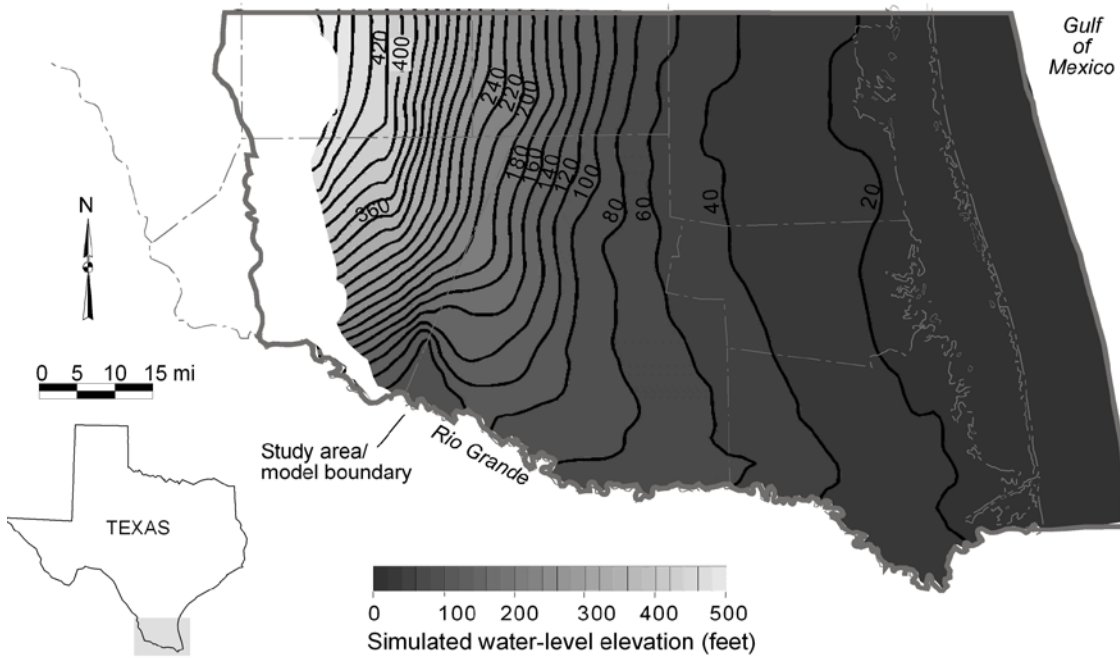


Figure 11-8. Simulated water levels in the Burkeville Confining System for the steady-state model (which represents conditions in 1980; mi = miles).

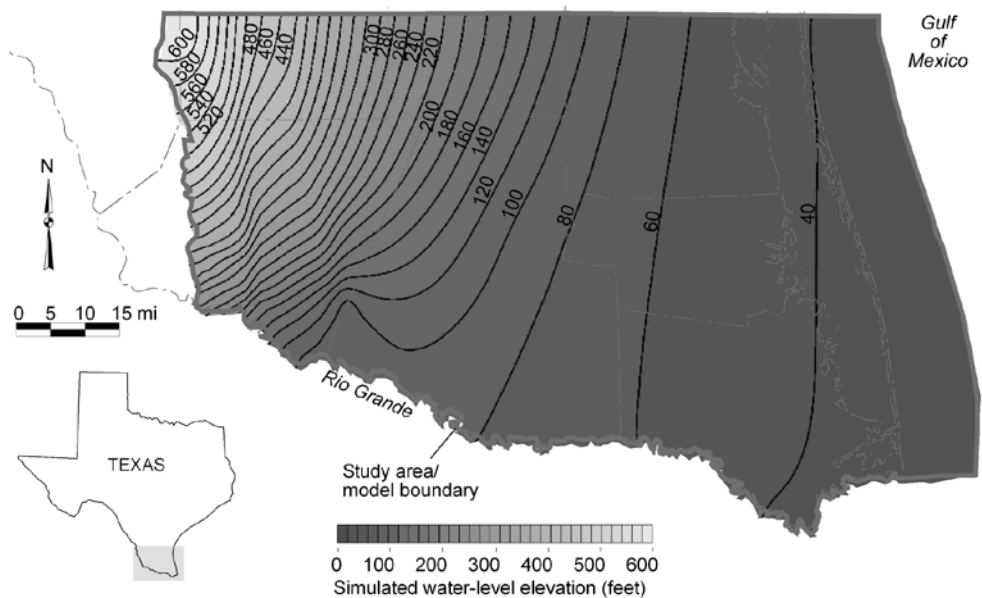


Figure 11-9. Simulated water levels in the Jasper Aquifer for the steady-state model (which represents conditions in 1980; mi = miles).

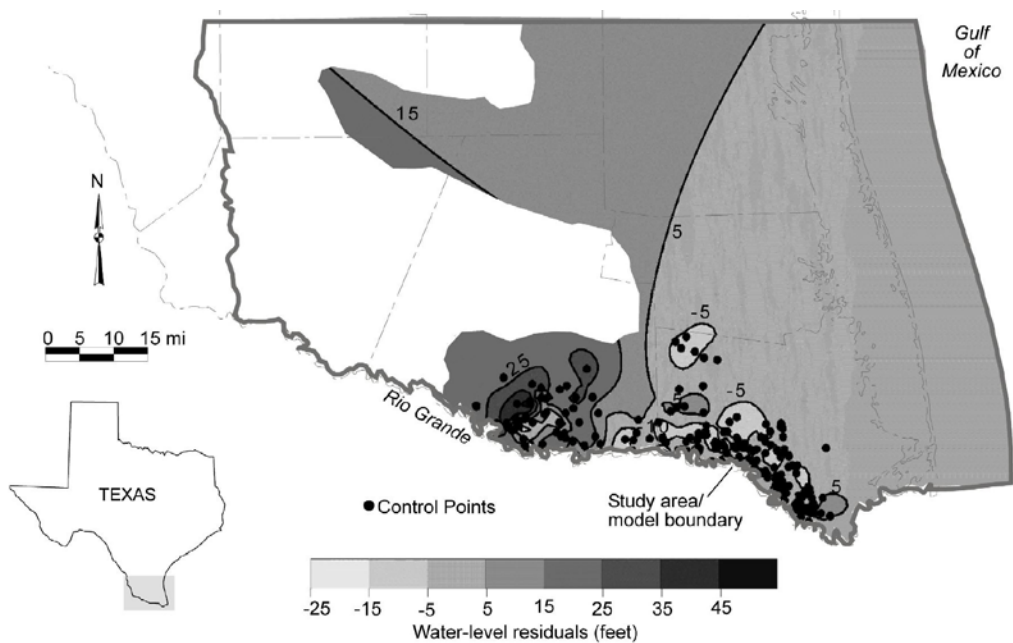


Figure 11-10. Spatial distribution of water level residuals (differences between simulated and measured water levels) in the Chicot Aquifer for the steady-state model (which represents conditions in 1980). A positive value means that the model is overestimating water levels, and a negative value means that the model is underestimating water levels (mi = miles).

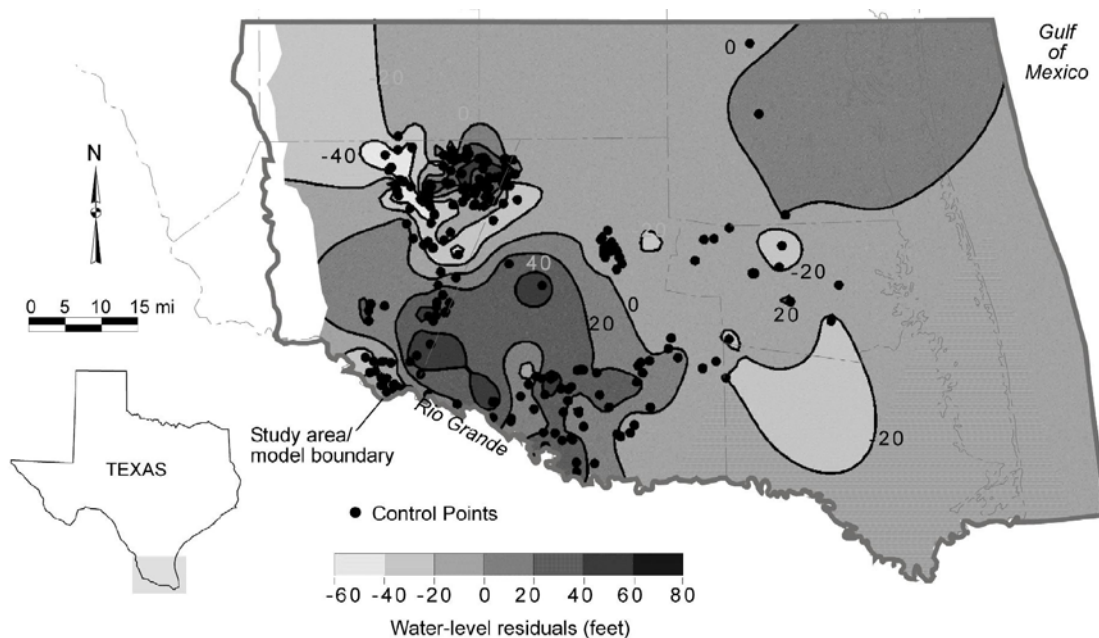


Figure 11-11. Spatial distribution of water level residuals (differences between simulated and measured water levels) in the Evangeline Aquifer for the steady-state model (which represents conditions in 1980). A positive value means that the model is overestimating water levels, and a negative value means that the model is underestimating water levels (mi = miles).

11.2 Water budget

We estimated the total volume of water that enters or leaves the Gulf Coast Aquifer using the calibrated steady-state model (Table 11-1). We found that about 88,000 acre-feet per year of water flows through the Gulf Coast Aquifer. Of this total flow, 47 percent comes from rainfall that directly falls on the land surface in the outcrop areas of the model and 53 percent seeps into the aquifers from the Arroyo Colorado and the Rio Grande. Nearly 62 percent of the total recharge from rainfall percolates through the Chicot outcrop, 32 percent percolates through the Evangeline outcrop, and the remainder (6 percent) percolates through the thin sliver of the Jasper outcrops. Of the total flow of about 88,000 acre-feet per year, 3 percent is lost through evapotranspiration, 15 percent discharges through pumping that existed during the 1980s, 32 percent flows into the Rio Grande and Arroyo Colorado (base flow component in Table 11-1), and 50 percent discharges to the Laguna Madre and Gulf of Mexico (Table 11-1). The amount of groundwater lost through evapotranspiration may appear low at the regional scale, but evapotranspiration may locally comprise up to 30 percent of recharge under steady-state conditions. Cross-formational flow is a significant component of the total flow in model layers. More water discharges upwards from the Evangeline Aquifer (about 15,000 acre-feet per year) to the Chicot Aquifer than recharges the Evangeline Aquifer (about 14,000 acre-feet per year; Table 11-1). This implies that groundwater in the Chicot Aquifer in the downdip areas can be composed of large fluxes of older saline water mixed with relatively younger, fresher water causing deterioration in the water quality.

Table 11-1. Water budget for the calibrated steady-state (1980), calibrated transient (1981-1999), and predictive run (2010-2050). All values are in acre-feet per year. Recharge is the amount of water that infiltrates into the aquifer, river leakage is the amount of water that leaks into the aquifer during high river stages; base flow is the amount of water that discharges into the river (Rio Grande and Arroyo Colorado) from the aquifer; evapotranspiration (ET) is the amount of water used by deep rooted plants (mainly mesquites in the area); and cross-formational flow (X-flow) is the amount of water exchanged between the aquifers. Cross-formational flow applies to both upper and lower faces of each of the model layers. X-flow (In) applies to water coming into the aquifer and X-flow (Out) applies to the amount of water that is leaving the aquifer. Net X-flow is the net amount of water exchanged in an aquifer. Storage refers to the amount of water stored in the aquifer that changes due to pumping and /or recharge conditions.

Year	Layer	Recharge	River	Baseflow	ET	Wells	X-flow Upper (In)	X-flow Upper (Out)	Net X- flow (Upper)	X-flow Lower (In)	X-flow Lower (Out)	Net X- flow (Lower)	Gulf of Mexico	Storage
1980	1	26,102	43,289	-27,422	-2,081	-11,470	0	0	0	15,514	-1,182	14,332	-42,749	0
	2	13,945	2,389	-870	-412	-2,462	1,182	-15,514	-14,332	2,256	-513	1,742	0	0
	3	204			0		513	-2,256	-1,742	2,221	-682	1,538	0	0
	4	1,611			-73		682	-2,221	-1,538	0	0	0	0	0
	All	41,862	45,678	-28,292	-2,566	-13,932	2,377	-19,990	-17,613	19,990	-2,377	17,613	-42,749	0
1991	1	30,615	50,866	-25,808	-2,275	-23,658	0	0	0	16,454	-1,580	14,874	-42,999	-1,616
	2	14,759	3,508	-601	-421	-4,546	1,580	-16,454	-14,874	3,197	-328	2,869	0	-695
	3	217	0	0	0	0	328	-3,197	-2,869	2,362	-708	1,654	0	998
	4	1,721	0	0	-100	0	708	-2,362	-1,654	0	0	0	0	32
	All	47,312	54,375	-26,409	-2,795	-28,203	2,616	-22,012	-19,396	22,012	-2,616	19,396	-42,999	-1,281
1999	1	22,267	48,891	-25,641	-2,066	-19,092	0	0	0	16,759	-1,494	15,265	-41,934	-2,311
	2	13,457	3,150	-806	-474	-3,700	1,494	16,759	-15,265	2,993	-281	2,713	0	-927
	3	165	0	0	0	0	281	16,759	-2,713	2,369	-685	1,683	0	-864
	4	1,348	0	0	-83	0	685	2,369	-1,683	0	0	0	0	-418
	All	37,236	52,041	26,448	-2,623	-22,793	2,460	35,887	-19,661	22,121	-2,460	19,661	-41,934	-4,520
2010	1	15,579	46,415	-25,979	-1,253	-12,501	0	0	0	14,978	1,355	13,623	-39,847	-3,964
	2	7,524	2,958	-589	-216	-3,635	1,355	14,978	-13,623	4,014	84	3,930	0	-3,650
	3	106	0	0	0	0	84	4,014	-3,930	2,508	558	1,950	0	-1,874
	4	865	0	0	-46	0	558	2,508	-1,950	0	0	0	0	-1,132
	All	24,075	49,373	-26,569	-1,515	-16,136	1,997	21,501	-19,503	21,501	1,997	19,503	-39,847	-10,619
2020	1	15,579	47,312	-25,753	-1,244	-13,648	0	0	0	14,919	1,353	13,566	-39,685	-3,872
	2	7,524	3,078	-554	-205	-3,789	1,353	14,919	-13,566	3,989	83	3,906	0	-3,606
	3	106	0	0	0	0	83	3,989	-3,906	2,531	541	1,990	0	-1,810
	4	865	0	0	-46	0	541	2,531	-1,990	0	0	0	0	-1,171
	All	24,075	50,390	-26,307	-1,495	-17,437	1,977	21,439	-19,462	21,439	1,977	19,462	-39,685	-10,460

Table 11-1. Continued.

Year	Layer	Recharge	River	Baseflow	ET	Wells	X-flow Upper (In)	X-flow Upper (Out)	Net X- flow (Upper)	X-flow Lower (In)	X-flow Lower (Out)	Net X- flow (Lower)	Gulf of Mexico	Storage
2030	1	15,579	48,105	-25,578	-1,239	-14,537	0	0	0	14,851	1,359	13,492	-39,589	-3,766
	2	7,524	3,138	-531	-197	-3,860	1,359	14,851	-13,492	3,966	83	3,883	0	-3,535
	3	106	0	0	0	0	83	3,966	-3,883	2,547	526	2,021	0	-1,756
	4	865	0	0	-46	0	526	2,547	-2,021	0	0	0	0	-1,202
	All	24,075	51,242	-26,109	-1,481	-18,397	1,968	21,364	-19,396	21,364	1,968	19,396	-39,589	-10,260
2040	1	15,579	48,514	-25,423	-1,236	-15,106	0	0	0	14,785	1,362	13,423	-39,491	-3,739
	2	7,524	3,206	-512	-190	-3,985	1,362	14,785	-13,423	3,947	83	3,864	0	-3,516
	3	106	0	0	0	0	83	3,947	-3,864	2,559	513	2,046	0	-1,712
	4	865	0	0	-45	0	0	0	-2,046	0	0	0	0	-1,227
	All	24,075	51,720	-25,935	-1,471	-19,091	1,445	18,732	-19,333	21,291	1,958	19,333	-39,491	-10,194
2050	1	15,579	48,727	-25,354	-1,233	-15,350	0	0	0	14,731	1,362	13,369	-39,429	-3,690
	2	7,524	3,238	-498	-184	-4,019	1,362	14,731	-13,369	3,918	83	3,835	0	-3,472
	3	106	0	0	0	0	83	3,918	-3,835	2,567	502	2,065	0	-1,664
	4	865	0	0	-45	0	502	2,567	-2,065	0	0	0	0	-1,245
	All	24,075	51,965	-25,852	-1,462	-19,369	1,947	21,216	-19,269	21,216	1,947	19,269	-39,429	-10,071
2050 ¹	1	25,558	46,280	-26,499	-1,278	-15,350	0	0	0	15,225	1,286	13,938	-42,437	213
	2	13,437	2,727	-741	-224	-4,019	1,286	15,225	-13,938	3,015	288	2,727	0	-31
	3	205	0	0	0	0	288	3,015	-2,727	2,460	3,015	1,859	0	-664
	4	1,628	0	0	-45	0	601	2,460	-1,859	0	0	0	0	-276
	All	40,828	49,007	-27,240	-1,547	-19,369	2,176	20,700	-18,524	20,700	4,589	18,524	-42,437	-758

¹ predictive run with average recharge. A positive sign indicates addition of water into the aquifer and a negative sign indicates a removal of water from the aquifer. Storage declines with increasing time due to lower recharge rates during drought-of-record conditions. Decline in storage is slowed throughout 2010 to 2050 due to steady pumping. Numbers presented represents fluxes for the specified year.

12.0 Sensitivity analysis

Sensitivity analysis determines uncertainties associated with a calibrated model. These uncertainties are primarily caused by the difficulties associated with estimating the aquifer parameters, stresses, and boundary conditions (Anderson and Woessner, 1992, p. 246). Sensitivity analysis assesses the adequacy of the model with respect to its intended purposes (ASTM, 1994). It also identifies hydraulic parameters that primarily control water levels, flows to springs, or leakage to streams.

We tested the sensitivity of water levels to changes in parameters in the Chicot, Evangeline, and Jasper aquifers, and the Burkeville Confining System. During the sensitivity analysis, we systematically varied (± 75 percent) the calibrated values of hydraulic conductivity, recharge, evapotranspiration, and river conductance one at a time in all four layers of the model. The magnitude of changes in the water levels in each active cell was considered a measure of sensitivity of the solution to that parameter. We quantified the changes in the water levels by calculating the mean difference (MD) in the water levels in each active cell according to:

$$MD = 1/n \sum (H_{sen} - H_{cal})$$

where n is the number of points, H_{sen} is the simulated water level, and H_{cal} is the calibrated water level.

The mean difference is positive if water levels are higher than the calibrated values and negative if lower than the calibrated values. We used the root mean squared error at well points to measure the sensitivity of varying river stages to model calibration results.

Water levels in the model are most sensitive to recharge and horizontal hydraulic conductivity in both the Chicot and the Evangeline aquifers (Figure 12-1). The Evangeline Aquifer showed more changes in water levels than the Chicot Aquifer presumably because it receives much less recharge from the Rio Grande than the Chicot Aquifer. Lower recharge values caused water levels to decline in the model while higher recharge values cause water levels to rise. Similarly, lower horizontal hydraulic conductivity caused water levels to rise, and higher horizontal hydraulic conductivity caused water levels to decline. When we varied evapotranspiration, river conductance, and vertical hydraulic conductivity values, the model showed very small changes in water levels indicating that these parameters are not sensitive within the range of variation. We found that the water levels were more sensitive to lower parameter values than higher parameter values. In other words, changes in water levels were much greater when the lower values of a parameter were used than higher values of that parameter.

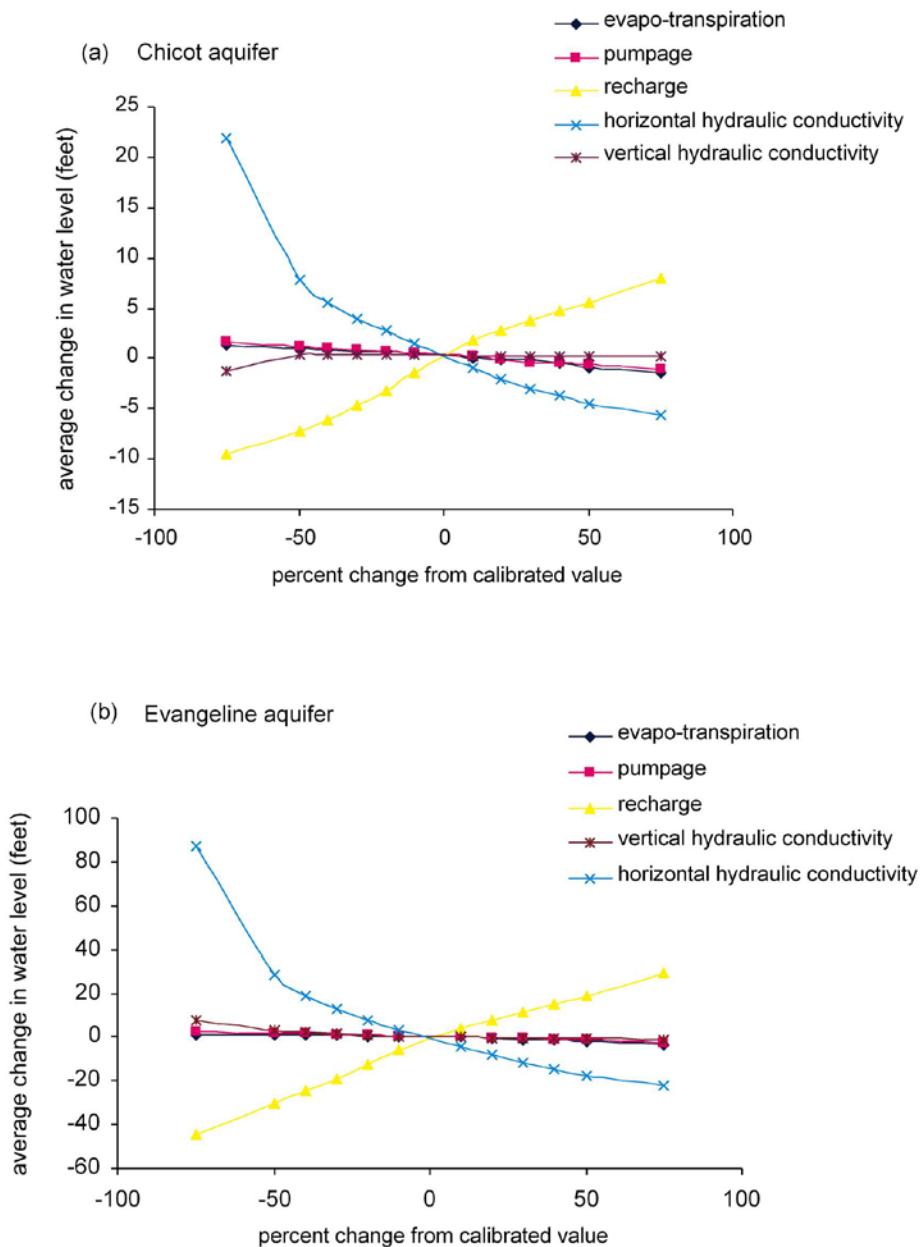


Figure 12-1. Sensitivity of simulated water levels to changes in recharge, hydraulic conductivity, evapotranspiration, and pumping from calibrated values for (a) the Chicot Aquifer and (b) the Evangeline Aquifer.

Table 12-1. Recharge/discharge relationships of the Rio Grande and Arroyo Colorado as obtained during sensitivity runs with varying river stages for (a) the calibrated case, (b) river stage at 5 feet less than the calibrated case, and (c) river stage at 5 feet more than the calibrated case.

	River	Recharge (in) (acre-feet/year)	Discharge (out) (acre-feet/year)
(a)	Rio Grande (Chicot)	7,821	19,049
	Rio Grande (Evangeline)	1,990	1,252
	Arroyo Colorado	34,900	8,597
(b)	Rio Grande (Chicot)	10,934	33,271
	Rio Grande (Evangeline)	6,167	368
	Arroyo Colorado	0	30,165
(c)	Rio Grande (Chicot)	14,202	18,078
	Rio Grande (Evangeline)	1,854	1,014
	Arroyo Colorado	45,518	6,809

We also examined sensitivity of the river stages used in calibration. Simulated water levels were sensitive to changes in the stages of the Rio Grande and Arroyo Colorado. Slight changes to the river stages resulted in switching the reaches of a losing stream to a gaining stream and vice versa. When we lowered the river stage by 5 feet from what we used during calibration, the

Arroyo Colorado turned entirely into a gaining stream, and the Rio Grande started to gain considerable volumes of water. During this sensitivity run, simulated water levels across the model were underestimated in most of the wells in the Chicot Aquifer resulting in an increase of the root mean squared error from 4.4 percent to 6.5 percent when we increased the river stages by 5 feet, the water budget changed due to higher flow from the river moving into the aquifer (Table 12-1). The root mean squared error was slightly higher for this sensitivity run. Therefore, our analysis indicates that the river stages that we selected from the U.S. Geological Survey topographic sheets are representative of the actual stage. The river stages used during calibration also closely match the measured stages from two gages (U.S. Geological Survey stations 08475000 and 08475000) along the Rio Grande. These sensitivity results also indicate that lowering the river stages during drought may result in a significant decrease in the recharge to the aquifers. This may considerably increase drawdown cones in the aquifers even when pumping remains steady.

13.0 Transient model

After we calibrated the steady-state model to water levels from 1930 to 1980, we calibrated the model to transient water levels for 1981 to 1990. We started the transient model calibration with hydraulic heads from the calibrated steady-state model so that the initial head and parameter inputs stayed consistent. We calibrated the model to measured water levels. In the transient

model, we estimated the storage parameters, keeping all other calibrated parameters unchanged. The transient calibrated model was then verified to water level changes during 1990 to 2000.

13.1 Calibration

We assigned annual stress periods for 1981 to 2000 except for the drought years in each decade, for which we assigned monthly stress periods (1988, 1989, 1990, 1994, 1995, and 1996). We reproduced the water levels using recharge that reflects rainfall distribution for the time period and corresponding groundwater pumpage for the calibration period. We reproduced the changes in water levels by calibrating the specific storage and the specific yield values. We were able to best reproduce water level changes using specific storage values of 0.000001, 0.000001, 0.00001, and 0.000001 per feet for layers 1, 2, 3, and 4, respectively, and specific yield values of 0.005, 0.001, 0.0001, and 0.05 for layers 1, 2, 3, and 4, respectively. The mean error is 4.5 feet for 1980, 0.17 feet for 1990, and 2.75 feet for 2000. The mean absolute error is 17.39 feet for 1980, 16.23 feet for 1990, and 15.34 feet for 2000. The root mean squared error is about 23 feet for 1980, 1990, and 2000, respectively. Comparison of simulated versus measured water levels for 1990 and 2000 shows a reasonable match between them (Figure 13-1). The root mean squared error remains the same for the steady-state and transient calibrations.

The transient model does a reasonable job of matching the measured monthly and annual water level trends throughout most of the model area with the exception of a shift between simulated and measured water levels (Figure 13-2). This shift in water levels has been carried over to the transient model from the steady-state model. In some wells, the shift was more pronounced than in others. This discrepancy is probably due to local scale heterogeneity in the aquifer materials that we were unable to capture at the scale of the regional model. In addition, a number of other factors, including a local overestimation in pumping, multiple screen intervals in wells, and/or local underestimation of hydraulic properties of the aquifer, may cause this shift. Calibration targets should coincide with model nodes—in most cases they do not. This may also cause differences between measured and simulated water levels.

The specific yield values of 0.05 to 0.001 that we have used in the transient calibration may appear low for the unconfined portions of the aquifer. Typical specific yields of sedimentary materials in unconfined aquifers range from 0.14 to 0.38 (Freeze and Cherry, 1979). We attempted to calibrate the model using higher specific yields but were unable to reproduce the required fluctuations to match the measured water levels. The lower specific yield that we used is more typical of semiconfined aquifers. The lower specific yields are appropriate for the Chicot, Evangeline, and Jasper aquifers as they contain numerous interbedded silt/clay lenses.

When we assigned smaller values of specific yields or specific storage, we observed a wider fluctuation in water levels (Figures 13-3 and 13-4). Water levels are slightly more sensitive to specific yield than specific storage.

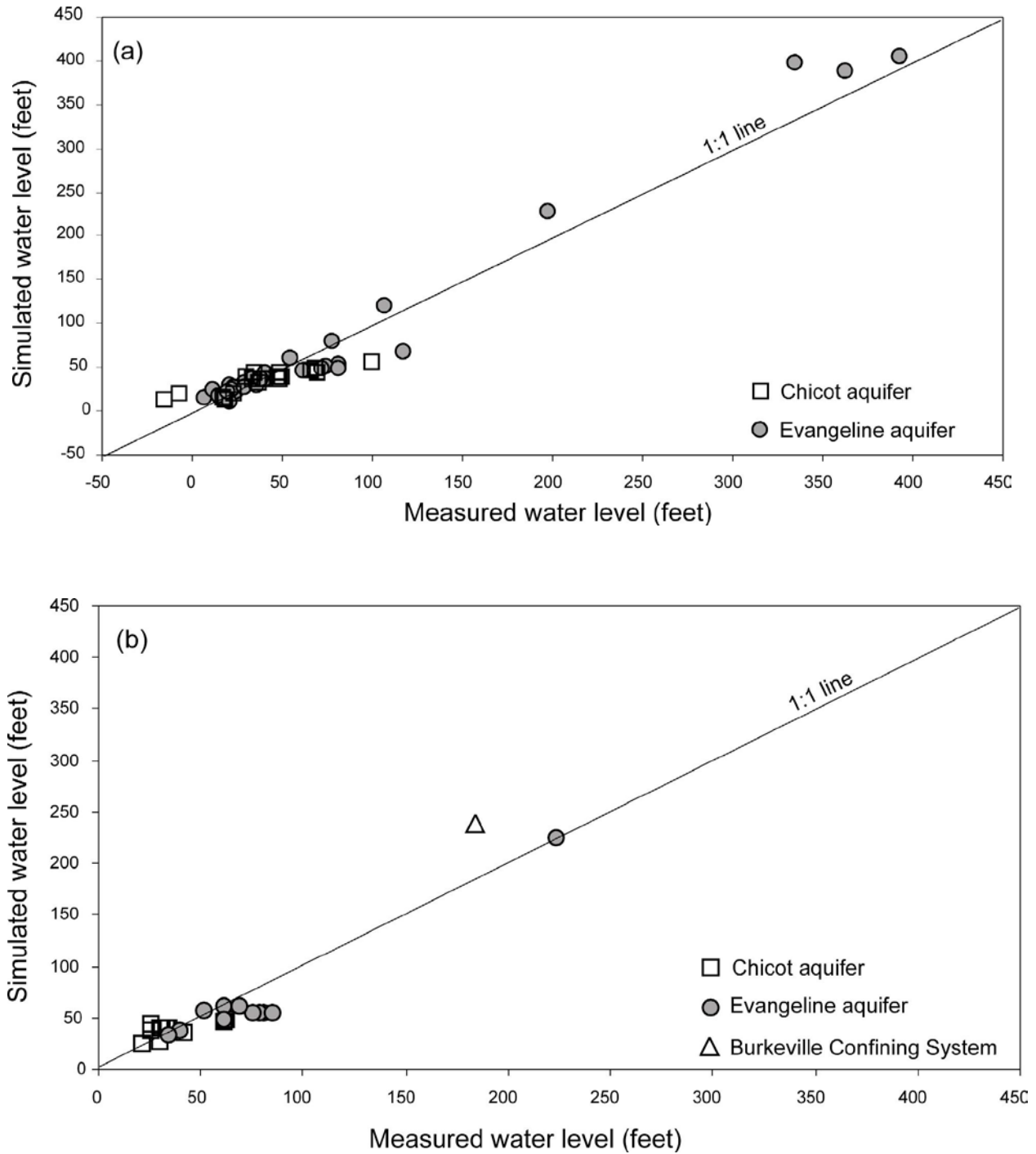


Figure 13-1. Comparison of simulated to measured water levels in the Chicot and Evangeline aquifers for (a) 1990 and (b) 2000. The solid line is the 1:1 line where the simulated water level would exactly match the measured water level.

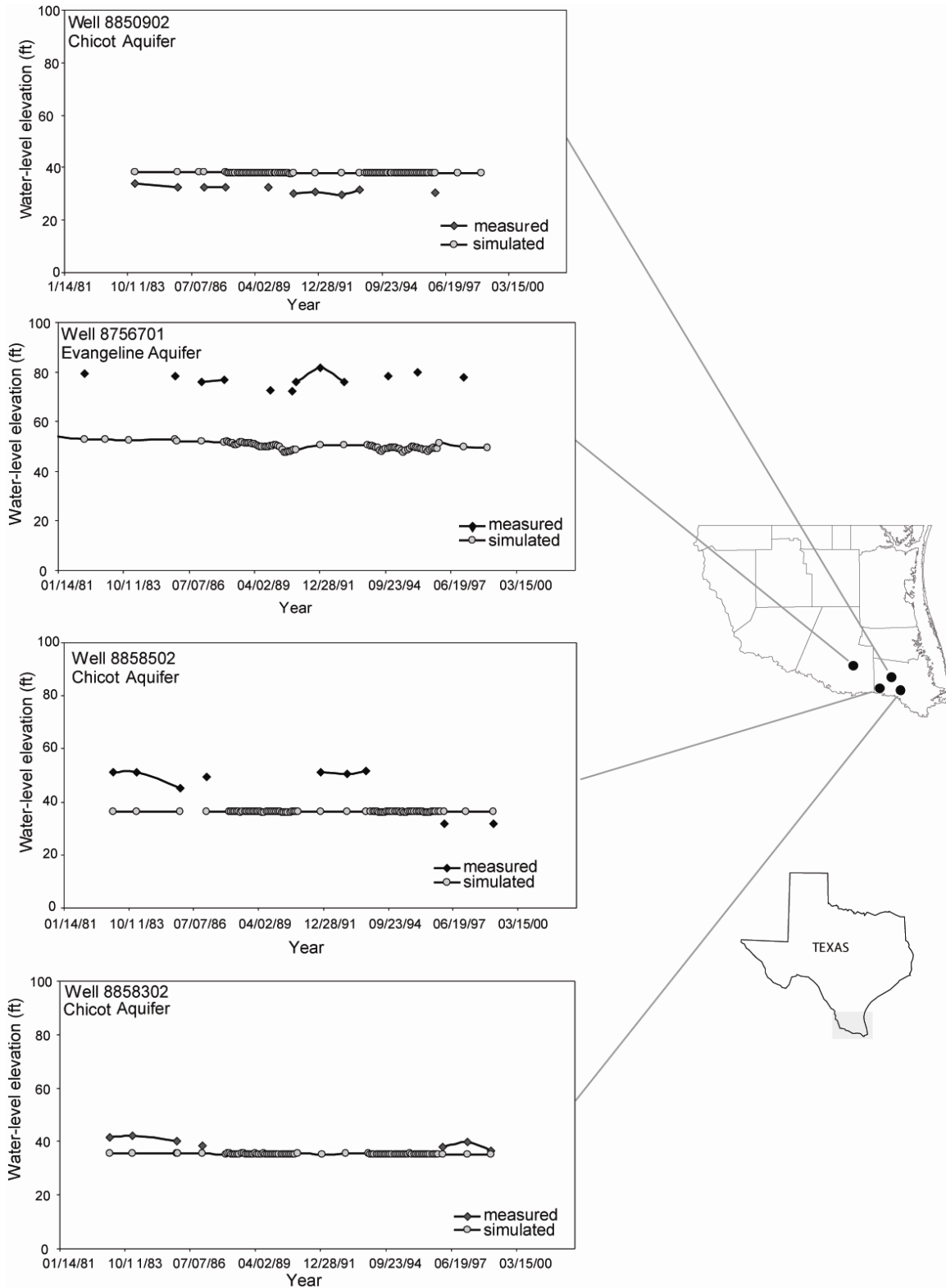


Figure 13-2a. Comparison of simulated water levels to measured water levels during the 1980s and 1990s (ft = feet).

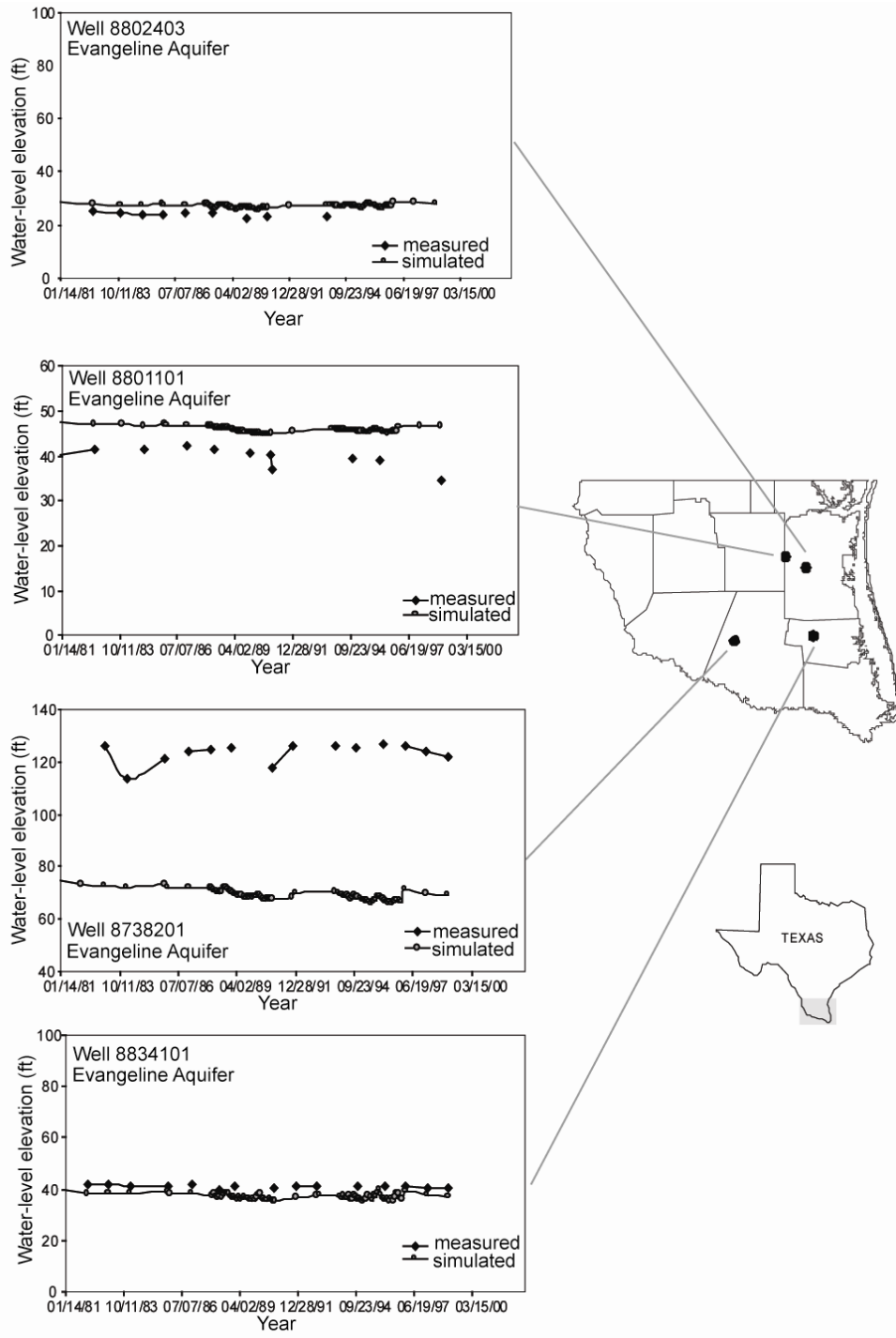


Figure 13-2b. Comparison of simulated water levels to measured water levels during the 1980s and 1990s (ft = feet).

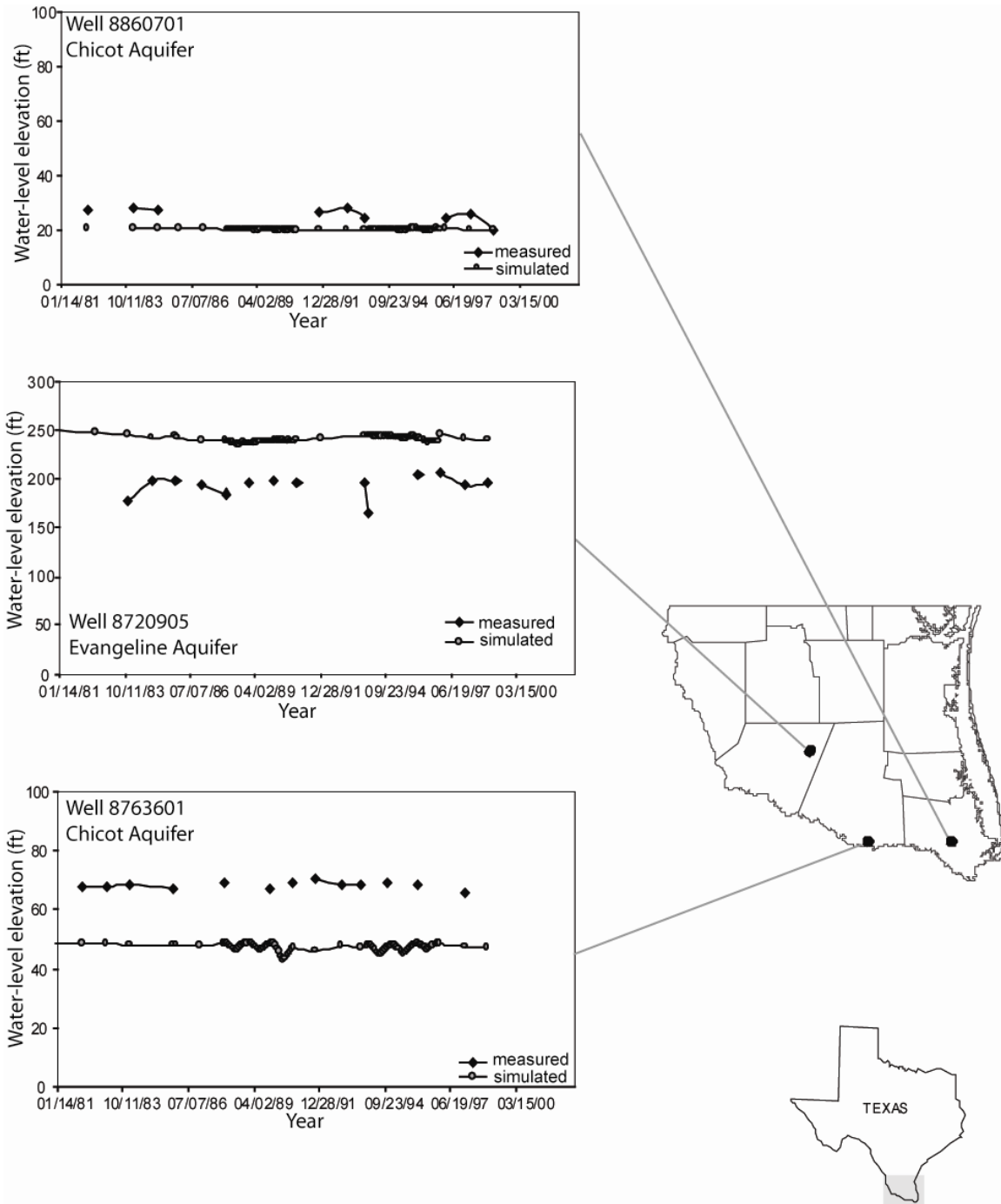


Figure 13-2c. Comparison of simulated water levels to measured water levels during the 1980s and 1990s (ft = feet).

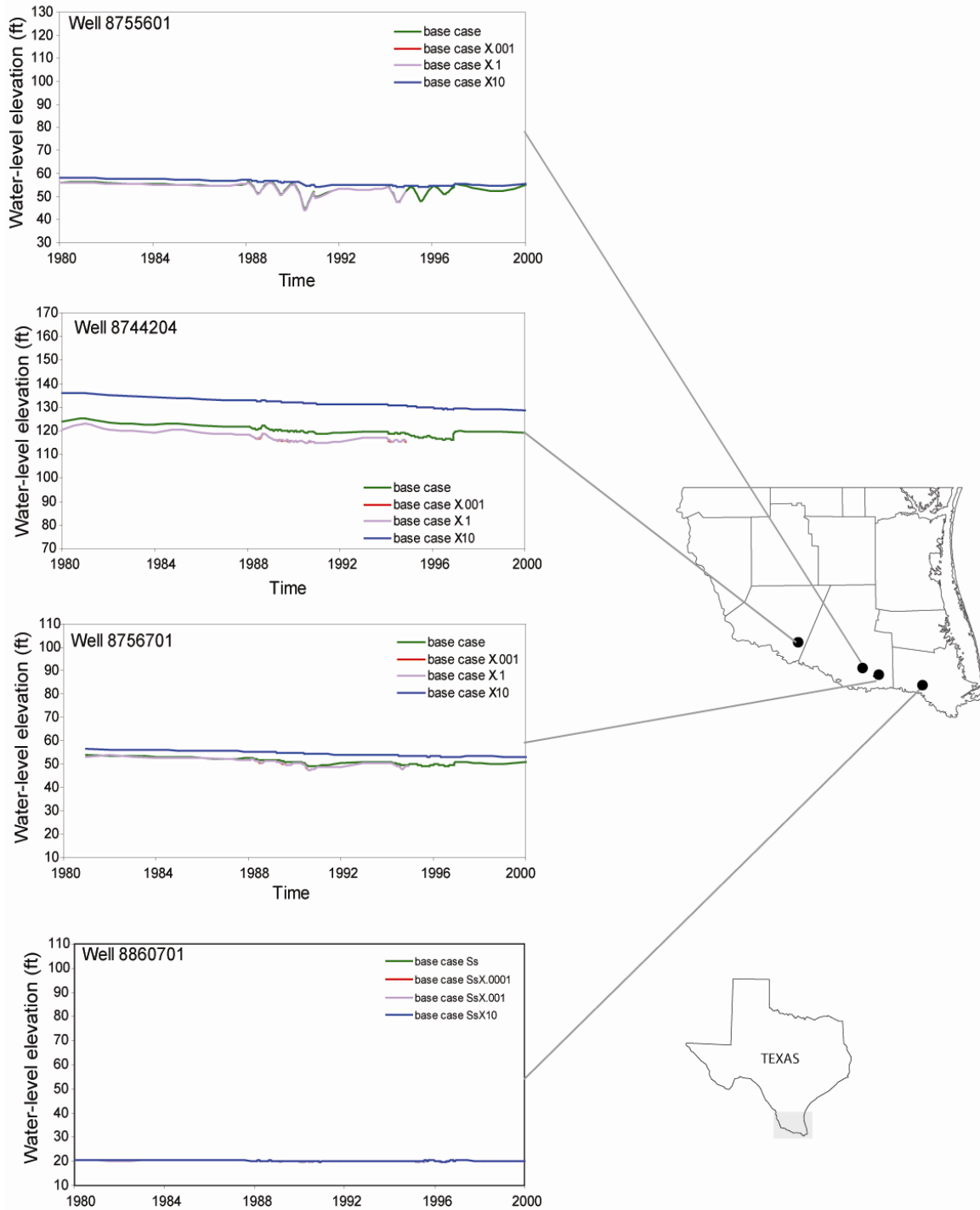


Figure 13-3. Sensitivity of simulated water levels to changes in specific yield (ft = feet).

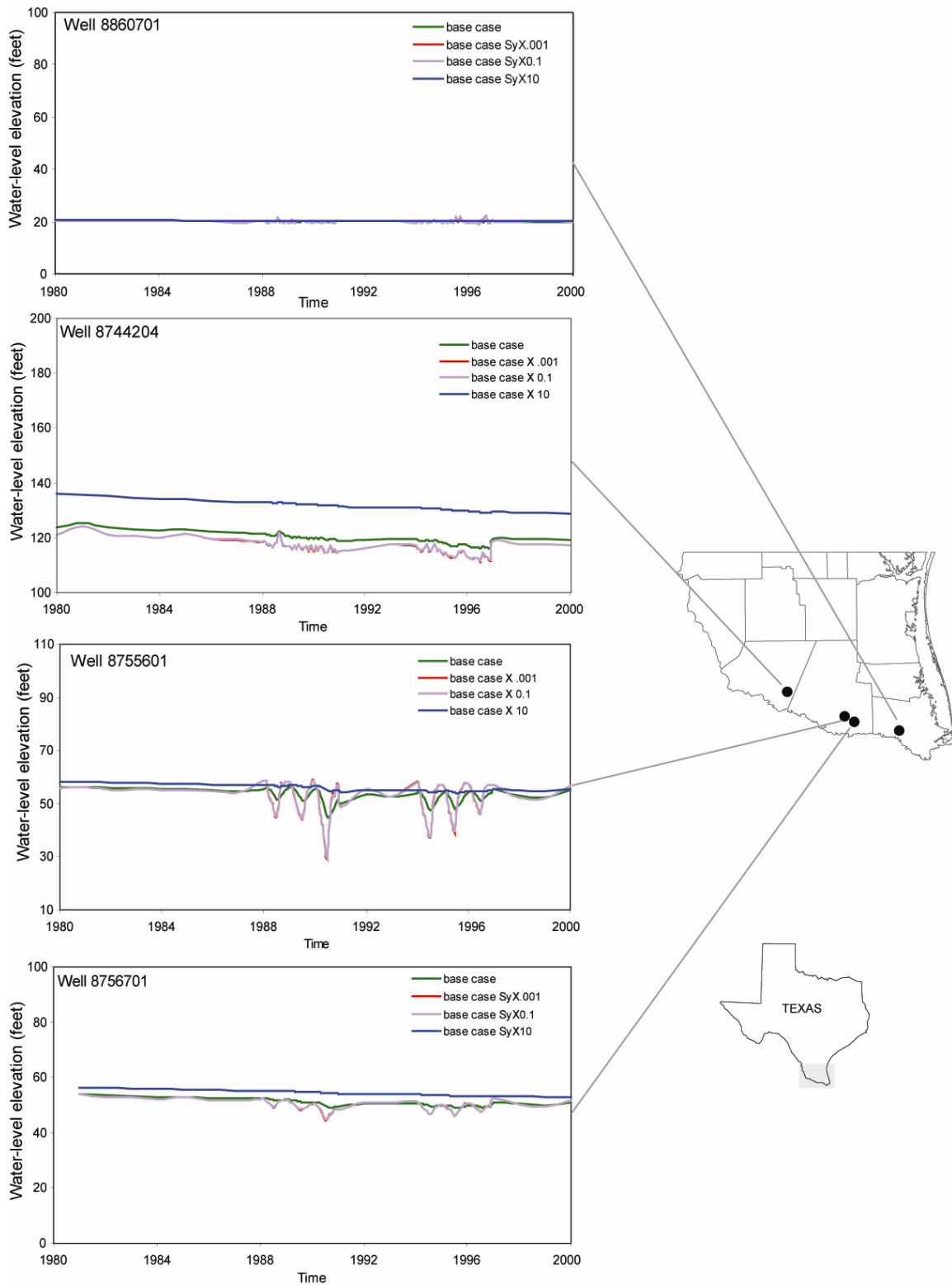


Figure 13-4. Sensitivity of simulated water levels to changes in specific storage (ft = feet).

14.0 Predictions

To help assess the future availability of groundwater in the Lower Rio Grande Valley, we used the calibrated model to predict future water levels using drought-of-record recharge as required by Senate Bill 1 and groundwater demand numbers as provided by the regional water planning groups. The purpose of using the drought of record is to ensure that the state's water needs are met during severe drought.

14.1 *Drought of record*

Drought is a normal, recurrent feature of the regular weather cycle. It coincides with abnormally dry weather that is sufficiently prolonged, resulting in a meteorological, hydrological, or agricultural imbalance in an area. Riggio and others (1987) reported that droughts lasting for more than 6 months are expected to occur once every 16 months and droughts of more than a year duration are likely to appear every 3 years in Texas. The recurrence of drought in Texas may be partly due to its location at about 30° North latitude where many deserts of the world occur (Jensen, 1996). The drought in the 1950s was the worst drought Texas has endured (Jensen, 1996). It lasted for seven years (1950 to 1956), although some observers believe that the drought started as early as 1949 in the Lower Rio Grande Valley and West Texas (Jensen, 1996).

The Parmer Drought Severity Index is widely used to gauge severity of droughts. The index considers rainfall, evaporation, and soil moisture. The Parmer Drought Severity Index is a meteorological drought index that represents abnormally dry or abnormally wet weather conditions. It provides (1) a measurement of the abnormality of recent weather, (2) an opportunity to place current conditions in historical perspective, and (3) spatial and temporal representations of historical droughts (Alley, 1984). Parmer Drought Severity Index values of 0 or more refer to wet conditions (extremely wet, 3.0 to 3.99; very wet, 2.0 to 2.99; moderately wet, 1.0 to 1.99; slightly wet, 0.5 to 0.99; incipient wet spell, 0.49 to -0.49; near normal). Values less than 0 refer to dry conditions (-0.5 to -0.99 incipient dry spell, -1.0 to -1.99 mild drought, -2.0 to -2.99 moderate drought, -3.0 to -3.99 severe drought, and -4.0 or less extreme drought) (Palmer, 1965).

Drought occurs more frequently in the Lower Rio Grande Valley than perhaps the rest of the state. Based on measured rainfall, we observed that nearly all rain gages recorded lower rainfall for the years 1950 to 1956 (Figure 14-1a). We, therefore, considered the years 1950 to 1956 as the drought of record for this area. The historical average rainfall for the years of record 1900 to 1999 is about 22 inches. Annual rainfall for the drought years 1950 to 1956 is about two-thirds (15 inches) of the historical average. The historical Parmer Drought Severity Index average for the years 1895 to 2000 in the Lower Rio Grande Valley is -0.28 (near normal). and for the drought of record the value is -2.81 (moderate drought) (Figure 14-1b). The value of -3.63 in 2000 indicates that the area is under severe drought conditions worse than that experienced during the drought of record.

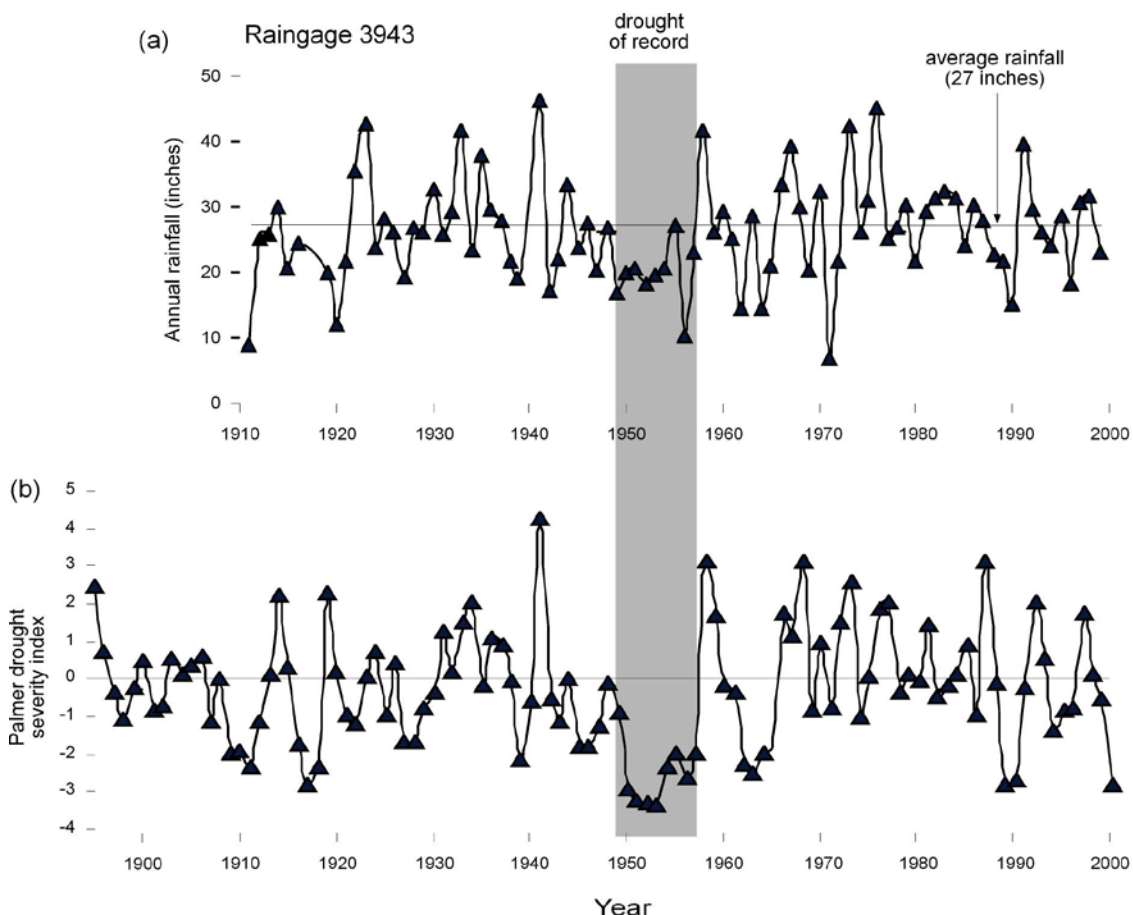


Figure 14-1. Measures of drought as indicated by (a) historical rainfall at a rain gage in Cameron County showing the drought of record (1949–1956) when rainfall was at a minimum and (b) historical Palmer Drought Severity Index indicating that during 1949–1956, the Lower Rio Grande Valley recorded the lowest index values.

We included the drought of record in the predictive simulations using the mean annual precipitation for 1949 through 1956 for each of the rainfall gage stations in the study area. To estimate rainfall for each grid cell, we interpolated the rainfall data for each year in Surfer using kriging. This formed the spatially distributed rainfall for the drought-of-record years and 0.52 percent of this formed the recharge for each year. We defined recharge for normal climatic conditions using the average precipitation data for the years 1960 to 2001 and the same percentage of precipitation as was used in the calibration of the model.

14.2 Predictive runs

We made six predictive runs of the calibrated model to assess future water levels in the aquifer:

- Baseline run: using average recharge through 2050;

- 2010 Run: using average recharge through 2002, using drought-of-record recharge from 2003 through 2010;
- 2020 Run: using average recharge through 2012, using drought-of-record recharge from 2013 through 2020;
- 2030 Run: using average recharge through 2022, drought-of-record recharge from 2023 through 2030;
- 2040 Run: using average recharge through 2032, using drought-of-record recharge from 2033 through 2040; and
- 2050 Run: using average recharge through 2042, using drought-of-record recharge from 2043 through 2050.

We calculated water level declines at the end of each decade by subtracting water levels at the end of 2010, 2020, 2030, 2040, and 2050 from water levels in 1999, the end of the transient calibration period (Figures 14-2, 14-3, 14-4, 14-5, and 14-6). Water levels declined with increased pumpage and lower recharge during the drought of record. When we assigned the drought-of-record recharge and currently projected demand numbers to predict future water levels for 2010, we observed that there were more changes in water levels and storage than the previous years. This depletion in storage is primarily caused by the drought-of-record recharge that is nearly one-third less than recharge in 1999. Subsequent predictive runs from 2020 through 2050 using the drought-of-record recharge suggest that water levels locally may rise. Changes in storage that increase to -10,619 acre-feet per year in 2010 slightly decrease to -10,071 acre-feet per year in 2050 due to a reduction in predicted pumping during this period (Table 11-1). Water levels decline by about 22 feet in the Chicot Aquifer and about 52 feet in the Evangeline Aquifer in 2050. These declines in water levels are minimal compared to 2010. When we used average recharge conditions throughout the next 50 years—an unlikely climatic event—and used predictive groundwater pumping, we observed predicted water levels that are similar to 1980 conditions and a slight increase in the river leakage, probably owing to higher pumpage.

Given the uncertainty in projecting pumping information, we made a model run assuming that the historical increasing trend in pumping continues into the future. We used the historical pumpage information to develop a trend equation and fitted the predicted usage to that trend (Figure 14-7). According to this trend, nearly 2½ times more groundwater could be used through 2050 if the trend in current groundwater pumping continues. For example, the prediction based on current projections states that in 2050 groundwater usage will be about 28,305 acre-feet per year, but groundwater usage is projected to be 68,745 acre-feet per year using historical trends. When we assigned the projected pumpage based on historical trends to the existing pumping distribution and ran the model with drought-of-record recharge, water levels in 2050 are considerably lower than those based on current projections. Under such a scenario, water levels locally may decline by up to 62 feet in the Chicot Aquifer and up to 170 feet in the Evangeline

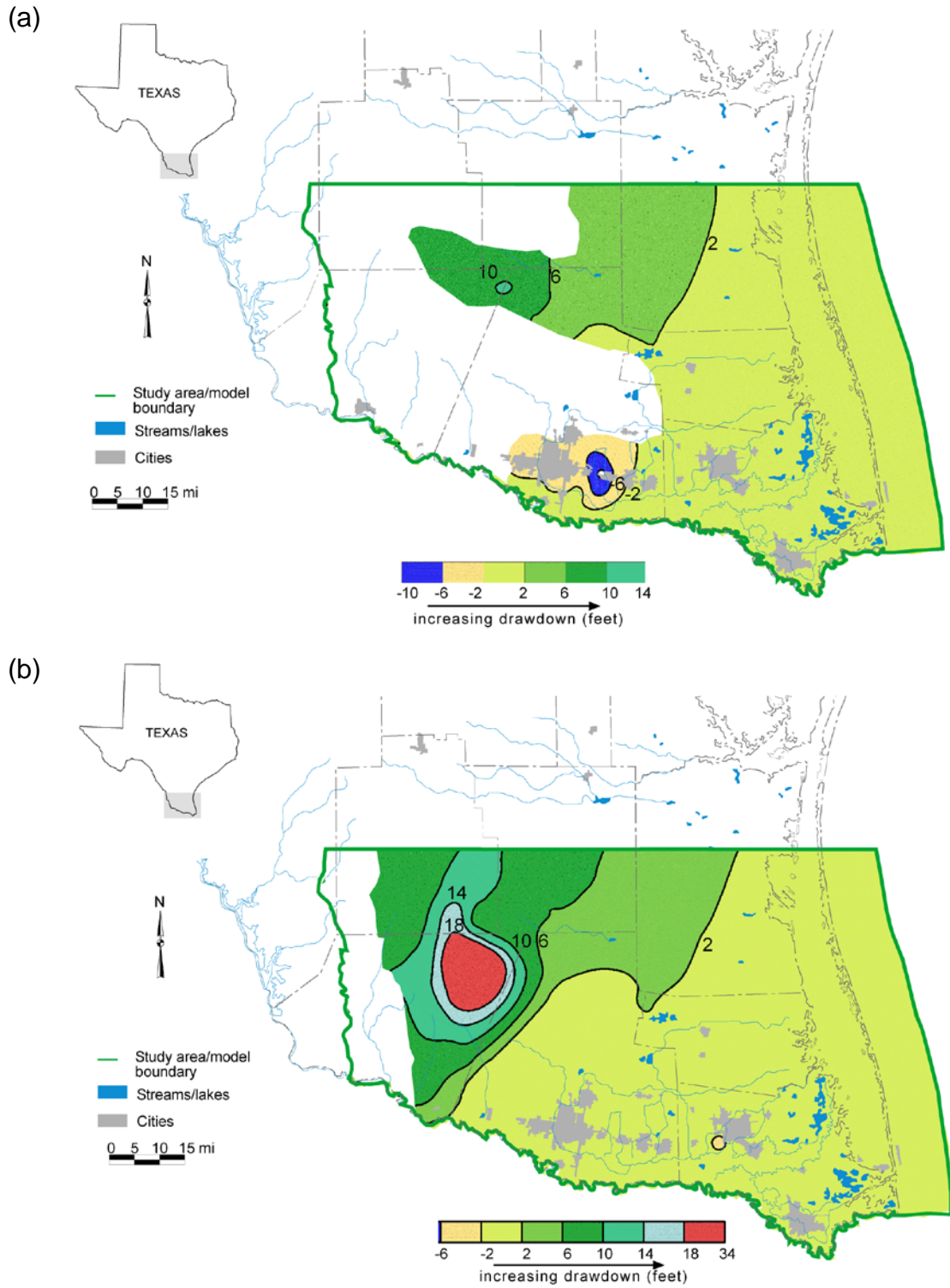


Figure 14-2. Groundwater drawdown in 2010 compared to water levels in 1999 for (a) the Chicot Aquifer and (b) the Evangeline Aquifer using drought-of-record recharge and dry demand numbers provided by the regional water planning groups in their 2001 regional water plans (mi = miles).

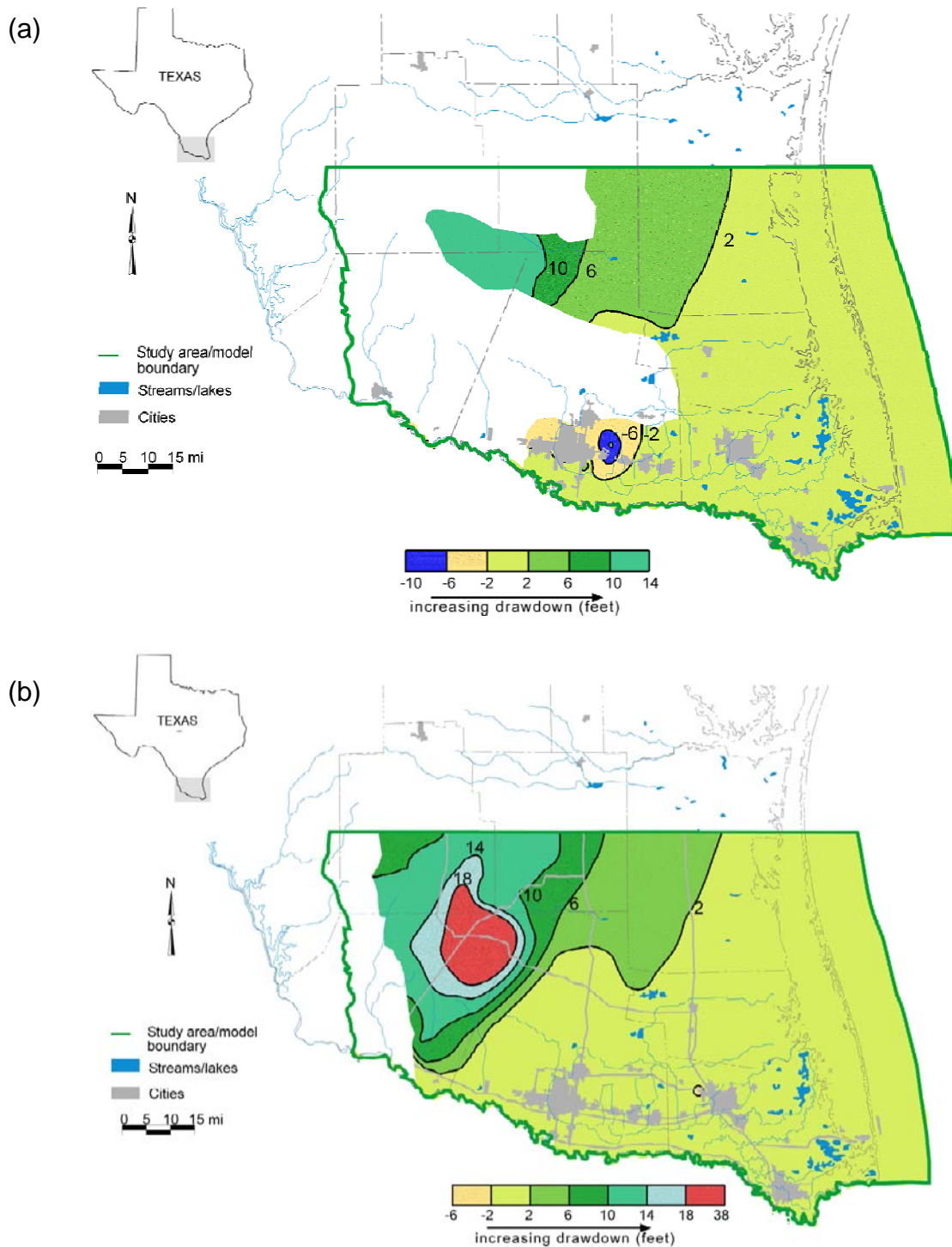


Figure 14-3. Groundwater drawdown in 2020 compared to water levels in 1999 for (a) the Chicot Aquifer and (b) the Evangeline Aquifer using drought-of-record recharge and dry demand numbers provided by the regional water planning groups in their 2001 regional water plans (mi = miles).

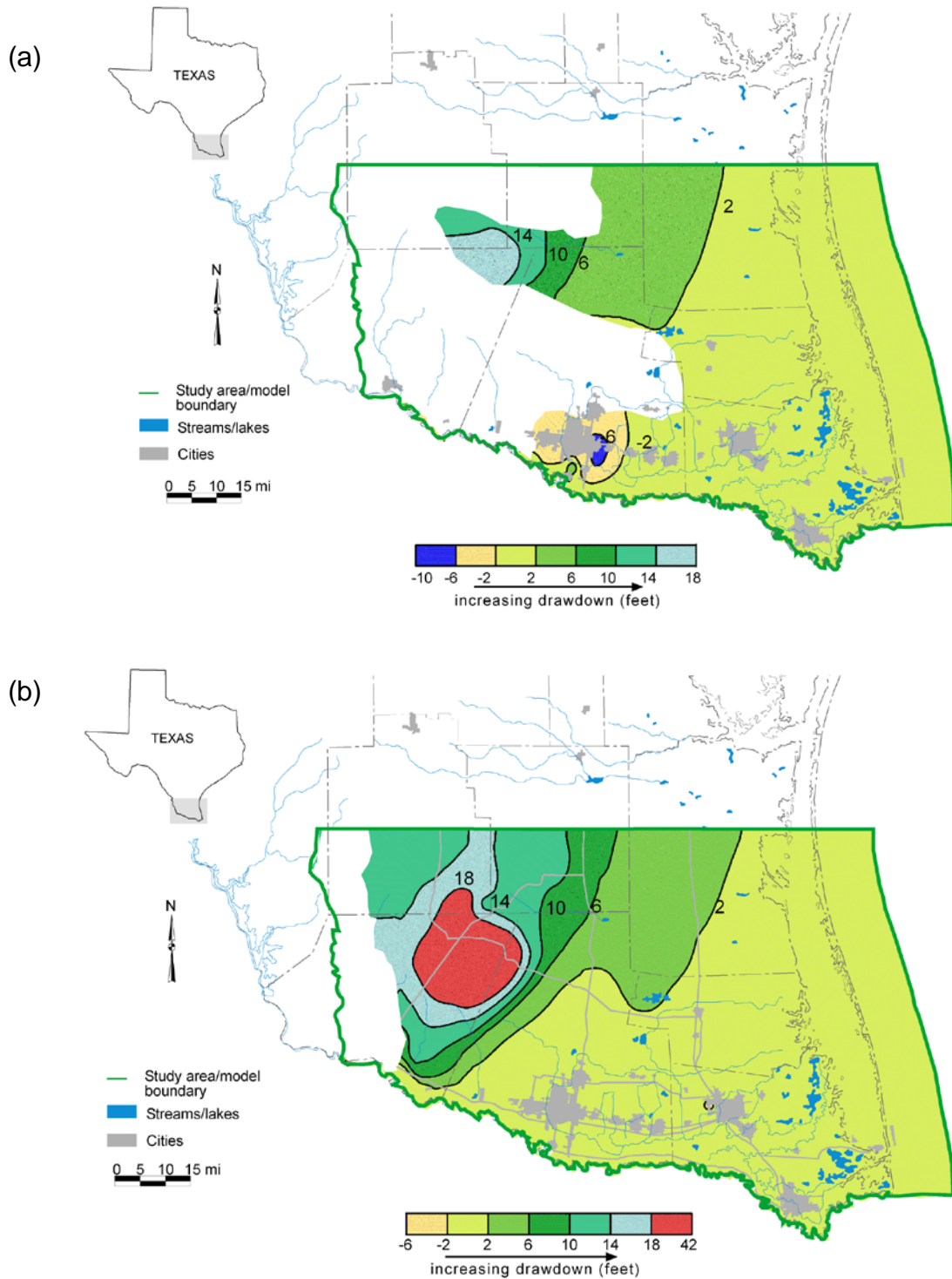


Figure 14-4. Groundwater drawdown in 2030 compared to water levels in 1999 for (a) the Chicot Aquifer and (b) the Evangeline Aquifer using drought-of-record recharge and dry demand numbers provided by the regional water planning groups in their 2001 regional water plans (mi = miles).

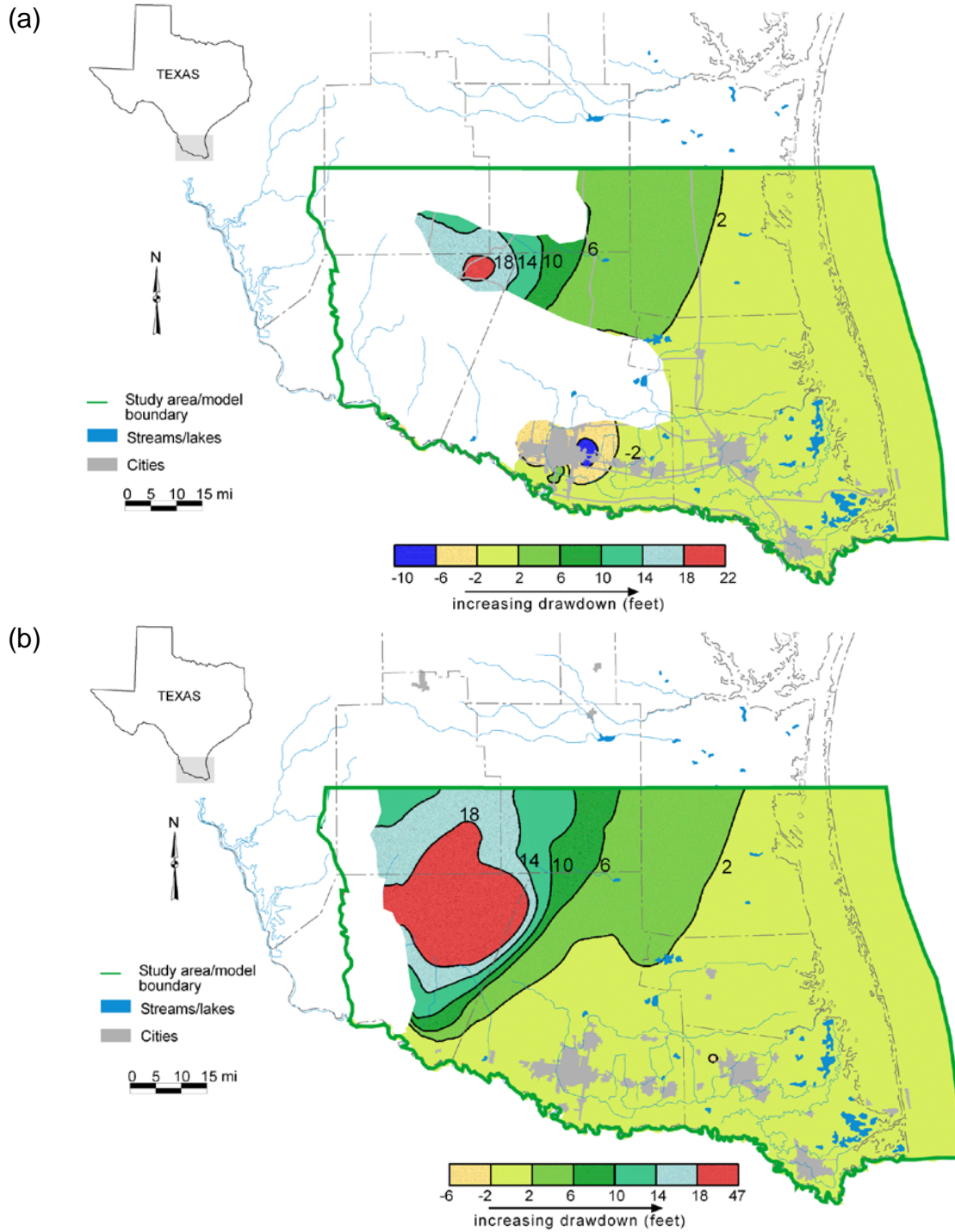


Figure 14-5. Groundwater drawdown in 2040 compared to water levels in 1999 for (a) the Chicot Aquifer and (b) the Evangeline Aquifer using drought-of-record recharge and dry demand numbers provided by the regional water planning groups in their 2001 regional water plans (mi = miles).

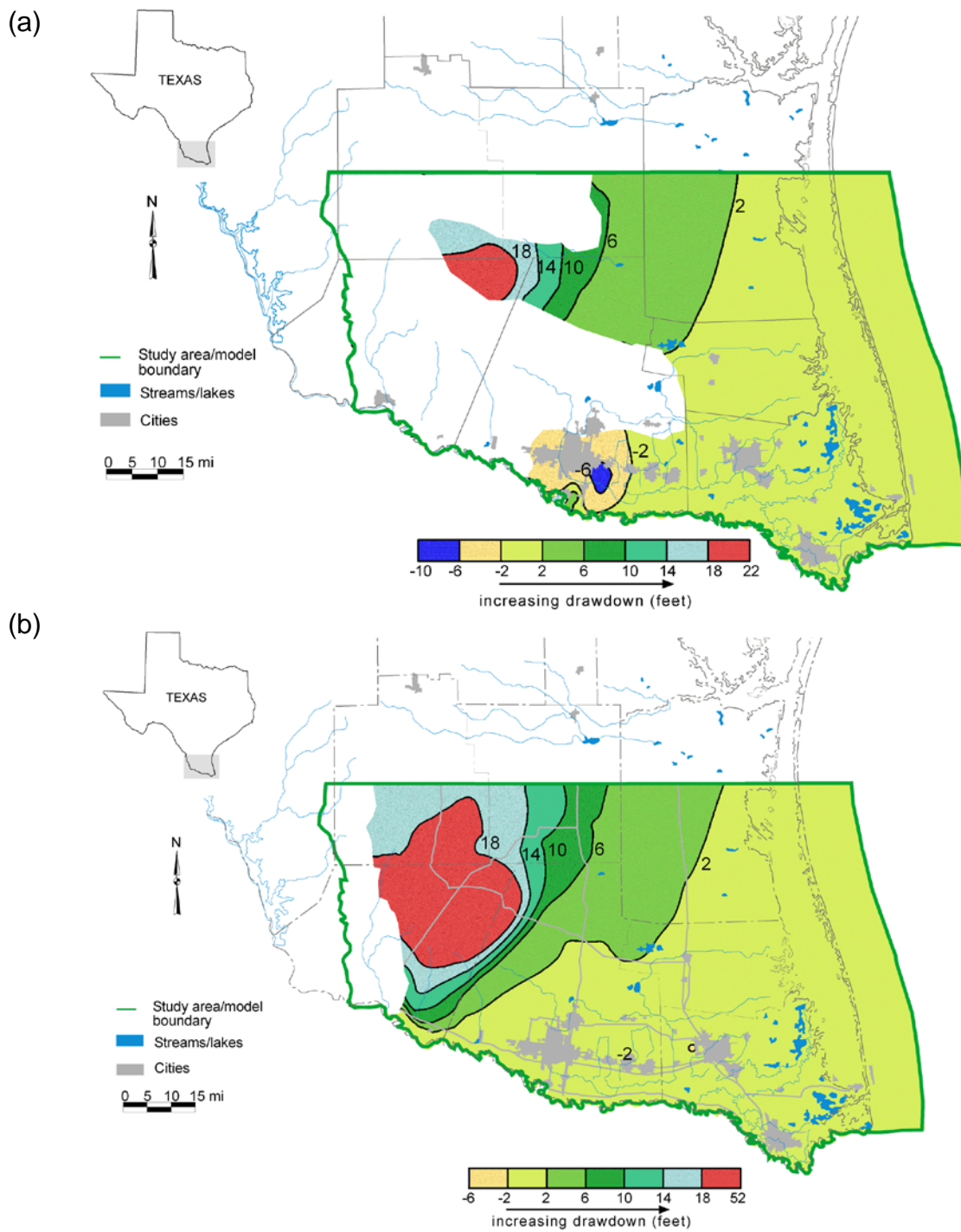


Figure 14-6. Groundwater drawdown in 2050 compared to water levels in 1999 for (a) the Chicot Aquifer and (b) the Evangeline Aquifer using drought-of-record recharge and dry demand numbers provided by the regional water planning groups in their 2001 regional water plans (mi = miles).

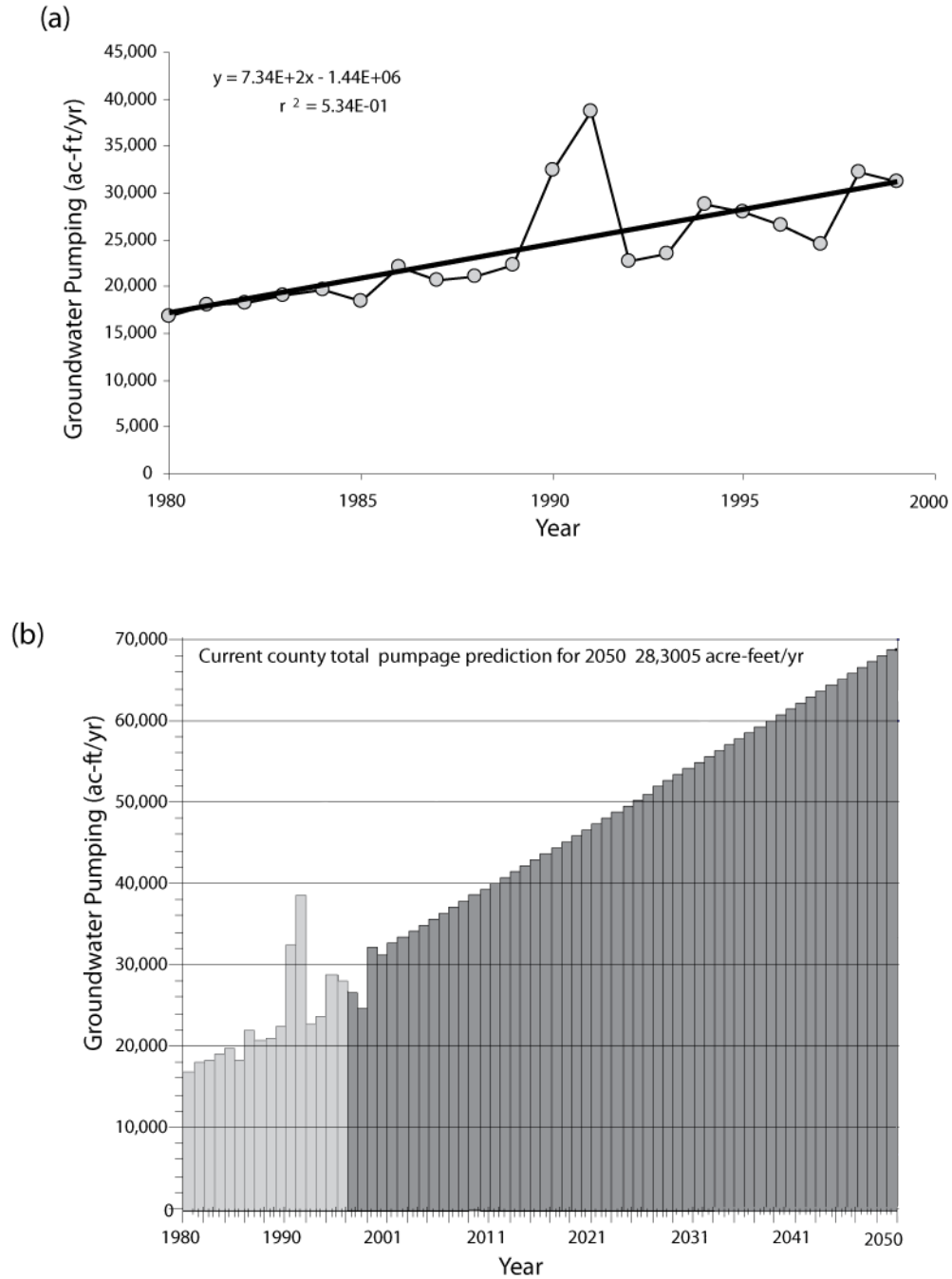


Figure 14-7. Development of an alternative predictive simulation based on historical trends. We first (a) used linear regression to develop an equation for a line to describe the trend since 1980 and (b) then used the line to project through 2050 (ac-ft/yr = acre-feet per year).

Aquifer. Water level declines in the Chicot Aquifer are much more widespread with water level declines of about 20 feet over two-thirds of the model area. This scenario, however, assumes that future pumpage increases by 2½ times and future pumping centers remain in the same locations as in the past.

15.0 Limitations of the model

All numerical models have limitations caused by (1) the quality and quantity of input data sets assembled to construct the model, (2) simplifications and assumptions that need to be applied during the implementation of the conceptual model into the model grid, and (3) the applicability of the model results due to scale of the model.

15.1 Input data

Uncertainties are introduced when approximations are made in gathering and analyzing input data. For example, in the absence of adequate control points that could help determine the aquifer geometry, the structure surfaces are generalized because of the complex stratigraphy of a fluvial-deltaic depositional setting. Without good seismic data, we did not consider faulting in the construction of the structure surfaces. We used the structure surfaces on the assumption that any growth faults present are not sealing faults to groundwater flow. This assumption is supported by a lack of any measured water level shifts in the study area. Moreover, any appreciable vertical displacement due to growth faulting would also likely affect deeper sediment sections in the downdip areas—areas not a focus of this investigation.

Hydraulic properties were based on all available specific-capacity and pumping test data. Even after including all this data, there are areas with few data points, particularly in the north in Jim Hogg and Kenedy counties. The areas with no data were populated with interpolated hydraulic conductivity values after we established their spatial relationship within the model area. Although this approach may be fine for the regional model, it may not be applicable for any local scale assessment or simulation. Much more detailed aquifer testing is necessary to characterize local scale hydrogeology.

Recharge rates are based on rainfall data provided by a limited number of rain gages, which do not evenly cover the entire model area. The interpolated values between the gages may not be an exact representation of the actual rainfall value in the area. We could not use the base flow data to further enhance the recharge because only three river gages presently exist along the Rio Grande and none exist in the rest of the model area. In addition, we have assumed that the relationship between precipitation and recharge is linear, which may not necessarily be the case. Therefore, we may be underestimating or overestimating the recharge in years with different amounts of precipitation. Irrigation return flow has not been accounted for as there was no estimate on what portion of it reaches the groundwater. This may result in underestimating the recharge reaching the groundwater.

Our current distribution of recharge is based on rainfall distribution for any respective year. However, local attributes, such as varying soil type in the updip outcrop and the downdip coastal

areas and topographic variations, may control recharge at a smaller-than-basin scale. A more accurate representation of the recharge rate could be determined by using long-term information on base flow and precipitation, which does not currently exist, and including more local attributes of soils and topography. In addition, recharge also partly depends on our estimation of the horizontal and vertical hydraulic conductivity of the aquifers.

Estimating the evapotranspiration proved difficult given its complexity and the multitude of variables that control this parameter. Our estimation of the evapotranspiration considered a number of factors, including (1) density of mesquite, (2) rainfall distribution, and (3) groundwater depth. A higher evapotranspiration rate at higher density may appear reasonable but may be simplistic because other factors, such as stand characteristics, were not considered. By incorporating the best combination of evapotranspiration and rainfall infiltration rate, we calibrated the recharge value in the model by trial and error, which is our best estimate of recharge.

There were few water level measurements for the Burkeville Confining System and the Jasper Aquifer for most of the model area. Therefore, their simulated water levels could not be calibrated except for a qualitative comparison in the outcrops. Most of the well measurements for the Chicot Aquifer were concentrated in the south near Rio Grande, with few data for the remaining two-thirds of the model area. There were also few water level measurements for the Evangeline Aquifer in Jim Hogg and Kenedy counties. Also, there was little water level information in the areas about 20 miles inland from the coastline. Limited availability of water level data tends to bias model calibration toward areas where water levels have been measured.

Only a few wells had monthly water levels during 1980 to 2000. While we were able to simulate seasonal fluctuations in water levels during the year, we were unable to compare them with the measured heads because of limited information. We selected water level records for the winter months of a given year. Given the limitation of water levels in certain locations, we had to widen the time frame to include additional water level information to assist in interpolating the data.

We used MODFLOW's River package to simulate interaction between the aquifers and the Rio Grande and Arroyo Colorado. It is possible that if pumping in the aquifers increases considerably in the future, any predicted drawdown could be underestimated. This is primarily because river leakage from the Rio Grande and the Arroyo Colorado could increase considerably due to an increase in the gradient of the water table. In addition, MODFLOW's River package does not allow the river to dry up.

An alternative to the River package is the Streamflow Routing package, which is designed to account for flow in the streams and simulate interaction between surface water and groundwater. This package could provide additional calibration parameters for flow through the Rio Grande that may prove helpful in assessing surface water discharge to the aquifers and the Gulf of Mexico. However, assessing that discharge could be difficult because of the lack of diversion information from the Rio Grande.

There appears to be considerable discrepancy between historic and predictive groundwater usage. The predictive pumping is considerably lower than historic usage, although population in

the model area is expected to more than double over the next 50 years. Predictive pumping may need to be examined in more detail because pumping is one of the most sensitive parameters in the model. We did, however, make a sensitivity run by increasing the predictive pumping so that it followed the trend of historic usage.

15.2 Assumptions

We used several assumptions to simplify construction of the model. Some of these assumptions are (1) dune sands in the northwest were included into the Chicot Aquifer, (2) there is no groundwater flow between the Jasper Aquifer and the underlying Catahoula Confining System, (3) all mesquite stands and root systems equally extract groundwater, and (4) differences in groundwater densities do not appreciably affect groundwater flow.

We included the dune sands within the Chicot Aquifer because we assumed that the surficial dunes are in hydraulic continuity with the Chicot Aquifer below. Pockets of the Goliad Sand outcrops in this area, and elevations from the topographic maps indicate that the dunes are probably as much as 50-feet thick.

The assumption that there is no flow between the Jasper Aquifer and the Catahoula Confining System probably holds true for most of the model area except in the outcrop where the Catahoula Confining System is relatively more sandy than in downdip areas. However, due to small lateral extent of the sandy areas of the Catahoula Confining System, flow from these areas may be insignificant.

All mesquite was assumed to have root systems that reach to a depth of 30 feet. Using a uniform 30-foot extinction depth to characterize root depth over the model area may under- or over-estimate evapotranspiration. Also, only a fraction of the recharge was removed by the evapotranspiration rate that we assigned to calibrate the model. We considered the calibrated evapotranspiration rate to be representative of the natural condition, since an increase in the evapotranspiration rate adversely affected our calibration results or caused to dry-up outcrop areas. Therefore, the evapotranspiration rate applied in the model is our best estimate based on what we know from the literature.

Most of the groundwater in the study area has a salinity (also known as total dissolved solids) much less than that of seawater (35,000 milligrams per liter). For example, more than 95 percent of groundwater in the Chicot Aquifer has total dissolved solids values less than 10,000 milligrams per liter. Therefore, density variations due to higher salinity should not be a concern except for along the coastlines and offshore where the salinity may approach that of seawater. The flow field can also change due to lowered groundwater density at higher subsurface temperature (at 50°C the density of water is 0.98 grams per cubic centimeter) (Anderson and Woessner, 1992). As most of the groundwater in our area occurs at relatively shallow depth, our assumption on density is probably appropriate.

15.3 Applicability

Like all regional groundwater flow models, this model has limitations. A regional flow model constructed with a grid size of 1 mile by 1 mile is best suited to evaluate regional-scale groundwater issues such as predicting aquifer-wide water level changes under various pumping or recharge conditions. The model in its current state will not predict water level declines around individual wells or small well fields. This is because local heterogeneities in storativity and hydraulic conductivity in the aquifer can not be translated at the scale of the model. However, the predicted water levels should be accurate at a regional scale when a group of wells or water levels in an entire county is considered. This model can be further refined to a smaller scale or, alternatively, analytical equations can be used to address local groundwater issues.

16.0 Future improvements

The validity of a model calibration largely depends on the quality of input data. There is a paucity of hydraulic conductivity and storage information in the Chicot and the Evangeline aquifers in Jim Hogg, Brooks, and Kenedy counties. Additional aquifer tests would help better characterize hydraulic properties of these two aquifers. The Streamflow Routing Package in MODFLOW could be used to better simulate groundwater-surface water interaction and flow at the two reaches of the Rio Grande within the model area where gages are present. The Streamflow Routing Package may allow simulation of river reaches that go dry as occurred in the downstream sections of the Rio Grande in 2000. Base flow from the Arroyo Colorado and Rio Grande could also be independently evaluated using analytical methods to provide greater confidence in the model. Additional gages may need to be installed to provide streamflow data that could be used to better simulate the flow.

Recharge was treated in the model as a direct function of the distributed rainfall. Including the outcrop soils and canal loss could help improve the recharge estimate. Evapotranspiration may require more detailed field examination as evapotranspiration may locally consist of a significant component of groundwater usage. Additional monitoring wells to record water levels, particularly water levels at monthly intervals, will also help future modeling.

17.0 Conclusions

We developed a numerical groundwater flow model for the Lower Rio Grande Valley using the U.S. Geological Survey MODFLOW-96 code. The model has four layers representing the Chicot Aquifer, Evangeline Aquifer, Burkeville Confining System, and the Jasper Aquifer. It covers parts or all of seven counties, extending from Jim Hogg County in the northwest to Cameron County in the southeast. The model has 27,007 active cells, each with a uniform grid size of 1 mile by 1 mile. We developed the conceptual model based on a review of previous work and assessment of information on water levels, recharge, and hydraulic properties. Our modeling approach included (1) calibrating a steady-state model to mean annual water levels of 1930 to 1980, (2) calibrating a transient model to measured water level fluctuations from 1980 to 1999, and (3) making predictive runs from 2000 to 2050 using demand numbers based on current projections and drought recharge conditions.

We calibrated the steady-state model to mean annual water levels as measured between 1930 and 1980 when water levels did not change much. The model generally replicates the spatial distribution of the water levels and groundwater flow toward the Gulf of Mexico and to and from the Rio Grande. The root mean squared error of the calibrated steady-state model is 23 feet which is about 4.4 percent of the total hydraulic head drop across the model area. We used about 0.52 percent of the average annual rainfall for 1930 to 1980 to calibrate the steady-state model. We found that about 88,000 acre-feet per year of water flows through the Gulf Coast Aquifer. Of the total flow, 47 percent of the recharge comes from rainfall, and 53 percent of the recharge seeps into the aquifers from the Rio Grande. Cross-formational flow is a significant component of the flow within individual aquifers, with deeper groundwater from the Evangeline Aquifer moving upward into the downdip areas of the Chicot Aquifer.

To determine uncertainty in the input data set, we tested the sensitivity of the model results to several parameters. We observed that the model is more sensitive to recharge and horizontal hydraulic conductivity of the Chicot and the Evangeline aquifers. The change in storage in the aquifers progressively increases from -1,281 acre-feet per year in 1991 to -4,520 acre-feet per year in 1999 due to increased pumping. When we assigned the drought-of-record recharge and currently projected demand numbers to predict future water levels for 2010, we observed that there is greater change in water levels and storage than in the previous years. Change in storage increases to -10,619 acre-feet per year in 2010 due to drought conditions, but slowly decreases to -10,071 acre-feet per year due to decreased pumping through 2050. When we used average recharge conditions throughout the next 50 years and projected pumping, we observed that the predicted water levels are similar to steady-state conditions in 1980, with a slight increase in the river leakage. However, if pumping in the future continues to grow at current trends, the model predicts that water levels and storage decline considerably.

Groundwater in the Lower Rio Grande Valley varies widely in composition from fresh to brine (198 to 37,752 milligrams per liter). The more saline waters occur at depths of less than 500 feet. Groundwater in southwestern Starr, south central Cameron, and northern Willacy counties appear to have the highest values of total dissolved solids. However, large areas in north central Brooks, northern Hidalgo, eastern Starr, and western Willacy counties also host fresh water. Using the aquifer thickness, cell dimensions of 1 mile by 1 mile, and a porosity of 0.15 for the Chicot and the Evangeline aquifers, we estimated the volume of fresh to moderately saline water in each aquifer. We estimate that about 39,000,000 acre-feet of fresh to moderately saline water is present in the Chicot Aquifer and about 230,000,000 acre-feet of fresh to moderately saline water is present in the Evangeline Aquifer within the study area.

18.0 Acknowledgments

We would like to acknowledge a number of people for their help to this modeling project: Mr. Roberto Anaya and Mr. Richard Smith for structure; Dr. Ian Jones and Ms. Cindy Ridgeway for preparing pumping data sets, Dr. Ted Way for preparing water levels, and Mr. Edward Angle and Ms. Merry Klonower for formatting and editorial review of the report. We also thank Mr. Robert Flores for information on planning issues and the Region M Regional Water Planning Group members for their contribution, patience, and participation through several

stakeholder meetings. We are also thankful to our senior management, Mr. Harald Petrini and Mr. Bill Mullican, for their encouragement, inspiration, and support.

19.0 References

- Allen, R.G., Pereira, L. S., Raes, D., Smith, M., 1998, Crop evapo-transpiration–Guidelines for computing crop water requirements: FAO Irrigation and Drainage Paper 56, Food and Agriculture Organization of the United Nations, Rome, 300 p.
- Alley, W.M., 1984, The Palmer Drought Severity Index–Limitations and assumptions: *Journal of Meteorology*, v. 23, p. 1100–1109.
- Anderson, M.P., and Woessner, W.W., 1992, Applied groundwater modeling: Simulation of flow and advective transport: San Diego, Academic Press, 381 p.
- ASTM (American Society of Testing and Materials), 1994, Standard guide for conducting a sensitivity analysis for a groundwater flow model application: American Society of Testing and Materials Standard D 5611-94e1, 6 p.
- Baker, E.T., 1965, Groundwater resources of Jackson County, Texas: Texas Water Development Board Report 1, 225 p.
- Baker, Jr., E.T., 1979, Stratigraphic and hydrogeologic framework of part of the coastal plain of Texas: Texas Department of Water Resources Report 236, 43 p.
- Baker, Jr., E.T., 1986, Hydrogeology of the Jasper Aquifer in the southeast coastal plain: Texas Water Development Board Report 295, 64 p.
- Baker, Jr., E.T., and Wall, J.R., 1976, Summary appraisals of the nation’s groundwater resources–Texas Gulf region: U.S. Geological Survey Open-File Report, 61 p.
- Baker, R.C., and Dale, O.C., 1961, Groundwater resources of the Lower Rio Grande Valley area, Texas: Texas Board of Water Engineers Bulletin 6014, 81 p.
- Berg, R.R., 1986, Slumped, delta-front reservoir sandstone in the Eocene Yegua Formation, East Sour Lake field, southeast Texas: *Gulf Coast Association of Geological Societies Transactions*, v. 36, p. 401–407.
- Berg, R.R., 1995, Sealing properties of Tertiary growth faults, Texas Gulf Coast: *American Association of Petroleum Geologists Bulletin*, v. 79, p. 375–393.
- Bornhauser, M., 1958, Gulf Coast tectonics: *American Association of Petroleum Geologists Bulletin*, v. 42, p. 339–370.
- Borrelli, J., Fedler, C.B., and Gregory, J.M., 1998, Mean crop consumptive use and free-water evaporation for Texas: Department of Civil Engineering, Texas Tech University, Lubbock, Texas, Texas Water Development Board Grant Number 95-483-137, 260 p.

- Bureau of Economic Geology, 1976, *Geologic Atlas of Texas, McAllen-Brownsville Sheet*: The University of Texas at Austin .
- Bureau of Economic Geology, 1997, *Tectonic map of Texas*: The University of Texas at Austin
- Canadell, J., Jackson, R.B., Ehleringer, J.R., Mooney, H.A., Sala, O.E., and Schulze, E.D., 1996, Maximum rooting depth of vegetation types at the global scale: *Oecologia*, v. 108, p. 583–595.
- Carlson, D.H., Thurow, T.L., Knight, R.W., and Heitschmidt, R.K., 1990, Effects of honey mesquite on the water balance of Texas rolling plains range land: *Journal of Range Management*, v. 43, no. 6, p. 491–496.
- Carr, J.E., Sandeen, W.M., and McLane, I.R., 1985, Digital models for simulation of groundwater hydrology of the Chicot and Evangeline aquifers along the Gulf Coast of Texas: Texas Department of Water Resources Report 289, 101 p.
- Carr, W.R., 2000, Natural vegetation types of Texas and their representation in conservation areas: Austin, The University of Texas at Austin, Ph.D. dissertation, 177 p.
- Chiang, W.H., and Kinzelbach, W., 1998, *Processing MODFLOW—A simulation system for modeling groundwater flow and pollution*: Software manual, Springer-Verlag, Berlin, 325 p.
- Chowdhury, A.H., and Mace, R.E., 2002, Groundwater flow modeling to estimate fresh and brackish water availability in the Lower Rio Grande Valley, South Texas, *in* Dutton, S.P., Ruppel, S.C., and Hentz, T.F. (eds.), *Transactions of the Gulf Coast Association of Geological Societies and Gulf Coast Section of the Society of Economic Paleontologists and Mineralogists*, v. LII, p. 122.
- Chowdhury, A.H. and Mace, R.E., 2004a, Estimating groundwater availability in the Gulf Coast Aquifer, South Texas, *in* *Groundwater flow understanding from local to the regional scales*, Proceedings: XXXIII Congress International Association of Hydrogeologists and 7th Asociación Latinoamericana de Hidrología Subterránea para el Desarrollo, Zacatecas City, Mexico, 4 p., CD-ROM, ISBN 970-32-1749-4.
- Chowdhury, A.H. and Mace, R.E., 2004b, Geochemical Evolution of the Groundwater in the Gulf Coast Aquifer of South Texas *in* *Groundwater flow understanding from local to the regional scales*, Proceedings: XXXIII Congress International Association of Hydrogeologists -and 7th Asociación Latinoamericana de Hidrología Subterránea para el Desarrollo, Zacatecas City, Mexico, 4 p., CD-ROM, ISBN 970-32-1749-4.
- Chowdhury, A.H., Wade, S., Mace, R.E., and Ridgeway, C., 2004, A groundwater availability model of the central Gulf Coast Aquifer System—Numerical simulations through 1999: unpublished report, Texas Water Development Board, 114 p.

- Chowdhury, A.H., Bogichi, R., and Hopkins, J., 2006, Hydrogeochemistry, salinity distribution and trace constituents: implications for salinity sources, geochemical evolution, and flow system characterization, Gulf Coast Aquifer, Texas: Aquifers of the Gulf Coast of Texas, Texas Water Development Board Report 365, p. 81–128.
- Clark, I., 1979, Practical geostatistics: London, Applied Science Publishers Limited, 129 p.
- Cloos, E., 1962, Experimental analysis of Gulf Coast fracture patterns: American Association of Petroleum Geologists Bulletin, v. 52, p. 420–444.
- Cuoma, C.J., Ansley, J., Jacoby, P.W., and Sosebe, R.E., 1992, Honey mesquite transpiration along a vertical site gradient: Journal of Range Management, v. 45, no. 4, p. 334–338.
- Custido, E., 1987, Hydrogeochemistry and tracers, *in* Custido, E. (ed.), Groundwater problems in coastal areas: Studies and reports in hydrogeology: UNESCO, no. 45, p. 213–269.
- Dale, O.C., 1952, Groundwater resources of Starr County, Texas: Texas Board of Water Engineers Bulletin 5209, 47 p.
- Dennis, J.G., Tieszen, L.L., and Vetter, M.A., 1978, Seasonal dynamics of above and below ground production of vascular plants at Borrow, Alaska, *in* Tieszen, L.L. (ed.), Vegetation and production ecology of the Alaskan Arctic Tundra: Ecological Studies 29, Berlin Heidelberg, New York, Springer, p. 113–140.
- Doering, J., 1935, Post-Fleming surface formations of coastal southeast Texas and south Louisiana: Bulletin of the American Association of Petroleum Geologists, v. 19, p. 651–688.
- Dutton, A.R., and Richter, B.C., 1990, Regional hydrogeology of the Gulf Coast Aquifer in Matagorda and Wharton counties, Texas—Development of a numerical flow model to estimate the impact of water management strategies: Report prepared for the Lower Colorado River Authority under contract (88-89) 0910, Bureau of Economic Geology, The University of Texas at Austin, 118 p.
- Eaton, T.T., and Feinstein, D.T., 2002, Representing bedrock subcrop hydrostratigraphy in a multi-layer MODFLOW grid, 21 p., <http://www.isgs.uiuc.edu/3DWorkshop/2002workshop/eaton.doc>
- Fipps, G., 2001, Potential water savings in irrigated agriculture in the Lower Rio Grande Basin of Texas: The Texas Water Resources Institute, TR-183, 66 p.
- Freeze, R.A., and Cherry, J.A., 1979, Groundwater: Englewood Cliffs, New Jersey, Prentice Hall, 604 p.
- Frye, R.G., Kirby, L.B., and McMahan, C., 1984, The vegetation types of Texas: Texas Park and Wildlife Department, http://www.tpwd.state.tx.us/gis/vegetation_types/.
- Galloway, W.E., 1977, Catahoula Formation of the Texas Coastal Plain, depositional systems, composition, structural development, groundwater flow, history and uranium distribution:

- The University of Texas at Austin, Bureau of Economic Geology, Report of Investigation no. 87, 59 p.
- Gardner, W.R., 1983, Soil properties and efficient water use—An overview, *in* Taylor, H.M., Jordan, W.R., and Sinclair, T.R. (eds.), *Limitations of efficient water use in crop production: American Society of Agronomy*, Madison, p. 311–314.
- Gatewood, J.S., Robinson, T.W., Colby, B.R., Hem, J.D., and Halpenny, L.C., 1950, Use of water by bottom-land vegetation in Lower Safford Valley, Arizona: U.S. Geological Survey Water Supply Paper W1103, 210 p.
- Gay, L.W., and Hartman, R.K., 1982, ET measurements over riparian salt cedar on the Colorado River: *Proceedings of Hydrology and Water Resources in Arizona and the Southwest*, v.12, p. 9–15.
- Groschen, G.E., 1985, Simulated effects of projected pumping on the availability of freshwater in the Evangeline Aquifer in an area southwest of Corpus Christi, Texas: U.S. Geological Survey Water Resources Investigation Report 85-4182, 103 p.
- Harbaugh, A.W., and McDonald, M.G., 1996, User's documentation for MODFLOW-96, an update to the U.S. Geological Survey modular finite-difference ground-water flow model: U.S. Geological Survey Open-File Report 96-485, 56 p.
- Harden and Associates, 2002, Availability of brackish groundwater from the Rio Grande alluvium, Cameron County, Texas: consultant report for the Southmost Regional Water Authority, 23 p.
- Hay, R., 1999, A numerical groundwater flow model of the Gulf Coast Aquifer along the South Texas Gulf Coast: Texas A&M University—Corpus Christi, M.S. thesis, 47 p.
- HDR, 2000, Desalination for Texas water supply: contract report prepared for the Texas Water Development Board, Nueces River Authority, Central Power and Light Company, City of Corpus Christi, and San Patricio Municipal Water District, 258 p.
- Ideker, J., 1991, Plants and habitat associations of Unit 1, Laguna Atascosa National Wildlife Refuge, Cameron County, Texas: *Sabal*, v. 8, no. 1, p. 1–4.
- Jensen, R., 1996, Why droughts plague Texas: *Texas Water Resources Institute Newsletter*, v. 22, no. 2, p. 1–13.
- Jorgensen, D.G., 1975, Analog model studies of groundwater hydrology in the Houston district, Texas: Texas Water Development Board Report 190, 84 p.
- Kasmarek, M.C., and Strom, E.W., 2002, Hydrogeology and simulation of ground-water flow and land surface subsidence in the Chicot and Evangeline aquifers, Houston area, Texas: U.S. Geological Survey Water Resources Investigation Report 02-4022, 62 p.

- Kasmarek, M.C., and Robinson, J.L., 2004, Hydrogeology and simulation of groundwater flow and land-surface subsidence in the northern part of the Gulf Coast Aquifer System, Texas, U.S. Geological Survey Scientific Investigations Report 2004-5102, 111 p.
- Knape, B.K., 1984, Underground injection operations in Texas: A classification and assessment of underground injection activities: Texas Department of Water Resources Report 291, variously paginated.
- LBG-Guyton Associates, 2003, Brackish groundwater manual for Texas Regional Water Planning Groups, report prepared for the Texas Water Development Board, 188 p.
- McCoy, T.W., 1990, Evaluation of groundwater resources in the Lower Rio Grande Valley, Texas: Texas Water Development Board, Report 316, 47 p.
- McCuen, R.H., and Snyder, W.M., 1986, Hydrologic modeling—Statistical methods and applications: Englewood Cliffs, New Jersey, Prentice Hall, 568 p.
- McDonald, M.G., and Harbaugh, A.W., 1988, A modular three-dimensional finite-difference groundwater flow model: Techniques of water-resources investigations, Book 6, Chapter A1: U.S. Geological Survey, Reston, Virginia, 576 p.
- Myers, B.N., and Dale, O.C., 1967, Groundwater resources of Brooks County, Texas: Texas Water Development Board Report 61, 87 p.
- Meyer, W.R., and Carr, J.E., 1979, A digital model for simulation of groundwater hydrology in the Houston area, Texas: Texas Department of Water Resources LP-103, 27 p.
- NCDC (National Climatic Data Center), 2002, Cooperative Summary of the Day, TD 3200 POR-2001 Data, Central United States: National Oceanic and Atmospheric Administration, Asheville, North Carolina.
- Noble, J.E., Bush, P.W., Kasmarek, M.C., and Barbie, D.L., 1996, Estimated depth to the water table and estimated rate of recharge in outcrops of the Chicot and Evangeline aquifers near Houston, Texas: U.S. Geological Survey Water Resources Investigations Report 96-4018, 19 p.
- Paine, J.G., Angle, E.S., and Petrossian, R., 2001, Identifying and assessing groundwater in the Lower Rio Grande Valley, Texas, using airborne electromagnetic induction: Bureau of Economic Geology, Texas Water Development Board Contract 99-483-310, 80 p.
- Palmer, W.C., 1965, Meteorological drought: U.S. Department of Commerce, Research Paper 45, 58 p.
- Phillips, W.S., 1963, Depths of roots in soil: Ecology, v. 44, p. 424.
- Plummer, F.B., 1933, Cenozoic Systems in Texas: Geology of Texas, vol. 1, Stratigraphy, University of Texas Bulletin 3232, p. 519–818.

- Preston, R., 1983, Occurrence and quality of groundwater in the vicinity of Brownsville, Texas: Texas Department of Water Resources Report 279, 98 p.
- Price, W.A., 1934, Lissie Formation and Beaumont Clay in south Texas: Bulletin of the American Association of Petroleum Geologists, v. 18, no. 7, p. 948–959.
- Prudic, D.E., 1990, Estimates of hydraulic conductivity from aquifer test analyses and specific capacity data, Gulf Coast regional aquifer systems, south-central United States: U.S. Geological Survey Water Resources Investigation Report 90-4121, 38 p.
- Quarles, M., 1952, Salt-ridge hypothesis of Texas Gulf Coast type of faulting: American Association of Petroleum Geologists Bulletin, v. 37, p. 489–508.
- Raber, O., 1937, Water utilization by trees, with special reference to the economic forest species of the north-temperate zone: U.S. Department of Agriculture, Miscellaneous Publication 257, 97 p.
- Rantz, S.E., Barnes, H., Benson, M.A., Bodhaine, G.L., Buchanan, T.J., Carter, R.W., Cobb, E.D., Dalrymple, T., Davidian, J., Hulsing, H., Kilpatrick, F.A., Kindsvater, C.W., Matthai, H.F., Pendelton, A.F., Smoot, G.F., and Tracy, H.J., 1982, Measurement and computations of streamflow: U.S. Geological Survey Water Supply Paper 2175, 631 p.
- R.J. Brandes Company, 1999, Evaluation of Amistad-Falcon water supply under current and extended drought conditions, Phase II, Lower Rio Grande Valley Regional Integrated Water Resources Planning Study, Lower Rio Grande Valley Development Council and the Valley Water Policy and Management Council of the Lower Rio Grande Water Committee, Inc.; Austin, Texas, variously paginated.
- Riggio, R.F., Bomar, G.W., and Larkin, T.J., 1987, Texas drought—Its recent history (1931-1985): Texas Water Commission Report LP 87-04, 74 p.
- Robertson, S.M., Lawrence, R.G., and Maurer, T.C., 1992, Contaminants survey of La Sal Vieja, Willacy County, Texas: U.S. Fish and Wildlife Services, Region 2, Contaminants Program, 15 p.
- Rohwer, C., 1948, Seepage losses from irrigation channels: Fort Collins, Colorado, A&M College, Technical Bulletin 38, 98 p.
- Rose, N.A., 1954, Investigation of groundwater conditions in Hidalgo, Cameron and Willacy counties in the Lower Rio Grande Valley: The Lower Rio Grande Valley of Chamber of Commerce, 30 p.
- Ryder, P.D., 1988, Hydrogeology and pre-development flow in the Texas Gulf Coast Aquifer systems: U.S. Geological Survey Water Resources Investigation Report 87-4248, 109 p.
- Sayre, A.N., 1937, Geology and water resources of Duval County, Texas: U.S. Geological Survey Water-Supply Paper 776, 116 p.

- Sellards, E.H., Adkins, W.S., and Plummer, F.B., 1932, *The Geology of Texas, Volume I, Stratigraphy*: The University of Texas at Austin, Bureau of Economic Geology, 1007 p.
- Selley, R.C., 1970, *Ancient sedimentary environments and their subsurface diagnosis*: Chapman and Hall, London, 286 p.
- Shafer, G.H. and Baker, E.T., 1973, *Groundwater resources of Kleberg, Kenedy and southern Jim Wells counties, Texas*: Texas Water Development Board Report 173, 153 p.
- Solis, R.F., 1981, *Upper Tertiary and Quaternary depositional systems, central Coastal Plain, Texas—Regional geology of the coastal aquifer and potential liquid-waste repositories*: The University of Texas at Austin, Bureau of Economic Geology Report of Investigations 108, 89 p.
- Strom, E.W., Houston, N.A., and Garcia, C.A., 2003a, *Selected hydrologic data sets for the Chicot Aquifer, Texas*: U.S. Geological Survey Open File Report 03-297, CD-ROM.
- Strom, E.W., Houston, N.A., and Garcia, C.A., 2003b, *Selected hydrologic data sets for the Evangeline Aquifer*: U.S. Geological Survey Open File Report 03-298, CD-ROM.
- Strom, E.W., Houston, N.A., and Garcia, C.A., 2003c, *Selected hydrologic data sets for the Jasper Aquifer*: U.S. Geological Survey Open File Report 03-299, CD-ROM.
- TBWE (Texas Board of Water Engineers), 1946, *Seepage loss from canals in Texas*: Texas Board of Water Engineers, Austin, 39 p.
- The Handbook of Texas Online, 2002, *Laguna Atascosa*, <http://www.tsha.utexas.edu/handbook/online/articles/view/LL/rol2.html>.
- Theis, C.V., 1935, *The relation between the lowering of the piezometric surface and the rate and duration of discharge of a well using groundwater storage*: Transactions of the American Geophysical Union, v. 2, p. 519–524.
- Theis, C.V., 1963, *Estimating the transmissivity of a water-table aquifer from the specific capacity of a well*: U.S. Geological Survey Water Supply Paper 1536-I, p. 332–336.
- TCB (Turner, Collie and Braden), 2000, *Regional water supply plan for the Rio Grande regional water planning area (Region M)*: Rio Grande Regional Water Planning Group, variously paginated.
- UCS (Union of Concerned Scientists), undated, *Salty balance: Laguna Madre and the south Texas Coastal Plain*: Union of Concerned Scientists.
<http://www.ucsusa.org/gulf/gcplaceslag.html>.
- USGS (U.S. Geological Survey), 1990, 1:250,000 Digital elevation model.

- USSCS (U.S. Soil Conservation Service), 1972, Soil survey of Starr County, Texas: U.S. Department of Agriculture Soil Conservation Services, 137 p. + aerial photo maps.
- USSCS (U.S. Soil Conservation Service), 1977, Soil survey of Cameron County, Texas: U.S. Department of Agriculture Soil Conservation Services, 94 p. + aerial photo maps.
- USSCS (U.S. Soil Conservation Service), 1981, Soil survey of Hidalgo County, Texas: U.S. Department of Agriculture Soil Conservation Services, 171 p. + aerial photo maps.
- USSCS (U.S. Soil Conservation Service), 1982, Soil survey of Willacy County, Texas: U.S. Department of Agriculture Soil Conservation Services, 137 p. + aerial photo maps.
- Vandertulip, J.J., McDaniels, L.L., and Rucker, C.O., 1964, Water-supply limitations on irrigation from the Rio Grande in Starr, Hidalgo, Cameron and Willacy counties, Texas: Texas Water Commission Bulletin 6413, 72 p.
- Van Hylckama, T.E.A., 1970, Water use by salt cedar: *Water Resources Research*, v. 6, p. 728–735.
- Weakley, A.S., Patterson, K.D., Landaal, S., Pyne, M., and Russo, M.J., 2000, International classification of ecological communities—Terrestrial vegetation of southeastern United States, Texas review subset (February 23, 2000): The Nature Conservancy, Chapel Hill, North Carolina.
- Weeks, A.W., 1937, Miocene, Pliocene and Pleistocene formations in Rio Grande region, Starr and Hidalgo counties, Texas: *Bulletin of the American Association of Petroleum Geologists*, v. 21, no. 4, p. 491–499.
- Weeks, E.P., Weaver, H.L., Campbell, G.S., and Tanner, B.D., 1987, Water use by salt cedar and by replacement vegetation in the Pecos River floodplain between Acme and Artecia, New Mexico: U.S. Geological Survey Professional Paper 491-G, 33 p.
- Weiss, J.S., and Williamson, A.K., 1985, Subdivision of thick sedimentary units into layers for simulation of groundwater flow: *Groundwater*, v. 23, p. 767–774.
- Wood, L.A., Gabrysch, R.K., and Marvin, R., 1963, Reconnaissance investigation of the groundwater resources of the Gulf Coast region, Texas: Texas Water Commission Bulletin 6305, 114 p.
- Wood, L. A. and Gabrysch, R. K., 1965, Analog model study of groundwater in the Houston district, Texas: Texas Water Commission Bulletin 6503, 103 p.